Assessing Impacts of Climate Change on Water Resources and Agriculture: A Case Study of Tonle Sap Basin, Cambodia

---

A thesis
submitted in partial fulfilment
of the requirements for the Degree of
Master of Water Resource Management

at
Lincoln University
by
Sokna Ly

Lincoln University
2020

Abstract of a thesis submitted in partial fulfilment of the requirements for the Degree of Master of Water Resource Management.

Assessing Impacts of Climate Change on Water Resources and Agriculture: A Case Study of Tonle Sap Basin, Cambodia

by

Sokna Ly

Cambodia's Tonle Sap Lake is the largest permanent freshwater body not just in Cambodia, but in Southeast Asia, and is also one of the world's richest lacustrine-wetland ecosystems. Agriculture and fisheries provide the primary livelihoods of people living in the area. Despite a high abundance of natural resources, the area around Tonle Sap Lake is known to be one of the poorest areas in Cambodia, where most people derive their livelihoods directly from the resources provided by the lake. This study aims to assess the impacts caused by climate change on water resources and agricultural production in the basin by looking into future changes of streamflow of the tributary rivers, flood pulse and the paddy rice areas supported by the Mekong River's flood pulse.

For this study, six climate change scenarios were employed to assess future change in rainfall and river flow. They are the result of the combinations between three global circulation models (GFDL-CM3, GISS-E2-R-CC and IPSL-CM5A-MR) and two representative concentration pathways (RCP4.5 and RCP8.5). HEC-HMS was used for simulating rainfall and runoff for 11 sub-basins that feed the Tonle Sap Lake. HEC-RAS was used for computing inundation areas around the lake. Both models were calibrated and validated using data for the year 2000–2005 and 2006–2007, respectively. The results from HEC-RAS were exported in a format that enabled further analysis in GIS to examine changes to paddy rice areas at both the basin- and sub-basin scales.

Both HEC-HMS and HEC-RAS model performances were evaluated using statistical indices NSE and R^2. The indices indicated satisfactory performance for both simulation models with NSE > 0.40 and R^2 > 0.60 for HEC-HMS and NSE > 0.60 and $R^2 \geq 0.90$ for HEC-RAS. The main findings in the study were the reduction of annual streamflow that is projected to occur in almost every sub-basin under all climate change scenarios up to the year 2030. The Dauntri sub-basin is projected to experience the highest streamflow decrease, up to 62.53%,

while streamflow in the Sen and Boribor sub-basins showed a slight increase. The results from HEC-RAS suggest a decrease of flood pulse extent under all climate change scenarios. The magnitudes of decrease are almost the same for each scenario with an average decrease of around 10%. The Sen sub-basin showed the greatest reduction of flooded areas (13.82%) while Sangker was projected to decrease the least (2.00%). Though the Sen and Boribor catchments show an increase in streamflow, the increase is offset by the reduced flows in the remaining catchments, thus contributing less flow to the lake overall, leading to its reduced area. The results also suggest a decrease in paddy rice areas supported by the flood pulse. Stuang is the sub-basin with the highest reduction of paddy rice areas of up to 28.36%, while Sangker remains the sub-basin with the least reduction (2.67%).

Some noteworthy implications arise from the main findings. The decrease of flows in the tributary rivers suggests an increase in drought risk and consequences for household water supply and surface irrigation that divert or extract water from those rivers. The change of the extent of flood pulse suggests that there will be lower nutrients and sediment loads and this would substantially impact the ecosystems in the lake and other connected parts. The reduction of paddy rice areas underscores the potential implications for social and economic development such as food insecurity, unemployment and economic impacts.

Keywords: Tonle Sap, Cambodia, climate change, RCPs, water resources, streamflow, flood pulse, paddy rice areas, HEC-HMS, HEC-RAS.

Acknowledgements

This work was made possible by the efforts of my supervisors, Crile Doscher and Geoffrey Kerr, and the support from my family and friends.

Thank to Crile for sticking with me through ups and downs to follow through with this thesis. Without your guidance and support, this work would not have been completed. Thank to Geoff for your advice and comments to improve my work.

Thank to my family, my parents, especially. Thank dad and mom for your unconditional love. Without your encouragement, I would not be able to go this far.

Thank to the Waterways Center for Freshwater Management for supporting me throughout my Masters Program.

Matti deserves special thank in this work for helping with data. I could not ask for anyone else who is more helpful and inspiring than you.

Lots of thanks to my best friends, Vysen and Lyda, for standing by me when I reached the lowest points during my research journey. Thank to all my Cambodian brothers and sisters in Christchurch, my flatmates and all my international friends who were with me throughout this journey.

Thank to people at MoWRAM, Pu Bunrith, Pu Vy, Pu Hak, Pu Vuth, Bong Davy, Pich, Bong Den, Pu Seng, and Bong Seyha for your support and help with data.

My whole Masters Program would not have been completed without financial support from New Zealand Scholarship Programme. Thank to the People of New Zealand.

Table of Contents

List of Tables

List of Figures

Chapter 1
Introduction

1.1 Introduction

Cambodia's Tonle Sap Lake is a unique lacustrine wetland ecosystem (Figure 1.1). Thanks to an annual flood pulse that brings nutrients and sediment load to agricultural areas, the lake is one of the world's most productive freshwater ecosystems with high levels of biodiversity from which many Cambodians derive their livelihoods (Varis et al., 2006). While around 30% of Cambodia's population is living in the Tonle Sap zone (MoP, 2009), the area attracts people from elsewhere in Cambodia to settle because it is relatively flat with good access to water and potential for farming and fishing (Campbell et al., 2009).

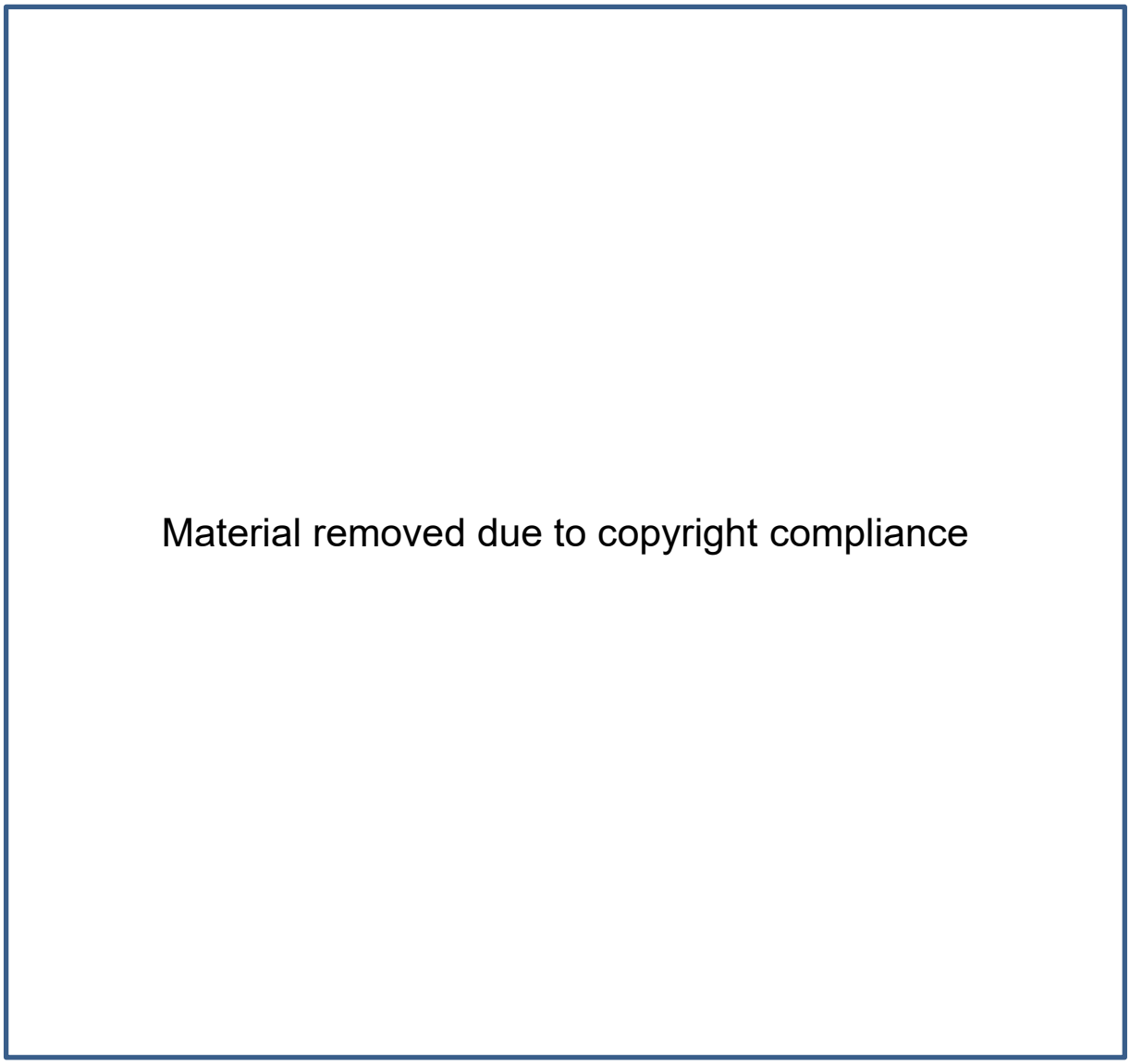

Figure 1.1 Map of Cambodia.
Source: UN OCHA (2017)

In the Tonle Sap area, the main livelihood strategies are rice cultivation and fishing (Keskinen et al., 2009). The type of agricultural cultivation people in the area mainly practice is flood recession paddy rice farming. As defined in the glossary database of the Food Agriculture Organisation (FAO), flood recession paddy rice areas are the areas along the river or lake exposed to floods, and cultivation occurs in those areas as floodwaters recede. This also includes floating rice (FAO, 2016). Flood recession farmers sometimes detain floodwater in bunds or man-made reservoirs and release this water to supply paddies during the dry season (Fox & Ledgerwood, 1999). If conditions permit, farmers in Cambodia prefer to grow flood recession rice as the yields are higher than for wet-season rice due to enhanced soil fertility from silt deposited by the floods (Fox & Ledgerwood, 1999). Rice cultivation in flood recession areas in 2006 covered 367,688 ha across Cambodia, which was approximately 50% of the total water managed areas (AQUASTAT, 2011).

Despite a high abundance of natural resources, the area around Tonle Sap Lake is one of the poorest areas in Cambodia when measured in monetary terms (Keskinen et al., 2007; Varis & Keskinen, 2003). The poor in the Tonle Sap area are highly dependent on land-based and water-based natural resources and are influenced by the dynamic hydrology of the lake, particularly the flood pulse system. They are, consequently, highly vulnerable to changes in the environment and the availability of different natural resources (Keskinen et al., 2009). Evidence from the past shows that several years of drought and flood, combined with poor soil and lack of proper water management, have weakened their farming capacity, forcing a large number to emigrate to the city and neighbouring countries for employment (Kimsun & Bopharath, 2013).

For the last couple of decades, water resources in the Tonle Sap Basin have been significantly affected by rapid population growth, massive changes in land use (urbanisation, deforestation, and agricultural expansion), and hydropower demand (Oeurng et al., 2019). This current situation is potentially exacerbated by climate change, leading to further degradation of the basin and floodplains. In 2019, for example, provinces in the basin were severely affected by droughts followed by extreme flooding events just a few months later.

To effectively manage water resources and efficiently ensure food security, it is crucial to understand future changes of significant hydrological aspects of the Tonle Sap system and its ability to support agricultural production under the threat of climate change. In this sense, future climate change impacts on streamflow and the flood pulsing system of the lake need to be accurately assessed before management strategies can be set out. A flood pulse is defined as the periodic inundation of lake and riverside areas due to high streamflow, which is the driving force in the river–floodplain ecosystem. The concept of flood pulse was formulated in 1986 during the first Large River Symposium in Toronto (Junk, 1989). It

focuses on the lateral exchange of water, nutrients and organisms between the river or lake and the connected floodplain. In this sense, a floodplain is considered as an integral part of the system that is seasonally connected and disconnected from the parent river by the aquatic or terrestrial transition zone (Junk & Wantzen, 2004).

Due to its unique hydrological characteristics and as an area of high importance for human and natural ecosystems, Tonle Sap Lake has been the subject of studies to comprehensively understand its dynamic hydrology such as its water balance (Kummu et al., 2014), sedimentation (Kummu et al., 2008), and the impacts to the lake due to upstream flow alterations resulting from hydropower dam construction, agricultural expansion and urban development (Arias et al., 2014; Kummu et al., 2004; Kummu & Sarkkula, 2008). Nonetheless, only one previously published study by Oeurng et al. (2019) looked into potential climate change impacts on Tonle Sap Lake. The study gave insight into future changes of streamflow for each tributary river under a number of climate change scenarios. The results indicate that there is a likely decrease of streamflow in both wet and dry season for most sub-basins under the three climate change scenarios (GFDL-CM3, GISS-E2-R-CC and IPSL-CM5A-MR) for three time horizons (2030s, 2060s, and 2090s). However, only the streamflow of tributary rivers was thoroughly examined in the study. To date, no attempt has been made to evaluate potential changes in other hydrological elements of the lake that are likely to be affected by climate change. This case study seeks to assess the potential impacts of climate changes on Tonle Sap's annual flood pulse and the paddy rice areas that depend on this flood pulsing system.

1.2 Research objectives

As highlighted above, knowledge about future hydrological changes in Tonle Sap Lake is vital in helping communities increase their resilience to climate change and ensuring sufficient resources to support the inhabitants of the areas. The primary goal of this study is to provide planners and decision-makers with supporting information to make sound decisions in water resources management and mitigation of the effects of climate change on the economy and the livelihoods of people living in the zone. The objectives laid out below helped to guide the study to achieve this goal:

- To determine the impacts of climate change on streamflow of Tonle Sap's tributaries;
- To assess the impacts of climate change on Tonle Sap's flood pulse contributed by its tributaries;
- To evaluate the impacts of climate change on flood recession paddy rice areas in Tonle Sap Basin.

1.3 Organisation of the thesis

This thesis is structured into seven chapters as follows:

Chapters 2 and 3 review the literature related to climate change in both the global and Cambodian contexts. Chapter 2 broadly explores the causes of climate change and the four projected emission scenarios used in the Fifth Assessment Report (AR5) by the Intergovernmental Panel on Climate Change (IPCC). The chapter also looks further into the impacts of climate change on a few significant aspects such as water, agriculture and economy at a global scale. Chapter 3 narrows down the scope to review the climate change situations in Cambodia. Prior to that, the chapter provides the background contexts and the country's risk and hazard profile. It then moves on to describe the current climate change situation in Cambodia, including the impacts, responses and challenges to climate change. The chapter wraps up with the future changes of climate that are likely to take place in Cambodia in the decades to come.

Chapter 4 describes the modelling framework for this research. The chapter starts with a detailed description of the study area and the rationale for modelling scenarios. The chapter also presents the hydrologic and hydraulic software that are used as model engines in this study: Hydrologic Engineering Centre – Hydrologic Modelling System (HEC-HMS), Hydrologic Engineering Centre – River Analysis System (HEC-RAS), and Geographical Information System (GIS). All datasets used as inputs to run the models are presented in detail with their features, sources, and time series. Lastly, the chapter describes the methods to analyse the data for each objective.

Chapter 5 contains the presentation of the results obtained from data analysis. The chapter begins with the assessment of model performance for HEC-HMS and HEC-RAS. The following parts of the chapter describe the results of the changes to tributary streamflow, flood pulse and flood recession paddy areas in comparison with the baseline. This chapter is facilitated by tables and figures to summarise and provide insights into the results.

Chapter 6 constitutes the discussions of the results presented in the previous chapter. Each objective is discussed by comparing with previous studies and connecting to the reviewed literature. The chapter then explores the potential implications of future changes in tributaries streamflow, flood pulse and paddy rice areas for the environment, society, and economy. The chapter concludes by addressing the research limitations in this study.

Chapter 7 provides a summary and conclusion of the thesis. The chapter summarises the outcomes by revisiting the research objectives. It concludes by recommending some perspectives for future research studies.

Chapter 2
Background: Climate Change and Its Impacts

2.1 Introduction

This chapter provides the background of climate change in the global context. The chapter also explores the causes of climate change and the four projected emission scenarios used in the Fifth Assessment Report (AR5) by the Intergovernmental Panel on Climate Change (IPCC). It then narrows down to the effects of climate change on the Southeast Asia region. Lastly, the chapter explores the impacts of climate change on a few important aspects such as water, agriculture and economy at a global scale.

2.2 Climate change: A global challenge

Climate change is one of the most significant global environmental challenges. Recent and future changes in extreme weather and climate events will likely create substantial impacts and serious problems for society (Karl et al., 2008). They pose various threats to socio-economic development such as decreasing agricultural productivity, increasing food insecurity and malnutrition and increasing vector-borne diseases – all of which affect the livelihoods of indigenous people (ADB, 2013; Dhar & Mazumdar, 2009). These impacts will also affect populations in areas where levels of climate-sensitive diseases are high, including for the urban poor in low- and middle-income countries (Akhtar, 2016). All these issues are challenges to sustainable development in developing countries, and are uncertainties the world is facing today.

The Earth's climate system has been significantly changing over the past few decades, and this phenomenon has been widely accepted in the scientific community (McCracken & Phillips, 2016). Sound evidence from the AR5 of the IPCC (Intergovernmental Panel on Climate Change) (2014) indicates that global mean sea level has risen approximately 0.19 m since the start of the twentieth century, and the global mean surface temperature has increased 0.8 °C since the immediate pre-industrial time. These changes have been scientifically explained as the result of increasing anthropogenic emissions of greenhouse gases (GHGs) in the Earth's atmosphere (Akhtar, 2016). Industrialisation, agricultural expansion, burning of fossil fuel, and transportation are the main drivers leading to an increase of GHGs in the atmosphere (Figure 2.1) (Shrestha, 2014). The concentrations of GHGs in the atmosphere influence the Earth's ability to reflect and absorb energy from the sun. As the level of GHGs increases, more heat is trapped in the atmosphere, causing the average surface temperature to increase (MoE & UNDP, 2011). With the ongoing emissions of GHGs, the climate system is projected to undergo changes well into and beyond the

twenty-first century. Nonetheless, the scale of such emissions remains unclear, and this uncertainty makes it difficult to forecast future climate change (McCracken & Phillips, 2016).

Figure 2.1 Total anthropogenic GHG emissions (gigatonne of carbon dioxide (CO_2) equivalent per year, $GtCO_2$-eq/yr) from economic sectors in 2010.
Source: Adapted from https://ar5-syr.ipcc.ch/topic_observedchanges.php (accessed May 2019)
Note: AFOLU: Agriculture, Forestry and Other Land Use

In light of this uncertainty, the IPCC developed four different 21st-century emission scenarios, or representative concentration pathways (RCPs). The RCPs integrate several scenarios of policy-level interventions, vulnerability mitigation practices, and adaptation strategies. They include a high greenhouse gas emissions scenario (RCP8.5), two intermediate scenarios (RPC4.5 and RCP6.0), and a stringent mitigation scenario (RCP2.6) (Figure 2.2) (IPCC, 2014). The number of each RCP (2.6, 4.5, 6.0 and 8.5) identifies projected radiative forcing levels (2.6, 4.5, 6.0 and 8.5 W/m^2) by the year 2100. Radiative forcing, expressed in watts per square metre (W/m^2), is the extra energy taken up by the Earth's system enhanced by the greenhouse effect. So, global temperature increases as the radiative forcing levels rise (van Vuuren et al., 2011).

Figure 2.2 GHG emission pathways 2000–2100.
Source: Adapted from https://ar5-syr.ipcc.ch/topic_pathways.php (accessed January 2020)

The RCPs are the products of an innovative collaboration between various modellers and experts. Van Vuuren et al. (2011) carried out a comprehensive overview of the four scenarios by describing the emission, environmental and socio-economic situations altogether for each RCP. Developed by PBL Netherlands Environmental Assessment Agency, the RCP2.6 low-emissions scenario projects that carbon dioxide emissions will remain at the present day levels until 2020, then decline and go lower than zero at the end of this century with CO_2 concentrations at about 400 ppm by 2100, corresponding to 2.6 W/m^2 of radiative forcing. To reach such low forcing levels, it would require a sharp reduction of GHG emissions through the declining use of oil, increases in the use of bio-energy products, and stronger climate change policies. On top of that, the scenario expects the world population to reach only 9 billion by 2100.

The lower-intermediate emissions scenario, RCP4.5, was developed by the Pacific Northwest National Laboratory in the US. This scenario projects the emissions of CO_2 to increase slightly before a decline around 2040. The scenario assumes future relatively low intensity of energy consumption and strong reforestation programmes (van Vuuren et al., 2011).

Another similar scenario is RCP6.0, a higher-intermediate emissions scenario. Developed by the National Institute for Environmental Studies in Japan, this RCP projects that CO_2 emissions will peak in 2060 at 75% higher than today's levels, then decline to 25% above current levels by 2100. The future anthropogenic activities consistent with these outcomes include a heavy reliance on fossil fuels and intermediate energy intensity along with the use of an array of technological approaches and strategies to reduce GHG emissions (van Vuuren et al., 2011).

Worst of all is the RCP8.5 – a continued high emissions scenario. This RCP was developed by the International Institute for Applied Systems Analysis in Austria. The scenario expects a world population of 12 billion in 2100 and CO_2 emissions to increase to be three times higher than today's levels as a result of heavy reliance on fossil fuels, high intensity of energy consumption, a lower rate of technology development and, more importantly, no implementation of climate policies to reduce emissions (van Vuuren et al., 2011).

Temperature is projected to rise over the 21st century under all emission scenarios (IPCC, 2014). This rising temperature will heat both land and ocean and melt the ice caps at the poles by various amounts. This will, in turn, lead to climatic phenomena such as sea-level rise, changes in rainfall patterns, heat and cold waves, increasing frequency and magnitude of droughts and floods, and other extreme weather events (MoE & UNDP, 2011). However, the effects of climate change will not be evenly distributed. Some places will experience higher surface temperature whereas others will be more prone to sea-level rise. While precipitation will increase in some areas, others will be drier (McCracken & Phillips, 2016). Climate change varies across the globe, and Southeast Asia is no exception.

2.3 Southeast Asia: A region at high risk from climate change

Southeast Asia, a region comprising 12 countries (Vietnam, Laos PDR, Thailand, Cambodia, the Philippines, Malaysia, Singapore, Indonesia, Timor-Leste and Papua New Guinea), was home to approximately 590 million people in 2010 (WB, 2013). The population is projected to reach 760 million in 2050, with 65% being urban-based (WB, 2013). The region has been affected by climate change in various sectors such as energy distribution, food security and water availability (Shrestha, 2014). Yusuf and Francisco (2009) used data on the spatial distribution of many climate-induced hazards to analyse 530 sub-national areas in Cambodia, Indonesia, Laos PDR, Malaysia, the Philippines, Thailand, and Vietnam. These mapping assessment results indicated that, either in part or in whole, each country (except Malaysia) is among the most vulnerable regions in Southeast Asia. All regions of the Philippines, almost all parts of Cambodia, Bangkok (Thailand), the Mekong River Delta of Vietnam, north and east parts of Lao PDR, and parts of the Sumatra and Java islands of Indonesia are regions identified as having a high exposure to climate hazards (Figure 2.3).

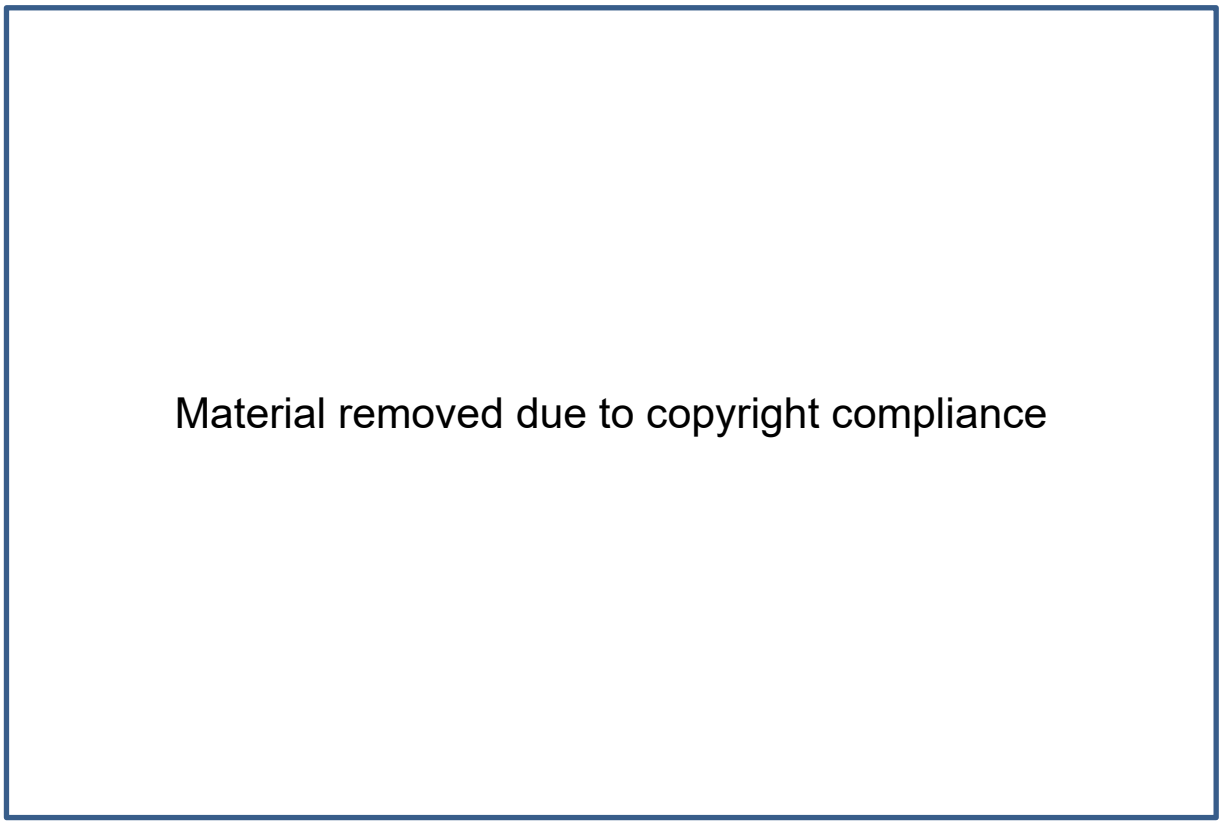

Figure 2.3 Climate change vulnerability map of Southeast Asia.
Source: Yusuf and Francisco (2009)

Southeast Asia has already been affected by climate change. Surface air temperature in the region increased between 0.1 and 0.3 °C per decade between 1951 and 2000 (ADB, 2009). Sea level has risen at the rate of 1 to 3 millimetres per year over the last 50 years. Heavy rainfall events increased significantly between 1900 and 2005, while tropical cyclones occurred more frequently between 1990 and 2003 (ADB, 2009).

Without any action, climate change is likely to intensify in the coming decades. Southeast Asia is expected to be warmer and become drier in many areas, while at the same time encountering higher risks of changes in the intensity of rainfall and a possible shift in monsoon patterns due to El Niño effects (Akhtar, 2016). Sea-level rise, coastal erosion and soil salinization are gradually engulfing Southeast Asia's arable lands and coastal areas (ADB, 2009). A projected 30-cm sea-level rise in 2040 would reduce rice production in the Mekong River Delta by about 2.6 million tons per year, or about 11% of 2011 production (WB, 2013). Sea-level rise will threaten coastal cities in Indonesia, the Philippines, Thailand and Vietnam and depress agricultural productivity in the delta regions. Populations and livelihoods in the river deltas are expected to suffer most because of the risks from rising sea levels (WB, 2013). Even though it is at the regional scale, the occurrence and consequences of climate change will not be homogeneously distributed throughout the region.

This unevenness makes the projection of regional climate change complicated, as it is challenging to incorporate all relevant regional aspects, exacerbating the uncertainties of

global modelling (McCracken & Phillips, 2016). Climate projections in Southeast Asia are particularly challenging because of a number of geographical factors such as complex terrain, a mixture of mainland, peninsulas, and islands, sea–land interactions, and a variety of complex climate phenomena that characterise the region's climate (WB, 2013). Despite the difficulties in modelling the scenarios, Southeast Asia stands as one of the most vulnerable to climate change, and the scenarios for climate change in Southeast Asia came under the spotlight in the recent Fifth IPCC Assessment (Akhtar, 2016). In 2009, the Asian Development Bank (ADB) carried out an economic modelling study of the impact of climate change and found that Southeast Asia is more likely to suffer from climate change than the world average. This could be equivalent to a mean loss of 2.2% of Gross Domestic Product (GDP) by 2100 on an annual basis when taking into account the market effects only, and 6.7% when considering the non-market and catastrophic risks also (ADB, 2009). This implication emphasises the necessity of future climate change projection in Southeast Asia to better guide adaptation and risk mitigation.

2.4 Impacts of climate change

The impacts of climate change are various and diverse. Identification of the magnitude of these impacts and whether they are beneficial or detrimental depends largely on location, time and the sector being discussed. For example, crops hit by severe drought, crops growing faster due to CO_2 fertilisation, rising heat stress, decreasing cold stress, increasing energy demand for cooling, decreasing energy demand for heating and so on. Although climate change may bring gains in the near future, in the long run, the negative impacts are likely to outweigh the positive ones (Tol, 2018).

2.4.1 Impacts on water

Water stress, the ratio of the total fresh water withdrawn by all major sectors to the total renewable freshwater resources, indicates the levels of potential impact on water resource sustainability and the potential conflict among water users (UN, 2018). Although the global average of water stress is only 11% (low water stress), 31 countries encounter water stress between 25% (defined as a minimum threshold of water stress) and 70%, while another 22 countries experience acute water stress above 70% (high water stress). Overall, over 2 billion people worldwide are living in countries under high water stress. The highest stress levels occur in Western, Central and Southern Asia and Northern Africa (UN, 2018). By 2050, two-thirds of the world population is projected to face high water stress conditions (Misra, 2014).

Water resources demand, and availability have been substantially impacted by climate change (UN-Water, 2010). Precipitation and temperature are the two essential indicators

reflecting the impacts of climate change on water resources (Men et al., 2019). Although there are some uncertainties and knowledge gaps, a growing body of scientific evidence (Huntington, 2006) has documented significant changes in the water cycle that can be anticipated in a changing climate. Climate change is the driver of a warmer atmosphere and faster water cycle through increasing evapotranspiration and precipitation (OECD, 2013). In general, climate change affects every aspect of the water cycle. The impacts on fresh water can be summarised as shifts in rainfall patterns, increasing water temperature, reduced water quality and increasing intensity and frequency of extreme weather events. Severe impacts are expected in the second half of the century when the consequences are anticipated to become apparent, while the rate of change is expected to accelerate over time (OECD, 2013).

Climate change will also affect groundwater availability and the depth of groundwater tables through changes in recharge rates due to changes in both amount and spatiotemporal distribution of rainfall (Kumar et al., 2017). Increasing evapotranspiration may also affect groundwater recharge, the extent of which remains unknown (OECD, 2013).

Water is a vital resource; impacts on fresh water will affect several key sectors (e.g., agriculture, energy, biodiversity, health and infrastructure) (OECD, 2013). Increased temperature will cause a higher rate of evapotranspiration and, in turn, further increase the demand for irrigation water that is already the most prominent water consumer (Kumar et al., 2017).

2.4.2 Impacts on agriculture

Historical evidence suggests that rice has played many important roles throughout civilisations in peace and war, dating back thousands of years. As a staple food, rice has supported and ensured food security for millions of people in the world. Today, around 50% of the world's population eat rice, and Asia accounts for more than 90% of global rice production (Cosslett & Cosslett, 2018). For the first half of this century, the global demand for food is expected to increase by 70%. Thus, new and traditional demand for agricultural production will exacerbate already scarce agricultural resources. Agriculture will be forced to compete for water and land with rapid urbanisation (FAO, 2009).

Under the threats of climate change, managing food security to achieve zero hunger for sustainable development is becoming more and more challenging and far from attainable. Despite substantial improvement and expansion in agricultural production, food insecurity is still an immense challenge for the world. A recent report jointly produced by five United Nations' agencies has indicated that more than 820 million people are living with hunger. Hunger is rising in almost all subregions of Africa, Western Asia, and Latin America (FAO et

al., 2019). During the 21st century, global agriculture is facing the new challenge of increasing food production to feed the growing population under the threat of climate change.

Climate change is expected to affect both irrigated and rainfed agriculture in the upcoming decades. Several studies (Aydinalp & Cresser, 2008; Keane et al., 2009) have summarised a number of possible ways climate change could, directly and indirectly, influence agricultural production such as:

- High temperature could affect crop growth rates and reduce soil moisture in many areas, especially some low and mid-latitude regions.
- Reduction in the quantity of water, either due to decreasing rainfall or increasing evaporation, influences both rain-fed and irrigated farming.
- Increase in atmospheric CO_2 concentrations influences the growth of crops as it changes one of the primary inputs for photosynthesis.
- Loss of productive land due to sea-level rise and associated salinization.
- Extreme weather events induced by climate change can influence production conditions, destroy crops and alter water supplies.

As the consequences of climate change are not evenly distributed, some regions will be adversely affected while others might benefit. The same studies above also highlight some possible positive effects that climate change could bring. An increase in temperature would expand agricultural production areas and extend the growing seasons in the regions where it is currently limited due to low temperatures. Also, some crops can use water more efficiently under higher CO_2 levels, because CO_2 fertilisation could increase their growth rate and reduce transpiration rates (Aydinalp & Cresser, 2008; Keane et al., 2009). Climate change is thus projected to alter the distribution of agriculture across the world. The poleward, shifting climate zones will increase the productive potential to high latitude regions, while agriculture in the low latitude regions will suffer yield loss due to heat stress and frequent severe weather events (UN-Water, 2010).

2.4.3 Economic impacts of climate change

Global and regional economies will be indirectly affected by climate change through the effects on other sectors such as water resources, agriculture, energy, and health. Due to the complexities of multi-sector involvement, little about the economic effects of climate change has been studied; however, it is not overlooked.

The OECD (2015) suggests that global annual GDP may decrease by between 2% and 10% by 2100 compared to the no-damage baseline scenario if temperatures continue to rise to a projected 4°C above pre-industrial levels by the end of this century. Changes in crop yields and labour productivity resulting from climate change are expected to have the most extensive negative consequences, which may cause losses to annual global GDP of 0.9% and 0.8% respectively by 2060.

The same report further highlights the regions where net economic consequences are projected to be mostly negative. Those regions are mainly in Africa and Asia, where the regional economies are vulnerable to heat stress and crop yield loss. South and Southeast Asia regions are projected to have GDP losses of 1.7% to 6.6% by 2060 (OECD, 2015).

2.5 Summary

The literature shows that the climate system has been undergoing significant changes. Increasing temperatures and sea-level rise are prominent examples of these changes. In response, the IPCC developed four RCP scenarios (RCP2.6, RCP4.5, RCP6.0, and RCP8.5) to project future climate change based on an integration of policy-level interventions, vulnerability mitigation practices and adaptation strategies. Meanwhile, Southeast Asia, a region projected to be home to 760 million people in 2050, has been identified to be at high risk of adverse effects of climate change. Some large coastal cities such as Bangkok, Ho Chi Minh, Jakarta, and Manila will be threatened by sea-level rise, while human health, crops and livestock will be influenced by increasing temperature.

The impacts of climate change are many and various. In the long run, these impacts are expected to be detrimental for relevant sectors such as agriculture, water and economy, although there could be localised exceptions to this. Water resources, which are already under high demand, have been and will be substantially affected by climate change. Both surface water and groundwater availability are projected to decrease due to changing rainfall patterns and increasing evapotranspiration. For centuries, securing adequate food for a growing population has always been a challenge for agriculture. Climate change will exacerbate this burden through several ways such as rising temperature, reducing water availability, increasing CO_2 concentration, reducing productive land due to sea-level rise and reducing crop yields due to extreme weather events. OECD (2015) suggests that global annual GDP may decrease between 2% and 10% by 2100 because of climate change effects. Africa and Asia are projected to face substantial economic loss due to heat stress and crop yield reduction.

Chapter 3
Cambodia in the Context of Climate Change

3.1 Introduction

Following from Chapter 2, this chapter also explores climate change, but the scope is restricted to the Cambodian context. Starting with an overview of Cambodia, the chapter provides some important information about the country's geography, climate, population, economy, and its risk and hazard profile. Then, the chapter moves on to describe the current situation regarding climate change in Cambodia, which cover the impacts, responses and challenges to climate change. The chapter concludes with the projection of future changes caused by climate change that are likely to take place in the country in the years to come.

3.2 An overview

3.2.1 Geography

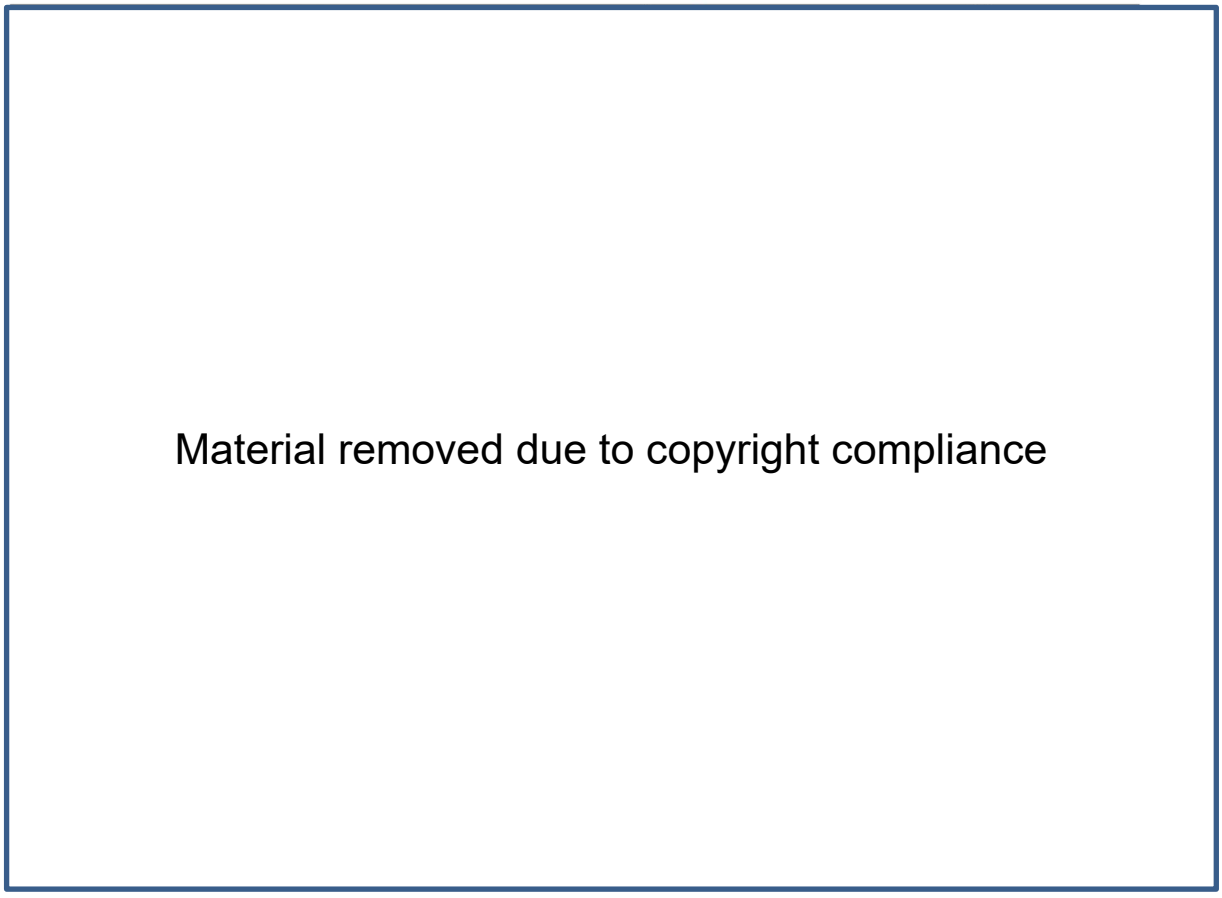

Figure 3.1 Administrative map of Cambodia.
Source: MoE (2009)

Cambodia, officially known as the Kingdom of Cambodia, is in mainland Southeast Asia located between latitudes 10° and 15° N and longitudes 102° and 108° E. Cambodia covers a land area of 181,035 km^2 and shares borders with Vietnam to the east and southeast, Laos PDR to the northeast and Thailand to the north and west (Figure 3.1). The total length of its land boundary is 2,572 km, and its coastline along the Gulf of Thailand is 435 km in length. Phnom Penh, the capital city of Cambodia, is located in south-central Cambodia, in the vicinity of the confluence of the Mekong, Tonle Sap and Bassac Rivers (MoE, 2015; UNISDR, 2010).

Around three-quarters of the country lies in low-lying alluvial plain at an elevation not more than 100 m above mean sea level (UNISDR, 2010). These areas are frequently susceptible to flooding, especially in the low-lying central plains, which include the Mekong River plain, Bassac River plain and Tonle Sap floodplain. This is understandable because the central plains are surrounded by mountain ranges to the north (the Dangrek Mountain adjoining the Korat plateau of Thailand), the east (Ratanakiri plateau and Chlong highlands merging with the central highlands of Vietnam) and the west and southwest (Cardamom and Elephant Mountains) (Figure 3.2) (MoE, 2009).

Figure 3.2 Cambodia's topographical landscape.
Source: Schmeling (2019)

In the heart of Cambodia lies a large permanent freshwater body known as the Tonle Sap Lake. The lake is part of the larger Mekong River Basin. Its hydrology is characterised by the unique seasonal reversal flow of the Tonle Sap River, which is primarily driven by the flow regime of the Mekong River. Water flows from the lake to the Mekong River in the dry season (November–April). During the wet season (May–October), however, the water level in the Mekong River increases, causing water flows back up to the lake through the Tonle Sap River (MRC, 2009). The lake is the most extensive wetland habitat in the Mekong River Basin and also functions as a natural floodwater reservoir for Cambodia and the Mekong system during the dry season (Kummu et al., 2014; MRC, 2009).

3.2.2 Climate

Like many other countries in Southeast Asia, Cambodia's climate is driven by tropical monsoons and is characterised by a rainy season from May to October and a dry season from November to April. Typically, the country receives heavy rainfall in September and October, while January and February remain the driest months. The mean maximum temperature is about 28 °C, and the mean minimum temperature is about 22 °C (MoE, 2015; UNISDR, 2010). The average precipitation rate for 11 years (1994–2004) is 1,598.4 mm. The Tonle Sap Basin and the lowlands along the Mekong River receive average annual precipitation of between 1,300 and 1,900 mm (MoWRAM, 2013).

Throughout the Mekong River Basin, the temperatures are reasonably stable, with only small variations from the average annual mean temperature of about 28 °C. However, in some years, the temperature can be as low as 10 °C in January and as high as 38 °C in April, before the rainy season arrives. Typically, the Vietnam bays are the protection wall against typhoons and tropical storms, mitigating the damage in Cambodia (MoWRAM, 2013).

3.2.3 Population and economy

Cambodia reached a population of 16.5 million in 2019, with an annual growth rate of 1.6% (UNFPA, 2019). The country's population is expected to increase to between 20 and 24 million by 2050 (Figure 3.3) (UN, 2019). A large proportion of the population (80%) lives in rural areas. A broader geodemography shows approximately 52% of the population lives in the central plains, 30% around the Tonle Sap Lake, 11% in the highland areas and 7% in coastal areas (MoE, 2015).

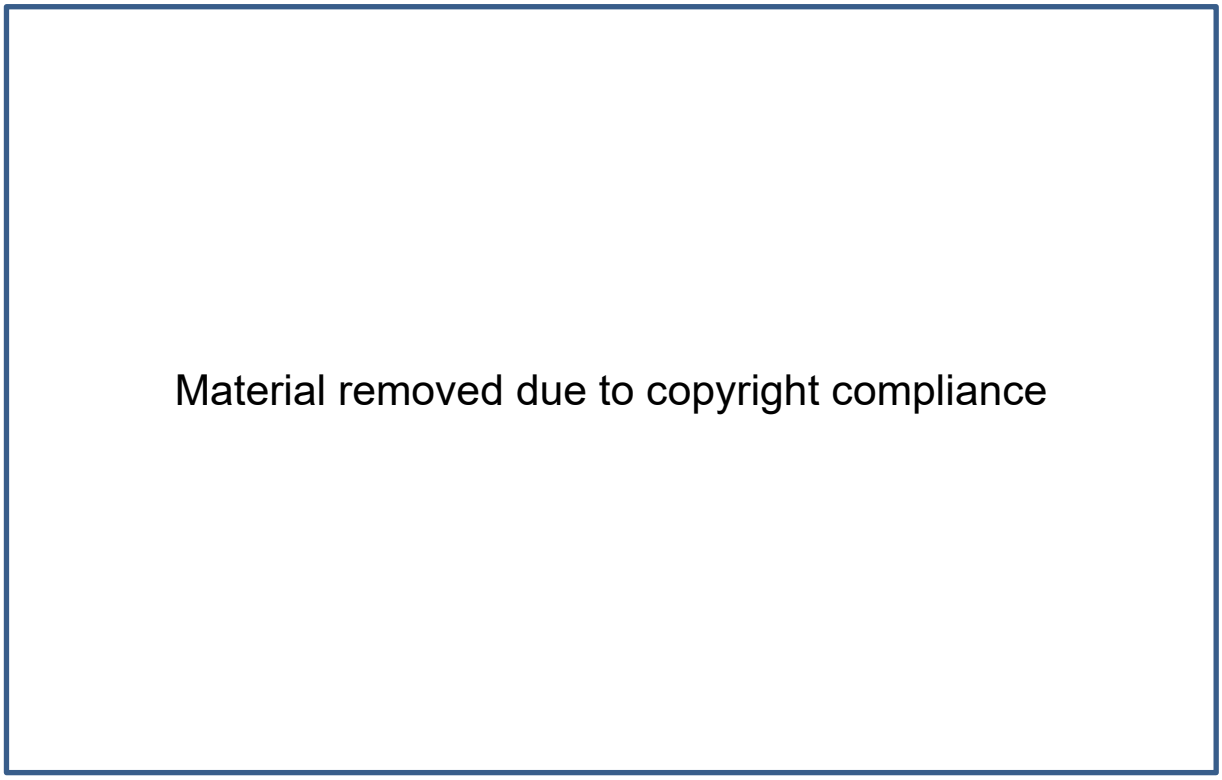

Figure 3.3 Cambodia: total population projection.
Source: Adapted from United Nations, DESA, Population Division. http://population.un.org/wpp/ (accessed August 2019)

In 2015, Cambodia advanced from a low-income to a lower middle-income country when the Gross National Income (GNI) per capita tripled from US$300 in 1994 to US$1,070 in 2015, thanks to rapid and sustained growth at an average rate of 7.6% between 1994 and 2015 (WB, 2017). This has made Cambodia one of the countries with the highest rates of economic growth in the world (MoE & UNDP, 2011). This sustained growth has been mainly driven by exports of goods and provision of services (garments and tourism). Recently, agriculture, construction, and real estate have become the country's pillars for sustaining strong economic growth (WB, 2017).

In 2015, Cambodia became a lower middle-income country when the gross national income (GNI) per capita tripled from US$300 in 1994 to US$1,070, thanks to rapid and sustained growth mainly driven by exports of goods and services (WB, 2017). In addition to this upgrade, economic development in Cambodia is expected to move forward in the coming years. As stated in the 'Rectangular Strategy Phase IV', the Royal Government of Cambodia (2018) has an ambitious vision to make Cambodia an upper middle-income country by 2030 and advance to a high-income country by 2050, with the aim of achieving sustainable economic growth of around 7% per annum.

3.2.4 Risk and hazard profile

Despite excellent performance in economic development for the last few decades, Cambodia is still exposed to numerous vulnerabilities due to extreme hazard events. Cambodia was ranked the second-highest disaster risk country in Southeast Asia in 2018, following the Philippines at the top of the list (Bündnis Entwicklung Hilft and Ruhr University Bochum, 2018). According to the synthesis report on disaster risks assessment of the ten ASEAN countries by UNISDR (2010), Cambodia is susceptible to various natural hazards such as floods, droughts, cyclonic storms and epidemics. The percentage distribution of disasters in Cambodia showed that between 1970 and 2009, the country suffered most from floods (47%), followed by epidemics (30%), drought (13%) and storms (10%).

Floods

Floods are the dominant risk in Cambodia. The Asia Pacific Disaster report in 2010 ranked Cambodia as the country in the region with the highest proportion of the population (12.2%) at risk of being affected by floods (UNESCAP, 2010). Between 1970 and 2009, floods killed 1,245 people, put 9.66 million people at risk, and caused economic losses of US$532 million. Among natural hazards, floods have the highest frequency of occurrence (35% of all natural hazards), the highest death rate (31.13 deaths/year) with an average annual loss of US$16.1 million (UNISDR, 2010).

Floods typically occur in Cambodia's 42 sub-basins, especially in the Mekong and Tonle Sap Basins. Flash floods frequently occur during the rainy season, especially near the plateau, whereas river floods frequently occur along Tonle Sap, Mekong and their tributaries (MoWRAM, 2013). According to Jha et al. (2012), floods that peak within six hours of the beginning of torrential rainfall are defined as flash floods and are almost impossible to forecast as they occur abruptly. River floods, on the other hand, occur when the volume of surface water runoff exceeds the capacity of waterways or constructed water channels to accommodate the flow. The excess water normally takes a considerable amount of time to overflow the banks of the water course and spread out to the low-lying areas or floodplains.

The bowl-like geography of Cambodia combined with its meteorological conditions (i.e., wet with high rainfall intensities) favours the development of floods in the low-lying areas (the central floodplain) almost every year. Also, floods in Cambodia can be attributed to other anthropogenic activities such as mass urbanisation and land-use change, along with underdevelopment of systematic water resource management practices and facilities (Ly et al., 2018).

Another major contributing factor that increases flood frequency is deforestation. In Cambodia, uncontrolled logging has long been a major environmental issue. Forest clearance, conversion of forests to agricultural land and illegal forestland encroachment are the main contributors to the country's decades of deforestation. In 1965, 73% of Cambodia was covered by forest. Forest cover rapidly decreased to around 59% (about 10.7 million ha) in 2006 (FA, 2010). The rate of deforestation from the 1980s to 1990s was estimated at approximately 2% per annum (200,000 ha/year) and declined to 0.8% per annum (75,000 ha/year) from 2002 to 2006 (MoE & UNDP, 2011). Forests are an effective tool for mitigating floods. They act as sponges by retaining water during heavy rainfall and later release it slowly into the waterways (CIFOR, 2012). Forests slow down runoff and thus reduce the severity of floods. The loss of a massive amount of forest therefore means an increase in flood severity and frequency.

Cambodia has suffered many major flood events in the last few decades. The intensity and magnitude of flooding along the Mekong River and Tonle Sap Lake have increased over time (Yu et al., 2019). Disaster statistics recorded by EM-DAT of the Centre for Research on Epidemiology Disasters (CRED) showed that Cambodia experienced nine climate-related disaster events (six floods, two droughts, one storm) from 1987 (the year in which the first disaster event in Cambodia was reported to EM-DAT) to 2000. From 2001 to 2015, however, the frequency of disaster events noticeably increased, especially flood events (twelve floods, three droughts, two storms) (EM-DAT, 2016 as cited in Kim et al., 2019).

One of the worst floods in Cambodia's history was a flood in 2000, where 374 lives were claimed, and total physical damage was estimated at US$150 million (RGC, 2014). After that, flood damage in 2011 ranked as the second most devastating event within the last two decades (MRC, 2011). Flooding in October 2011 affected 18 of the 24 provinces in Cambodia and caused severe damage to 350,274 households (equivalent to 1.64 million people including 700,000 children), 432,449 ha of rice fields, large amounts of communal infrastructure with a total estimated loss at US$630 million, and over 200 fatalities (Yu et al., 2019). MRC (2012) evaluated the average annual area of crop damage due to flooding in Cambodia to be 122,000 ha, with the average annual total flood cost being US$18 million per year. Turunen et al. (2011) found that 46% of Cambodian farmers experienced significant crop damage and 6% suffered total crop loss due to flooding in the 2008–2009 wet season.

Droughts

An uneven distribution of monsoon rainfall can sometimes result in drought conditions. When evapotranspiration far exceeds precipitation, and river flow drops, many places face water shortages, resulting in growing competition for water. Droughts can be classified as meteorological, hydrological or agricultural and socioeconomic. According to FAO (2017),

meteorological droughts occur when the amount of rainfall over a given period of time is significantly lower than the average. Agricultural drought happens when there is insufficient soil moisture to meet the needs of a particular crop at a specific time. Agricultural drought normally occurs after meteorological drought but before hydrological drought. Hydrological drought occurs when there are deficiencies in surface and subsurface water supplies, and socioeconomic drought occurs when reduced water availability begins to affect people individually and collectively. Meteorological droughts can stimulate hydrological droughts and together they can have impacts on rice yield production (MRC, 2014). In Cambodia, the most drought-prone area is the south-eastern region and drought is more likely to happen in the late monsoon season (September to November) (MRC, 2014).

The extensive drought in 2002, for example, devastatingly affected 650,000 people and caused an economic loss of US$38 million (UNISDR, 2010). In terms of average economic cost, MRC (2012) found that floods and droughts are the primary disasters in Cambodia and have been estimated to cost about the same amount (about US$70 million) per event.

3.2.5 Agriculture

Cambodia is predominantly agricultural, and rice is the most crucial crop in Cambodia. It dominates the country's economy, employing 75% of the national population and occupying 2.3 million ha of a total 2.8 million ha of cultivated area (ADB, 2005). The World Bank (WB) (2015) reported impressive growth of Cambodian agriculture over the past decade. The real agricultural GDP growth rate was 5.1% annually between 2002 and 2012. This remarkable growth has contributed significantly to poverty reduction in the country. The overall poverty headcount declined from 50.1% to 20.5% from 2007 to 2011. This is due to improving rural households' conditions, thanks to the direct impact of higher rice prices and the increase in rice production.

The wet season rice crop is the dominant source of Cambodia's food supply and accounted for 77% of total rice production in 2012 (Johnston et al., 2013). In Cambodia, rice is mainly produced for home supply, but producing a surplus for sale has grown lately. Rice production is thus not only important for maintaining food security but also for exporting as a significant crop, particularly for some high-value aromatic types (Johnston et al., 2013). Agriculture is one of the principal sources of family and national incomes. Despite the series of floods and droughts in some years, areas of rice cultivation have increased annually since 1980. In 2010, average rice yield was 2.76 tonnes per ha and 4.2 tonnes per ha in the wet and dry seasons, respectively (Smith & Hornbuckle, 2013).

3.2.6 Water resources

Cambodia's economy is highly dependent on water. The importance of water for food security, rural livelihoods and economic development is acknowledged in the Cambodia Government's Rectangular Strategy on Growth, Employment, Equity and Efficiency (Phase 2, 2008) and the National Strategic Development Plan (2009–2013) (MoWRAM, 2013).

Sources of water

Cambodia is one of the water-abundant countries in the region, thanks to the Mekong River and extensive aquifers. The dominant waterways in Cambodia are the Mekong River and its tributaries. The most significant tributaries of the Mekong River in Cambodia are the Tonle Sap Lake and its system. Tonle Sap Lake and the Mekong River are the key components to sustain the livelihood of millions of Cambodian people by providing an invaluable resource for agriculture, fish production, biodiversity, water transportation and hydropower. In addition to the two main river basins, Cambodia has another 42 sub-basins that offer significant amounts of water for domestic use and national economic development, especially agricultural production (MoWRAM, 2013).

Surface water is sourced from rainfall and water flowing from the Mekong River to the Tonle Sap Lake, before running further south to the Mekong Delta (in Vietnam) and the South China Sea (MoWRAM, 2013).

Groundwater is used for irrigation only for small-scale vegetable gardens or fruit farms in the dry seasons when surface water is limited. Though it has been developed and used for irrigation in the southern and eastern parts of Cambodia, groundwater has been used rarely in the northwestern areas of the country, where surface water is abundant (MoWRAM, 2013).

Water use

Water is used in various sectors including household, agriculture, industry, tourism, and energy production. According to the Ministry of Water Resources and Meteorology (MoWRAM), the average annual total water use in Cambodia is estimated to be 7.9 billion m^3, of which 7.59 billion m^3 (96% of total use) is consumed by irrigated agriculture (sourced from surface water). Domestic use accounts for 0.24 billion m^3 (3% of total use), and 0.07 billion m^3 (1% of total use) is for industrial use (MoWRAM, 2013).

Despite having abundant fresh water during the wet season, the country faces a shortage of water during the dry season and a 'small dry season' in the wet season. In principle, water is scarce when there is a lack of sufficient rainfall. Irrigation infrastructure is inadequate, old and run-down, which hugely affects water distribution and supply (MoWRAM, 2013). Without

supplementary irrigation, increasing water scarcity frequently leads to crop damage. Competition for water resources intensifies with the coming of irrigation development and population growth (ADB, 2005). In addition to the demand for water for irrigated agriculture, domestic consumption, and industrial use, water availability in Cambodia is likely to be influenced by climate change.

3.3 Climate change in Cambodia

3.3.1 Current situations

Background

Figure 3.4 shows the cumulative amount of CO_2 emitted by each country. Developing countries produce less CO_2 than developed countries. Between 1751 and 2016, Cambodia produced 97.29 million tonnes. New Zealand, by comparison, has emitted almost 18 times more than Cambodia (1.74 billion tonnes). Figure 3.5, on the other hand, indicates the Climate Risk Index (CRI) for every country. CRI indicates the level of exposure and vulnerability each country encountered in a specific period of time. CRI score is the result of four indicators analysed: (1) death toll, (2) deaths per 100,000 habitants, (3) total losses in Purchasing Power Parity (PPP), and (4) losses per unit of GDP (Germanwatch, 2019). According to Figure 3.5, developing countries tend to be more susceptible than rich countries to the risks of climate change. Climate change has unequal impacts across the globe. People who have contributed the least to the cause of climate change are expected to feel its effects the most, and those people are the poorest citizens in the poorest countries.

Figure 3.4 Cumulative CO_2 emissions for each country between 1751 to 2016, measured in tonnes.

Source: Adapted from https://ourworldindata.org/co2-and-other-greenhouse-gas-emissions (accessed May 2019)

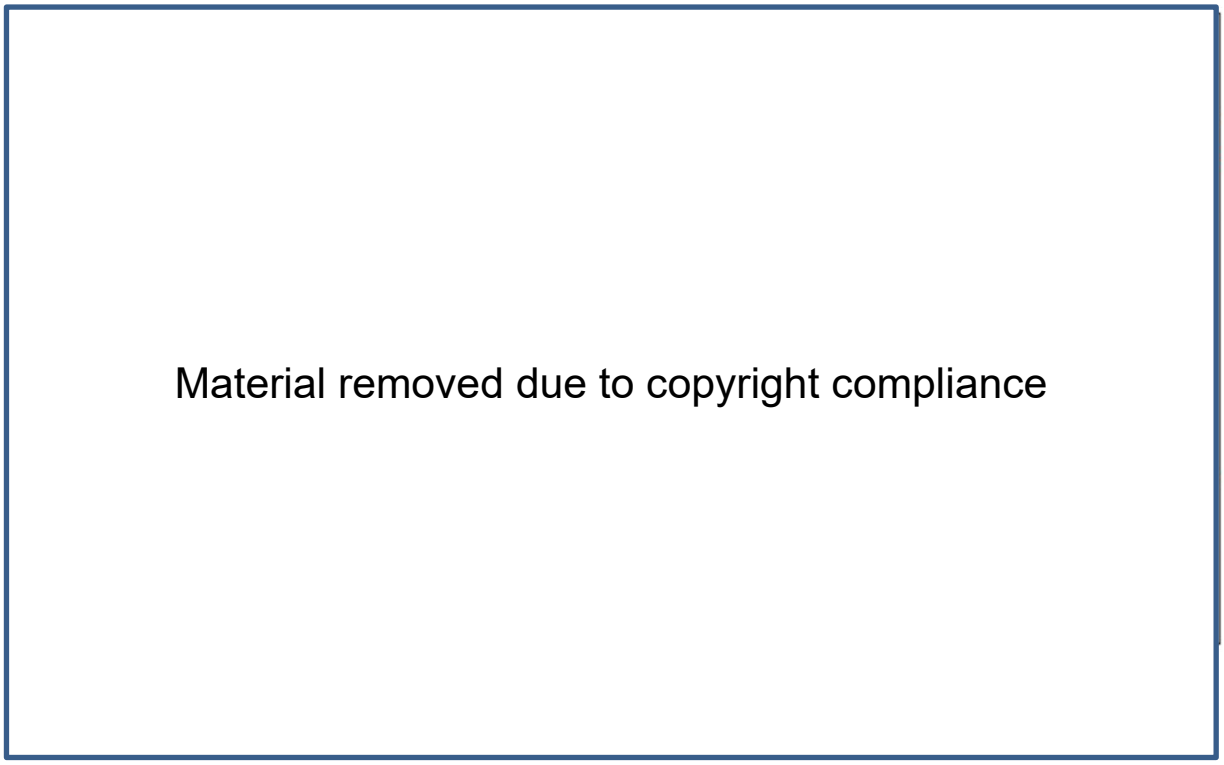

Figure 3.5 World map of the global climate risk index 1998–2017.
Source: Germanwatch (2019)

At 0.5 ton of CO_2 emissions per capita (per capita CO_2 emissions for New Zealand is 7.7 tons, and the world average was 4.8 tons in 2017) (Global Carbon Atlas, 2018), Cambodians contribute little to global warming, yet are highly vulnerable to the impacts of climate change. In the next few decades Cambodian agricultural land, water resources, food resources, biodiversity and coastal ecosystems are expected to decline due to the effects of climate change (ADB, 2012). In Cambodia, the livelihoods of the poor are highly dependent on natural resources, so an inability to access these resources will seriously affect the poor and put them at higher risk given their low capacity to adapt to environmental change (Kimsun & Bopharath, 2013).

Climate change is already being felt in Cambodia (MoE & UNDP, 2011). The Ministry of Environment of Cambodia (MoE) in 2016 carried out the second study (KAP2) on the public perception of climate change in Cambodia in terms of knowledge, attitude, and practices (the first one, KAP1, was done in 2011). The study surveyed 1,000 respondents across the 25 provinces. A large proportion, 91%, of the respondents had heard about climate change, and of that 91%, 98% agreed that climate change is affecting Cambodia. A majority of the respondents noticed climate variability through its impacts on their own and family members' health. Other consequences include difficulty in farming, lower crop yields, more droughts, increased temperatures and more flooding (Figure 3.6) (MoE, 2016b).

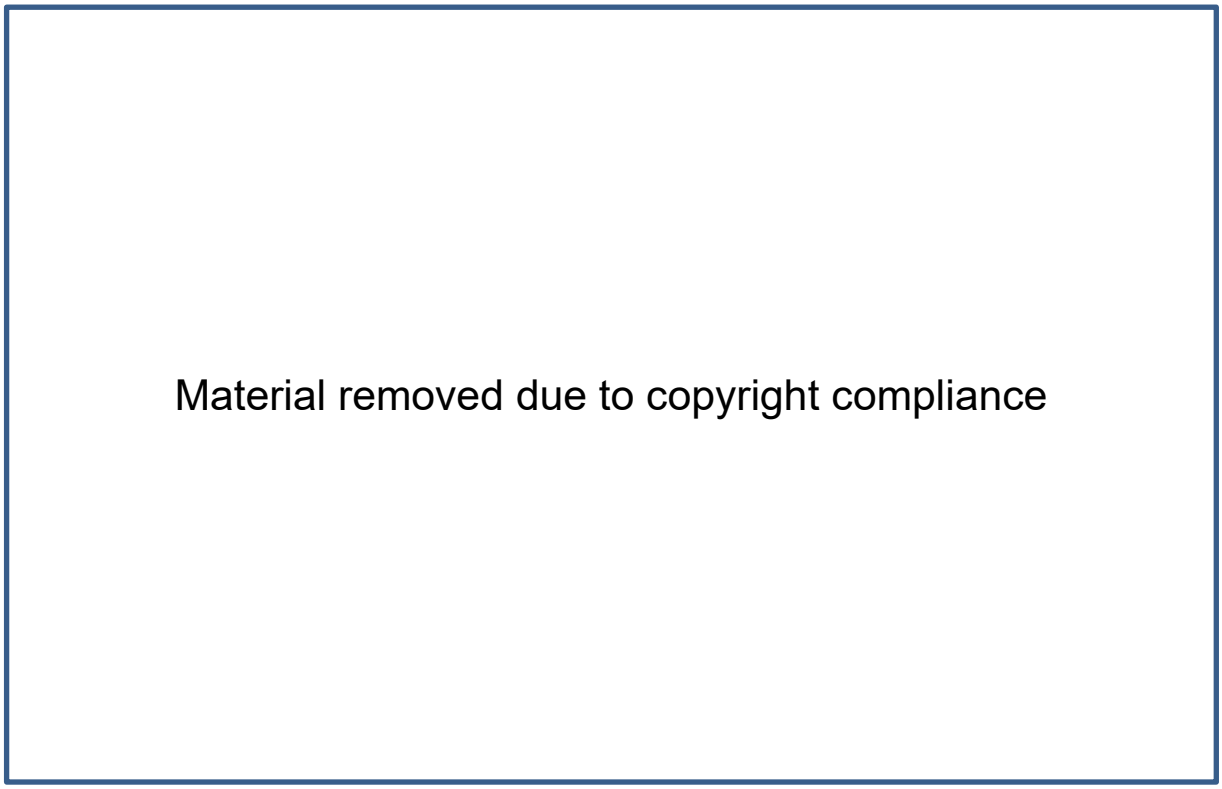

Figure 3.6 Climate change impacts on Cambodia.
Source: MoE (2016b)
Note: KAP1: The first nationwide study on public perception (knowledge, attitudes, and practices) of climate change in Cambodia in 2011. KAP2: The second national study on public perception (knowledge, attitudes, and practices) of climate change in Cambodia in 2016.

Impacts

In some parts of the world, the effects of climate change can be obvious and easily identified. For example, low-lying areas are exposed to sea level rise, and arid zones are highly exposed to severe water shortage due to their geography. In Cambodia, climate change affects the country's main elements of the social, political, and economic sectors, resulting in, for example, degradation of agriculture, fisheries, and ecosystems leading to broader and more intensive problems of poverty, economic development, legal and market institutions, and dependency on foreign aid (MoE & UNDP, 2011).

Climate change is definitely one of the main barriers for development in Cambodia. Agriculture, fisheries, ecosystem services, social and economic development are adversely affected. Climate change impacts combined with the issues of population growth, urbanisation, agricultural intensification, industrialisation, energy, and transportation development left almost one-third of Cambodians living at or below the national poverty line (MoE, 2016b). Rural communities, poor people, women, children, ethnic minorities, older people and people with disabilities are identified as being the most vulnerable to climate change, as they have limited alternative livelihood options, social roles and norms, sensitivity to climate changes, and low adaptive capacity (MoE, 2016b).

Climate change causes tremendous economic implications everywhere in the world, and the costs could be higher than average for developing countries like Cambodia. In 2009, ADB carried out a regional study (Indonesia, the Philippines, Thailand, and Vietnam) of economic loss due to climate change. The study found that under the 'business as usual' scenario, climate change could cause economic losses up to 6.7% of GDP by 2100 (ADB, 2009). Given the higher level of vulnerability that Cambodia is susceptible to, the cost of economic losses is expected to be higher.

Responses to challenges

In response to the issues threatened by climate change, the government of Cambodia has firmly committed to mitigate and find sustainable solutions for climate hazards. The efforts can be evidenced through the signing and ratifying of international conventions, adopting and implementing policy measures for climate change adaptation, disaster risk reduction and resilience building (MoE, 2016b).

Despite how well thought-out and planned at the policy-making level, the policy implementation on the ground cannot be fully effective unless there is an inclusion of a wide range of technical information, sources of knowledge and informed debate among stakeholders. According to a study conducted by MoE in 2016, 37% of the respondents did not know how to respond to climate change, while another 22% did nothing in response to climate change (MoE, 2016b). This illustrates that almost half of the respondents are unaware of or lack of capacity to deal with the impacts that are happening to them.

The report finally suggested that further steps towards enhancing knowledge to best adapt to climate change are to promote awareness and understanding among the public, especially rural people who are most sensitive to environmental changes, about the causes and consequences of climate change and its impacts on human health and livelihoods, and to build local capacity to address both climate change and disaster risk. Also, the absence of a proper response mechanism and planning at local levels (due to lack of understanding about associated issues and limited local institutional capacity – financial, technical, and human resources) is identified as the most significant challenge to overcome regarding climate change and climate variability (Kim & Chem, 2014; MoE, 2016b).

Future projections

Predicting future climatic is riddled with uncertainty. With many determining factors in play, future climate will undoubtedly vary significantly from one place to another. However, by incorporating past and new data with refined climate models, there exists a significant

consensus on the likely changes Cambodia will encounter within the next century. According to MoE and UNDP (2011), predictions of climate change in Cambodia are

- increasing temperature (temperature has already been rising and will keep rising),
- changes in seasonal patterns of rainfall – both timing and duration (shorter, wetter rainy season and longer, drier dry season),
- increasing flood and drought frequency and intensity,
- sea-level rise in the coastal regions.

However, the magnitude of temperature increase is expected to vary depending on location. In low-altitude areas, such as central Cambodia and the northeast, the rate of temperature increase is projected to be highest (0.036 °C per year), while in the high-altitude regions, such as the southwest, the projected rate of increase is only 0.013 °C per year (MoE & UNDP, 2011).

Predictions of rainfall are complicated and involve many uncertainties. The projections are scenario-based (depending on the selection of GHG emission scenarios, climate models and duration of the time period to be covered). The study of past and future precipitation changes cannot be accurately done due to the lack of reliable data, leading to technical challenges. Despite a clear need for more data and further research, a common consensus that emerges is that precipitation varies in different locations and at different periods within this century. These variations have implications for water availability (MoE & UNDP, 2011).

Sea level is projected to rise by between 0.18 m and 0.56 m by 2090, depending on the global GHG emission scenarios (MoE, 2016a). Under the high GHG emission scenario, the rise is projected to be at the rate of 1.7 cm per year, causing some 25,000 ha in the coastal zone to be permanently inundated (MoE & UNDP, 2011). Furthermore, risks of increased salinization due to sea-level rise will limit water availability for people living in the coastal areas (MoE & UNDP, 2011).

Overall, different parts of Cambodia will be affected by climate change in different ways. The coastal zone is projected to experience sea-level rise, increased salinization, and reduction of freshwater availability. The shift in natural hydrology exacerbating existing pressures on land and resource use around the Tonle Sap Lake will significantly affect biodiversity and fisheries. Changes in annual seasonal patterns will make it harder for Cambodian farmers, as this may mean changes to growing time and water availability as well as reduced productivity and fewer crop varieties. (MoE & UNDP, 2011).

3.4 Summary

Cambodia, a country in mainland Southeast Asia, shares borders with Vietnam, Thailand and Laos PDR. The annual population growth rate is 1.6%, and population is expected to reach between 20 and 24 million by 2050. Since 2015, Cambodia has become a lower middle-income country. Three-quarters of the country lies in the low-lying alluvial plain and is susceptible to flooding. Cambodia's climate is driven by tropical monsoons with six dry months and six wet months. As a tropical country, Cambodia encounters several natural disasters such as floods, droughts, storms and epidemics. Cambodia is an agrarian country. Agriculture dominates the economy, generating some 31.4% of GDP. Water resources are not only crucial for agricultural production but also the rural livelihoods of many Cambodian people. Surface water is the primary source of water supply. Irrigated agriculture is the leading consumer, followed by domestic use and industrial use.

Previous literature shows that climate change is currently affecting and will continue to affect Cambodia in a number of ways. Climate change represents a challenge to sustainable development in Cambodia and keeps many Cambodian people in poverty. In this agrarian country, many rural Cambodians depend highly on agriculture to sustain their livelihoods. Agricultural production systems in Cambodia, however, entirely rely on rainfall and annual flooding. These circumstances highlight the threatening role climate change is playing on rural people's livelihoods. Fisheries and ecosystems are also vulnerable to climate change. This degradation of natural resources has broader implications for the economic, social and political development of the country. In response to this challenge, the government has firmly committed to mitigate and find sustainable solutions to climate hazards.

Chapter 4
Methodology

4.1 Introduction

This chapter provides an overview of the study area, which includes the description of the geographical location and hydrological characteristics of the Tonle Sap system. Climate change scenarios that are the drivers of this modelling study are also included in this chapter. Presented in section 4.4 is the relevant information (sources, time series, and extraction processes of each data set) used as inputs in this modelling study. HEC-HMS, HEC-RAS, and GIS are the model engines used for simulation and computation, and the chosen methods for each software are described in section 4.5.

4.2 Study area

4.2.1 Geography

The Tonle Sap system consists of two main connected waterbodies linked to the Mekong River – Tonle Sap Lake and the Tonle Sap River (Figure 4.1). The Tonle Sap River connects to the Mekong system at the Chaktomuk confluence, near Phnom Penh, the capital city of Cambodia (Arias et al., 2014; Perera et al., 2017).

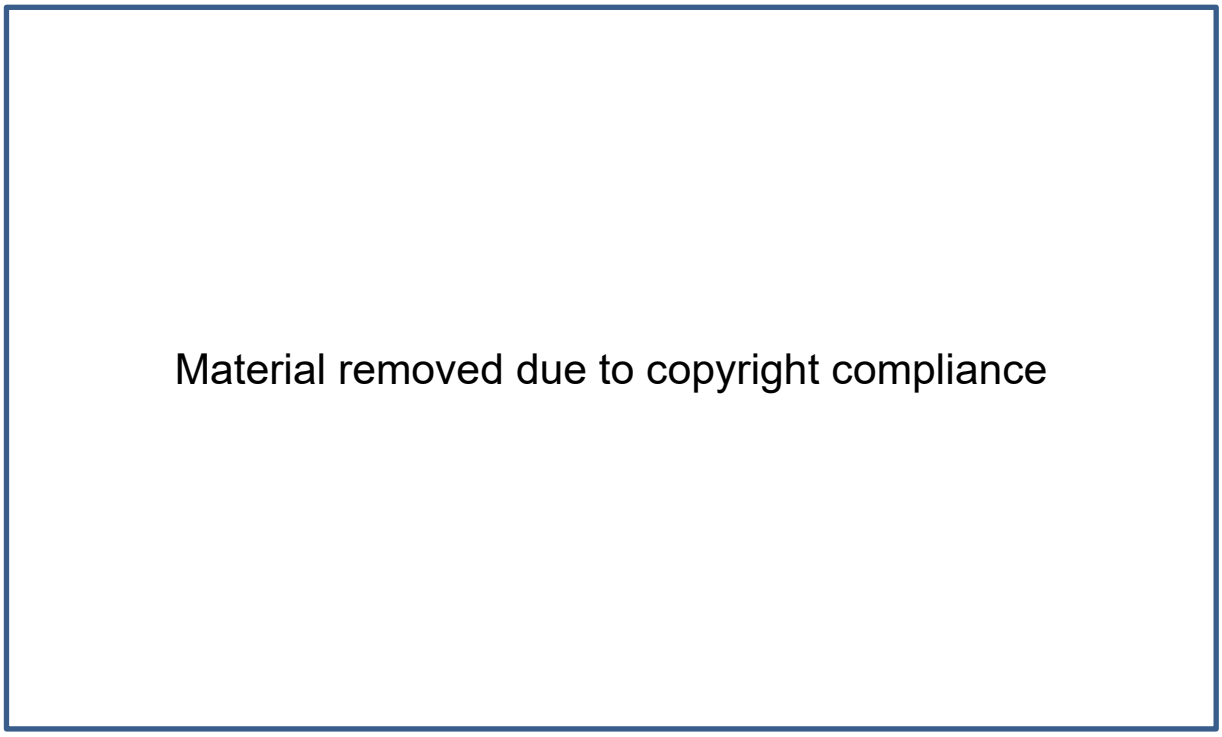

Figure 4.1 Main waterways in Cambodia.
Source: Doyle (2012)

4.2.2 Hydrology

Hydrologically, the lake is fed by 11 principal sub-basins, namely Chinit, Sen, Staung, Chikreng, Siem Reap, Sreng, Mongkol Borey, Sangker, Dauntri, Pursat, and Boribor (Figure 4.2). The Tonle Sap Basin has a total area of 85,790 km^2, which is around 47% of Cambodia's total area.

Tonle Sap Lake's hydrology is primarily driven by the monsoonal flood regime of the Mekong River. The unique reversal flow of the Tonle Sap River merits some mention. During the wet season (May to September), the Tonle Sap River reverses its flow, moving backwards into Tonle Sap Lake. This is due to water level increases in the Mekong River under a tropical monsoon climate. As the flow in the Mekong River begins to drop off at the end of the wet season, the flow of the Tonle Sap River switches back downstream (from Tonle Sap Lake into the Mekong River). In the wet season, the mean depth of the lake increases from 1 m to between 6 and 9 m while the area of the lake accordingly expands from 2,500 km^2 to 15,000 km^2. The volume also increases from less than 1.5 km^3 to between 60 and 70 km^3, depending on the year in question (MRC, 2009).

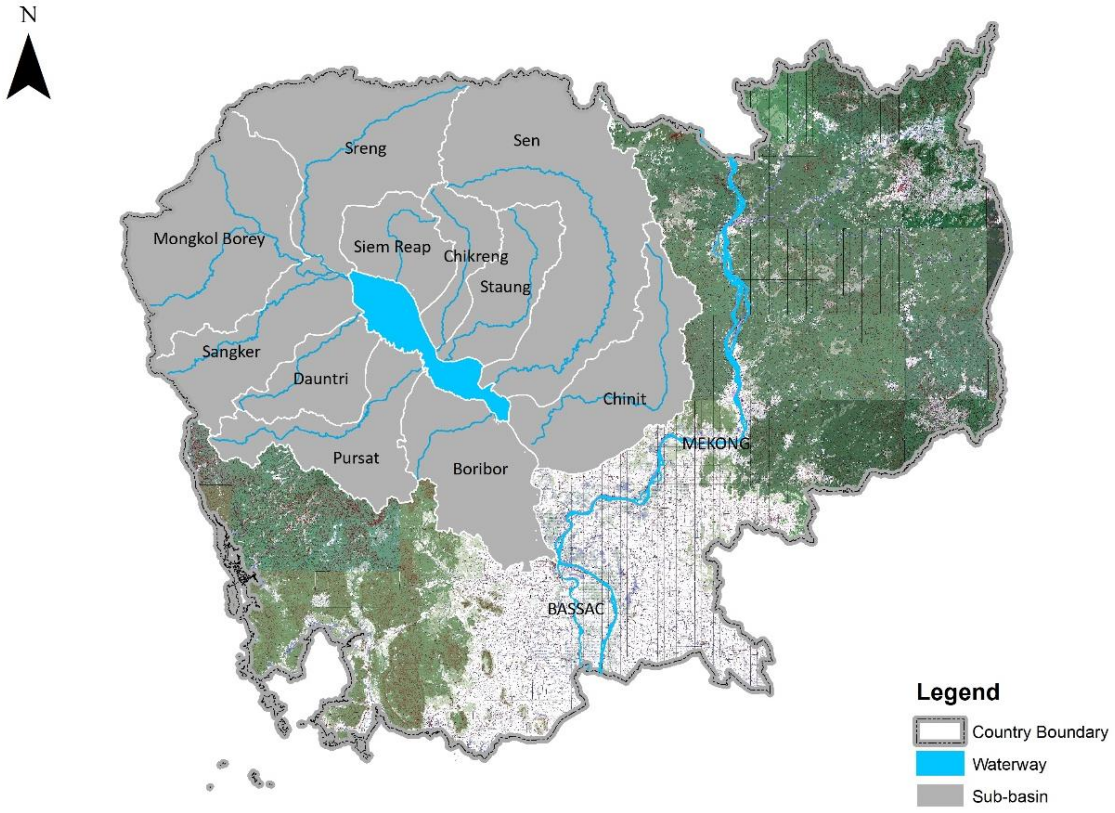

Figure 4.2 Tonle Sap Basin and its eleven principal tributaries.

A study of water balance for the Tonle Sap Lake-floodplain system by Kummu et al. (2014) determined that the annual inflow to the lake is mainly sourced from the Mekong mainstream (53.5%), both via the Tonle Sap River (50.3%) and overland flow (3.2%). Also, the tributaries of the system contribute 34%, and the rest (12.5%) is derived from precipitation. On a

monthly timescale, the Mekong shows the highest inflow from June to September while during October to January the tributaries contribute most (Figure 4.3).

The same study also assessed yearly outflow from the lake. The outflow is dominated by the discharge into the Mekong mainstream via the Tonle Sap River (84%), whereas the overland flow over the floodplain back to the Mekong mainstream constitutes only 3%. Evaporative losses are estimated to be approximately 13% (Kummu et al., 2014). On a monthly scale, the discharge into the Mekong is the dominant outflow from October to April, while during May and September the discharge and evaporation have an equal share (Figure 4.3) (Kummu et al., 2014).

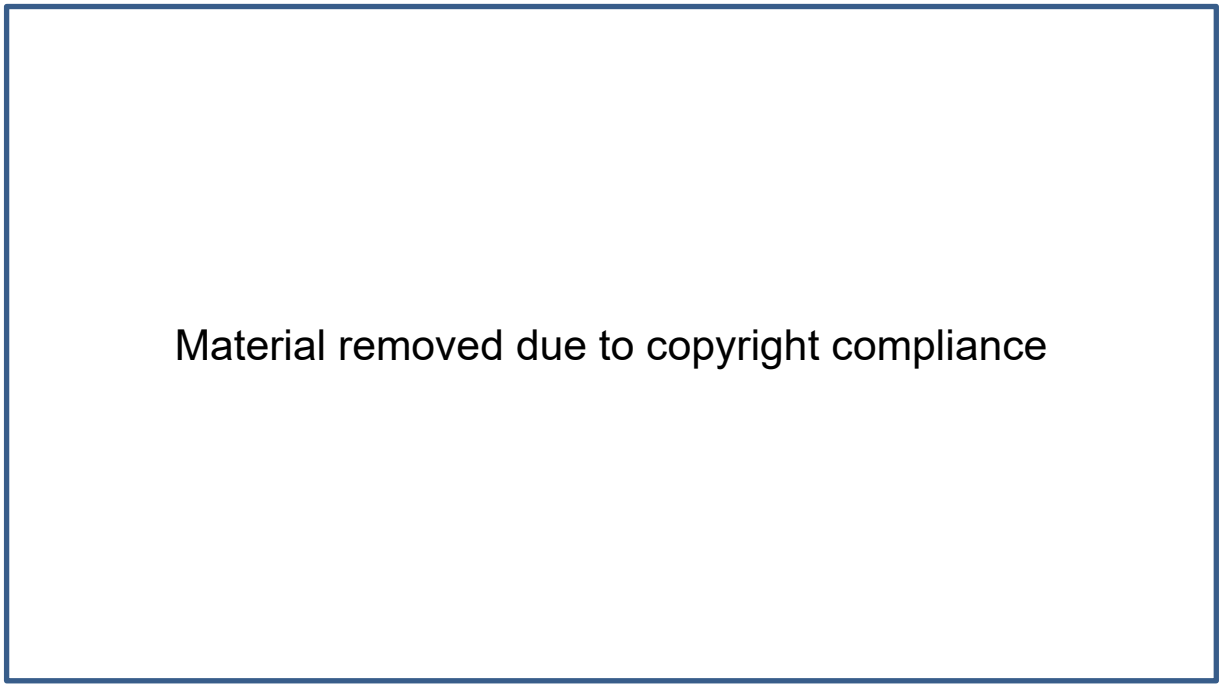

Figure 4.3 Monthly average water balance for Tonle Sap Lake.
Source: Kummu et al. (2014)

4.3 Modelling Scenarios

Despite excellent performance in economic development, Cambodia faces a number of environmental trade-offs on the other side of the equation. Over the last two decades, unsustainable economic activities, practices and management have substantially degraded the country's natural resources (WB, 2017). The pathways to achieve 2030 and 2050 visions are expected to be similar. While focusing more on economic development, Cambodia may not be able to invest much into sustaining the environment. These challenges are confirmed in the Rectangular Strategy Phase IV, which identifies that increases in natural resource utilisation, deterioration in environmental quality, limited capacity in technology and limited cooperation and participation are likely to be the key challenges for ensuring environmental sustainability (RGC, 2018).

In response to climate change, the Royal Government of Cambodia, through the Rectangular Strategy Phase IV, aims to continue to implement several environmental policies and strategic plans including the 'National REDD+ Strategy', 'National Strategic Plan on Green Growth 2013-2030', 'National Environmental Strategy and Action Plan 2016-2023', 'Cambodia Climate Change Strategic Plan 2014–2023', and to allocate social and environmental funds efficiently to ensure economic development with low-carbon emissions and resilience to climate change (RGC, 2018).

The high uncertainty in future risk analysis is often addressed by using different scenarios. The goal of working with scenarios is not to predict the future, but to better understand future uncertainties to help reach robust decisions about the future under a wide range of possible conditions (Moss et al., 2010). The scenario-based approach enables explorative study of potential impacts induced by climate change because it offers quantitative information on the uncertainty that is useful for risk assessment (Muis et al., 2015).

Taking into account the direction of economic development and political aspects mentioned above, this study will look into two RCP scenarios with respect to the Tonle Sap Basin that represent possible future pathways of climate conditions in the context of Cambodia's socioeconomic variability. From the four scenarios, one intermediate scenario – RCP4.5 – has been chosen as it best represents Cambodia's future socioeconomic and emission pathways based on the development scenarios mentioned above. On the other hand, it is prudent to study what the worst-case scenario of future climate change would bring to the basin, and thus, the RCP8.5 scenario will be applied to this modelling study.

4.4 Data Preparation

To apply the hydrologic and hydraulic models in this study, various secondary data were needed, but Cambodia is not a data-rich country. Data related to hydrology and topography (i.e., observed precipitation and discharge data and digital elevation model), are either not available or not easily obtained in a timely manner. To overcome this constraint, data from some internationally acknowledged open sources were chosen as inputs for this modelling study.

4.4.1 Shuttle Radar Topography Mission (SRTM)

A Digital Elevation Model (DEM) is a digital representation of the ground surface in raster format with a two-dimensional array of cells, where elevation value is included in each grid cell (Sharma & Tiwari, 2014). DEMs play an essential role in mapping and can be derived from many different sources, such as contour interpolation, LiDAR point clouds, optical stereo images (ASTER DEM) and radar interferometry (SRTM) (Sharma & Tiwari, 2014).

To generate a globally consistent DEM using a radar interferometer, NASA's Jet Propulsion Laboratory (JPL) collaborated with the National Geospatial Intelligence Agency (NGA) to create the Shuttle Radar Topography Mission (SRTM) (Rodríguez et al., 2006). SRTM consisted of a specifically modified Synthetic Aperture Radar (SAR) system that flew onboard the Space Shuttle Endeavour, which was launched into space on 11 February 2000 (Anirudh & Giridhar, 2015). For more than a decade, the near-global DEMs extracted from SRTM have been exploited for a range of applications including research studies in hydrology, geomorphology, seismology, volcanology, glaciology, and forest ecology (Boncori, 2016).

This study employed the DEM derived from SRTM version 4 at 90 metres resolution. In order to get a full picture of the study area, two SRTM files (102.5°N, 12.5°E; 107.5°N, 12.5°E) were downloaded and merged using GIS to produce a basin-wide elevation layer (Figure 4.4).

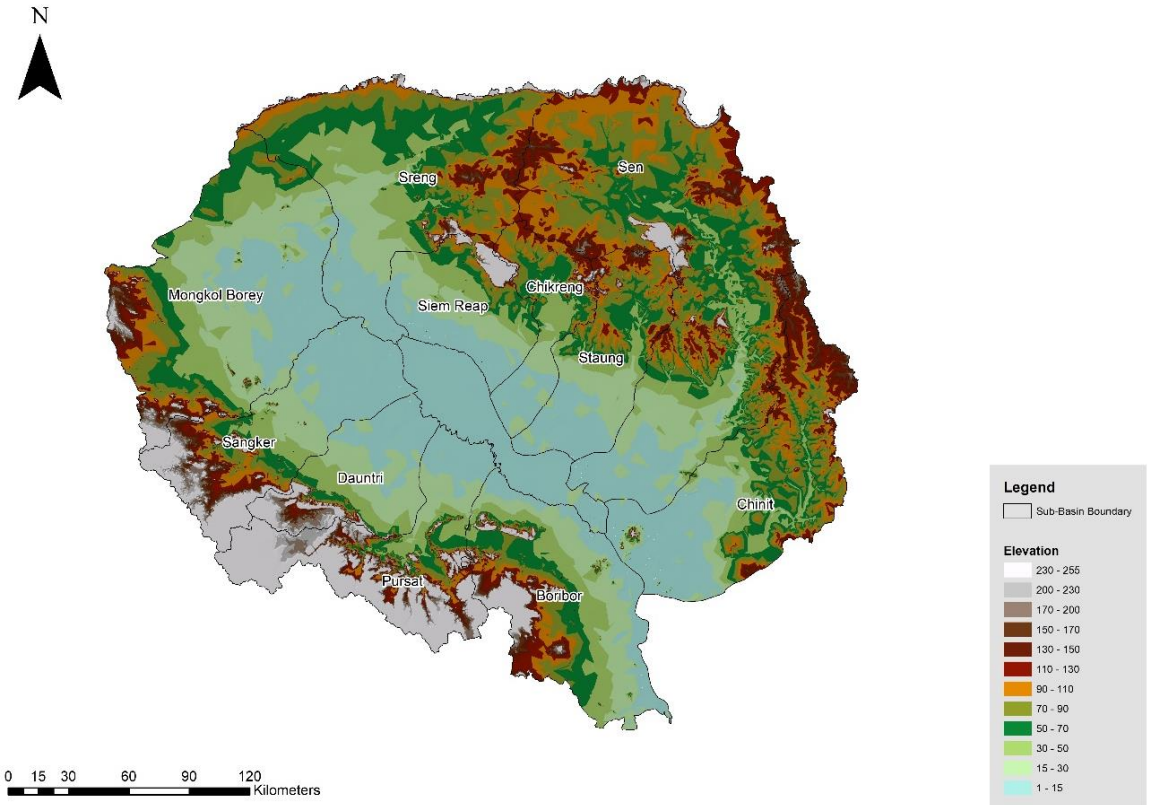

Figure 4.4 Digital Elevation Model of the Tonle Sap Basin.

4.4.2 Tropical Rainfall Measuring Mission (TRMM)

Hydrological simulation of large-scale river basins generally requires a considerable amount of meteorological data. However, in some areas, the available rain gauge stations may be sparse, their distribution does not cover the whole watershed, and often the quality of historical measurement data can be questioned. Many river basins in the 'Monsoon Asia' region, including the Mekong River Basin (excluding the areas in Thailand), suffer from poor availability of rainfall data (Lauri et al., 2014).

Despite being subjected to a variable range of errors depending on the use of the sensor, satellite data are advantageous for hydrological modelling of large river basins (Quirino et al., 2017). For the last few decades, the application of datasets derived from satellite products has been increasing due to their extensive spatiotemporal coverage, promising results, relative ease of use as input data for modelling in the areas where observed data are inadequate or not available, and the fact that many are free of charge and publicly available (Lauri et al., 2014; Tan & Duan, 2017).

The NASA Tropical Rainfall Measuring Mission (TRMM) is a US–Japan joint space mission to provide a comprehensive and detailed dataset of rainfall distribution and latent heating over tropical and subtropical continents and oceans (40°S–40°N). Launched on 27 November 1997, TRMM has become a significant data source for hydrological, meteorological and other research activities throughout the globe (Liu et al., 2012).

The TRMM data products are classified into three categories, namely the orbital products, gridded products and other TRMM-related products. The standard gridded products are averaged spatially (0.25° × 0.25° to 5° × 5°) and temporally (hourly to monthly) (Table 4.1).

Despite the unsatisfying result yielded in the study of Huang et al. (2014), suggesting that a relatively large deviation of the temporal variation of rainfall is present in TRMM 3B42 version 7, a considerable amount of existing research suggests that this product can be used for the simulation of large river basins with satisfying results. Lauri et al. (2014) evaluated the accuracy of four satellite datasets over the Mekong River Basin and recognised that TRMM 3B42 version 7 performed well in comparison with similar products of its kind with Nash–Sutcliffe Efficiency (NSE)[1] values exceeding 0.88 in all stations and average NSE of 0.932. Quirino et al. (2017) also suggested that higher reliability was seen in TRMM 3B42 version 7 over a study area in Brazil. Sahoo et al. (2015) highlighted similar quality findings when applying TRMM 3B42 version 7 to assess large-scale meteorological drought globally.

[1] Nash–Sutcliffe efficiency (NSE) is the normalized statistic that compare predicted variance and observed variance. The value of NSE ranges from negative infinity to 1. High positive values of NSE indicate better model simulation (Oeurng et al., 2019).

Table 4.1 Standard TRMM gridded data products.

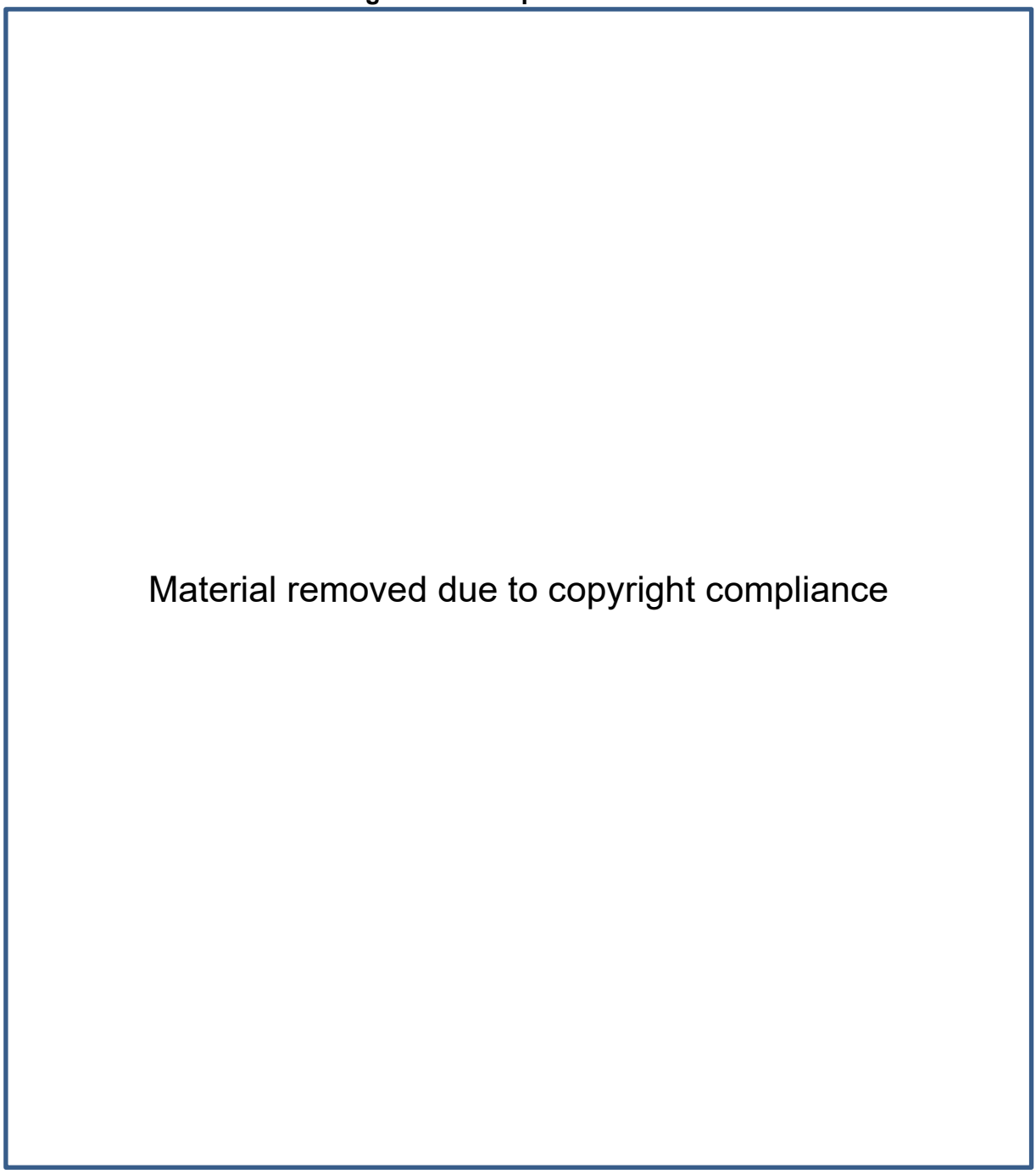

Source: Liu et al. (2012)

In this study, TRMM 3B42 Daily 0.25° × 0.25° data were employed, owing to their higher spatial resolution and suitable time scale. Earthdata's distribution, Mirador, offers raw data in netCDF format for daily rainfall. A raster layer was displayed from the netCDF file using Multidimensional Tools in GIS (Figure 4.6). Daily rainfall data were extracted from the output raster layer based on the rain gauge points (summarised in Table 4.2 and shown in Figure 4.5) by using Extract Multi Values to Points in Spatial Analyst Tools in ArcGIS. As one single file contains precipitation data of one day, 5844 files were downloaded, and each file was processed separately in ArcGIS (Figure 4.7) to extract daily rainfall data from 01 January 2000 to 31 December 2015.

Table 4.2 Location coordinates of each rain gauge.

No	Sub-basin	Rain Gauge	X	Y
1	Chhinit	Santuk	505220	1388954
2	Sen	Kampong Thom	488838	1402335
3	Staung	Staung	452924	1433440
4	Chikreng	Chikreng	427570	1451985
5	Siem Reap	Siem Reap	378354	1477782
6	Sreng	Oddar Meanchey	339661	1568911
7	Mongol Borey	Banteay Meanchey	279560	1505395
8	Sangker	Battambong	306355	1447803
9	Dauntri	Maung Russey	331281	1413040
10	Pursat	Pursat	381819	1386972
11	Boribor	Rolea B'ier	451852	1352125

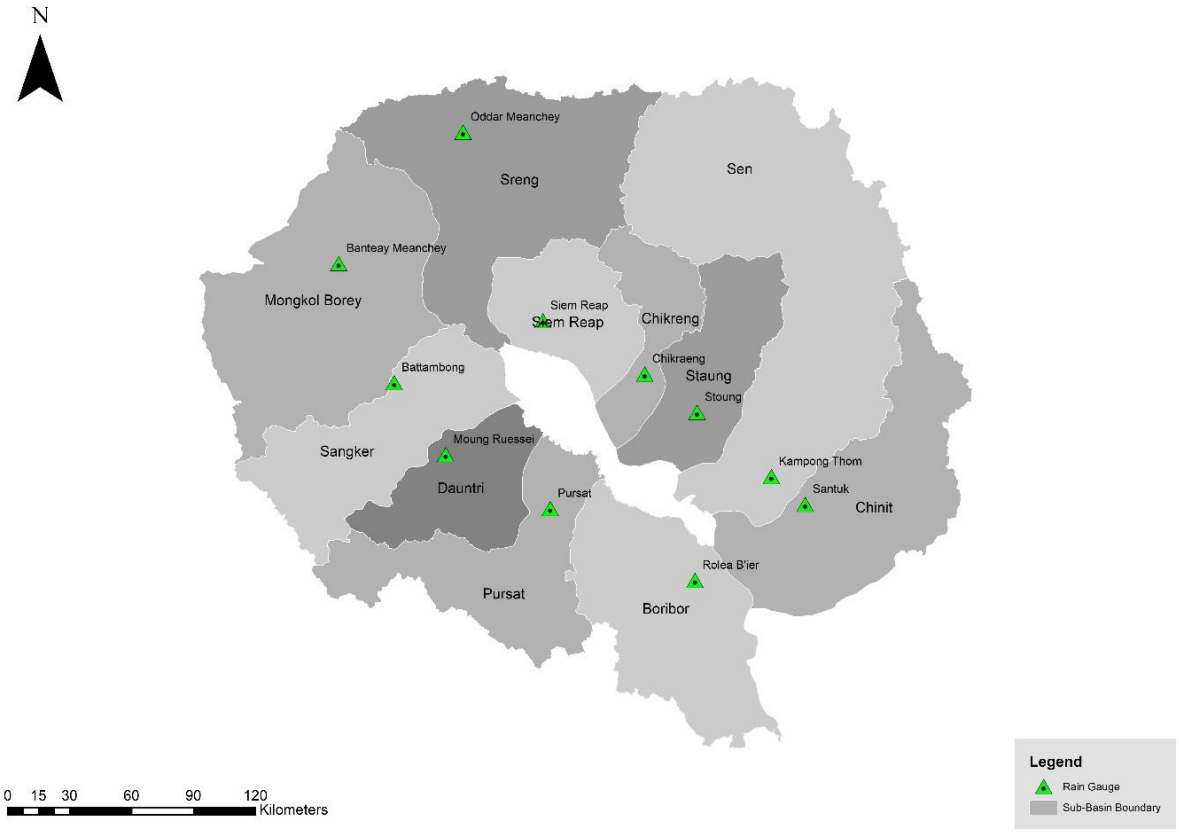

Figure 4.5 Location of rain gauge for each sub-basin of Tonle Sap Basin.

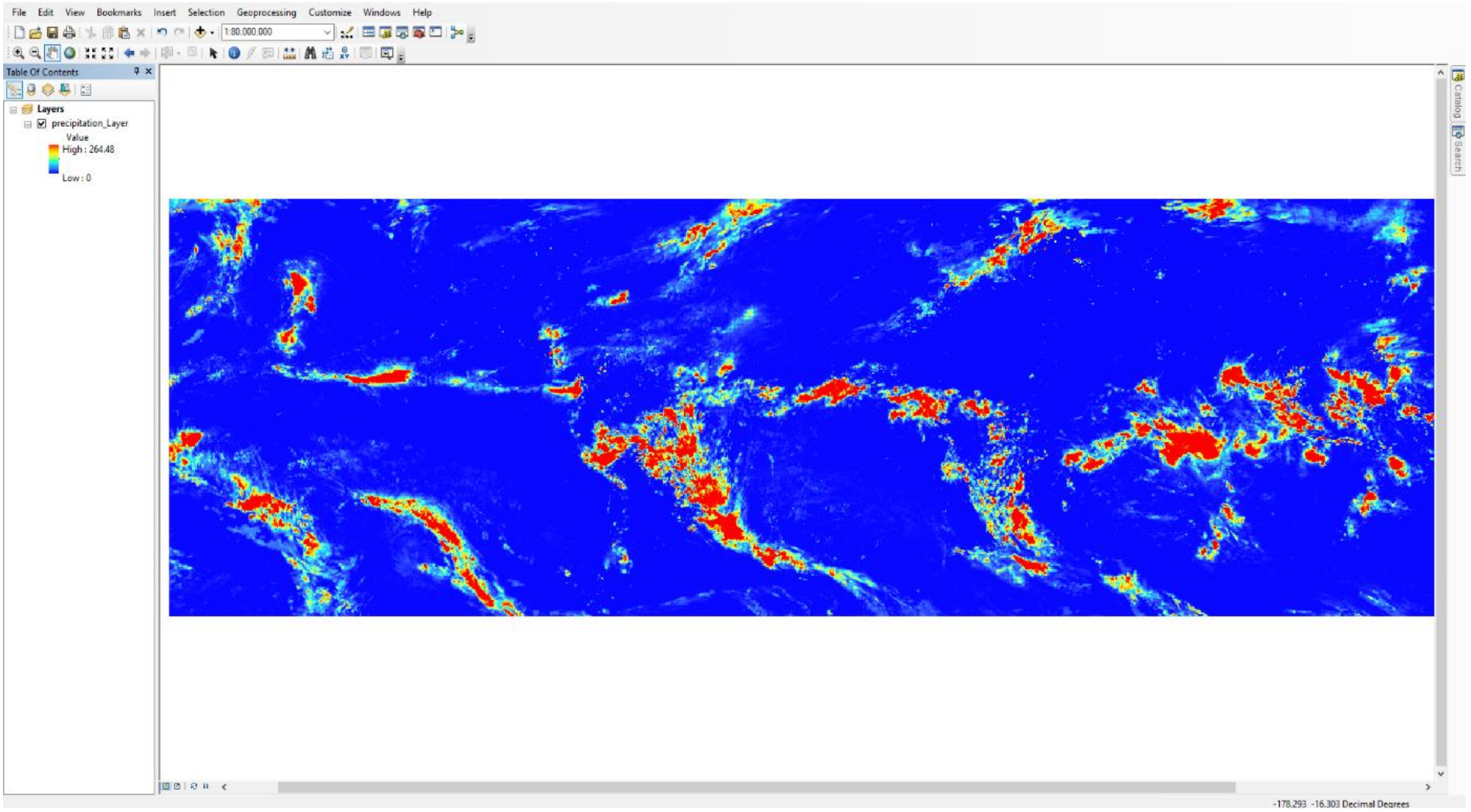

Figure 4.6 The display of raster layer in netCDF file in ArcGIS.

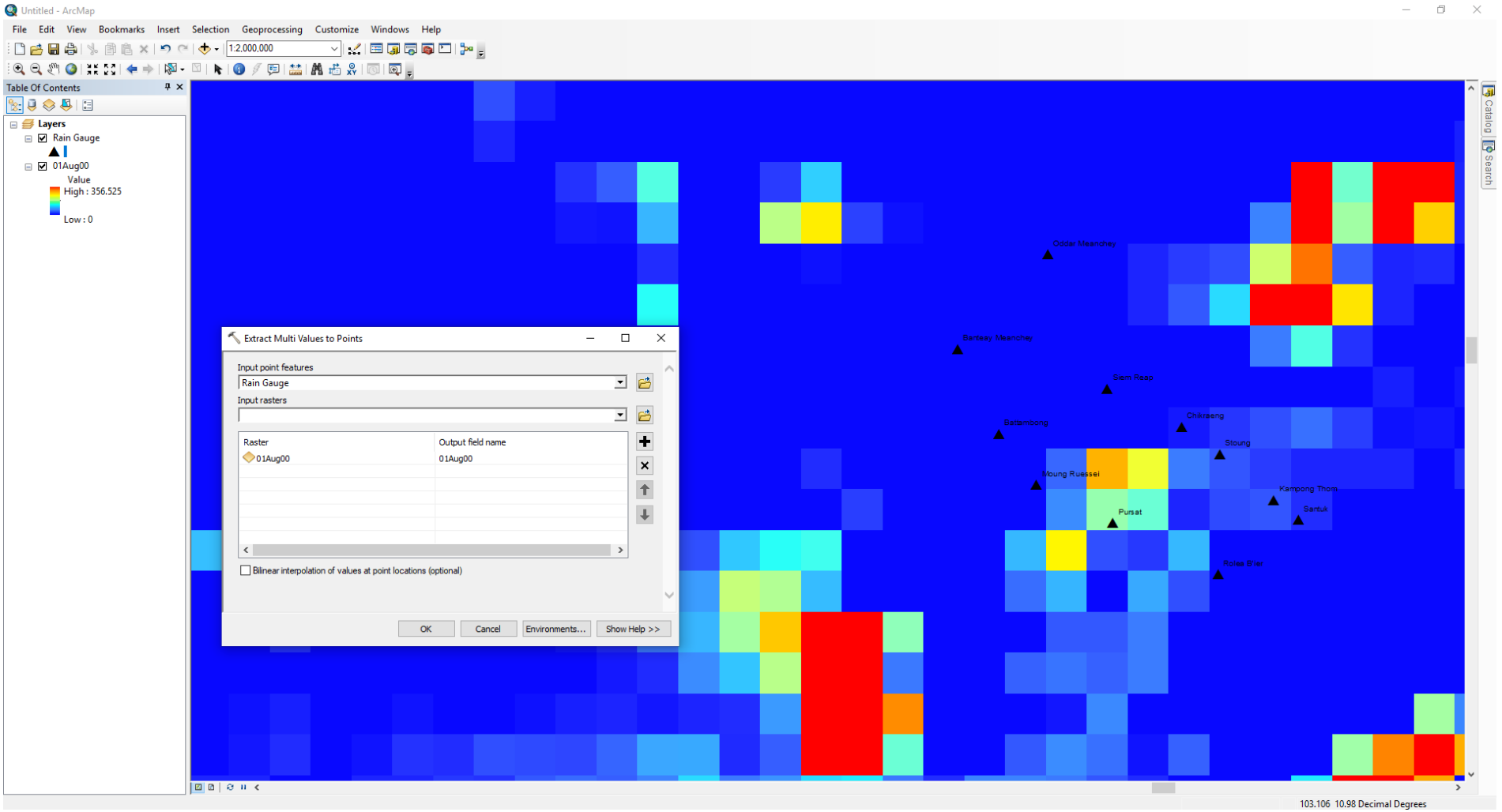

Figure 4.7 Precipitation data extraction using Extract Multi Values to Points function in ArcGIS.

4.4.3 Land cover data

In 2010, the Mekong River Commission (MRC) published land cover maps for the Mekong River Basin. Fifty-seven time-series Landsat 5 Thematic Mapper images for four member countries (Cambodia, Laos, Thailand, and Vietnam) and field surveys at 9,357 points in 703 areas across the basin were conducted for ground-truthing to build this map. This land cover dataset covers both wet and dry periods in 2010. Based on characteristic features of elevation and topography, the Mekong River Basin has been classified into seven distinct biogeographical zones and is categorised into 19 types of single-class land cover based on the FAO Land Cover Classification System version 3. In 2016, the dataset was updated (MRC, 2016).

Land cover used in this study is derived from the MRC Land Cover 2010, the latest version. According to MRC's Technical Report No.59 which was produced to support the land cover dataset, Tonle Sap Basin extends over Lowlands and Southern Uplands zones. Out of the 19 land classes, Tonle Sap Basin covers 16 land classes (Figure 4.8 and Table 4.3).

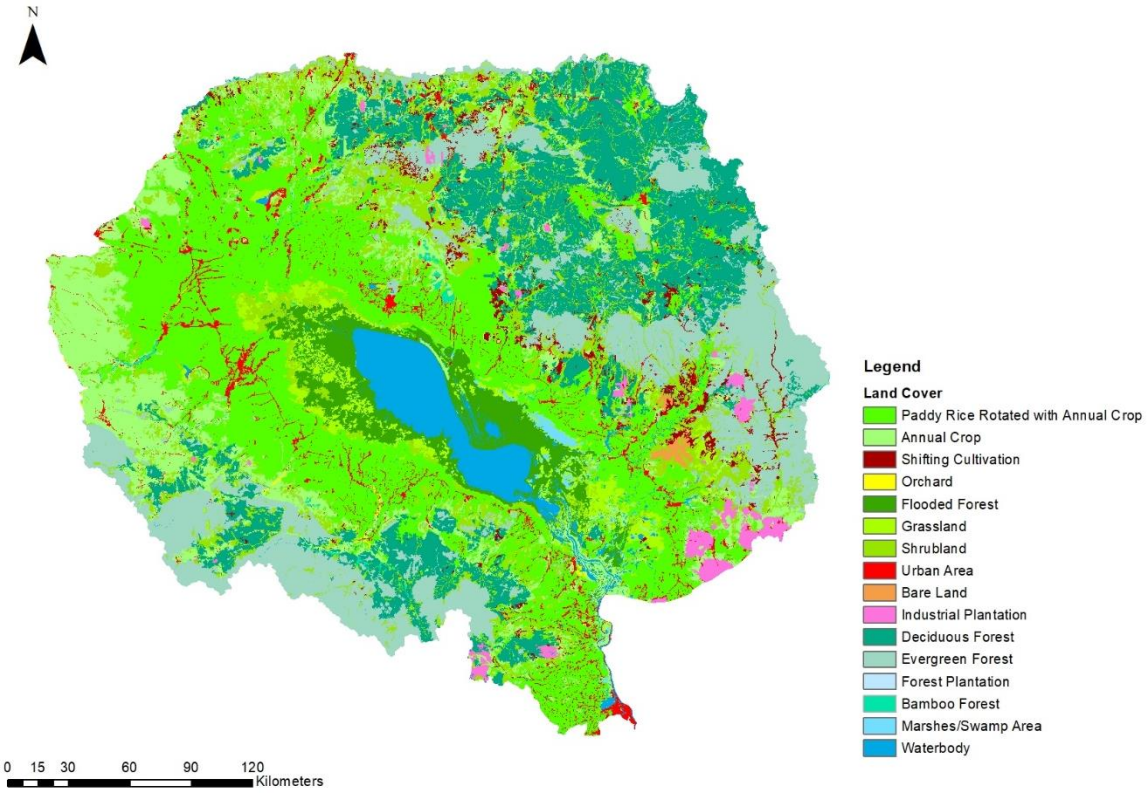

Figure 4.8 Types of land cover in Tonle Sap Basin.

Table 4.3 Area and Percentage of each Land Cover Type in Tonle Sap Basin.

No	Land Cover Type	Area (km^2)	Percentage (%)
1	Paddy Rice Rotated with Annual Crop	22583.35	27.66
2	Annual Crop	9537.52	11.68
3	Shifting Cultivation	1397.38	1.71
4	Orchard	87.37	0.11
5	Flooded Forest	3527.06	4.32
6	Grassland	2168.99	2.66
7	Shrubland	8620.19	10.56
8	Urban Area	2314.48	2.84
9	Bare Land	166.35	0.20
10	Industrial Plantation	985.08	1.21
11	Deciduous Forest	13187.19	16.15
12	Evergreen Forest	13123.41	16.08
13	Forest Plantation	0.82	0.00
14	Bamboo Forest	196.13	0.24
15	Marshes/Swamp Area	337.95	0.41
16	Waterbody	3402.47	4.17

4.4.4 Climate change data

The MRC Data Portal (www.portal.mrcmekong.org/interactive-climate-change-atlas) offers readily available data for projected climate change throughout the Mekong River Basin. The data provided are for projected precipitation and temperature from 2010 to 2100 on a yearly basis with four emission scenarios (RCP 2.6, RCP 4.5, RCP 6.0 and RCP 8.5) and three types of General Circulation Model (GCM), namely GFDL-CM3, GISS-E2-R-CC, and IPSL-CM5A-MR, with spatial resolution of 1 × 1 km.

The data for these future projected scenarios offered by MRC Data Portal were generated using SimCLIM. SimCLIM is a New Zealand-made software modelling system developed by the International Global Change Institution (IGCI) for investigating the impacts of and adaptations to climate change and variability. The software was initially built in 1993 for a New Zealand model called CLIMPACTS (Warrick et al., 2005). SimCLIM has been developed to project different climate variables for temporal and spatial scales based on statistical downscaling methods. It is incorporated with 40 GCMs retrieved from the Coupled Model Inter Comparison Project, Phase 5 (CMIP5) and Earth System Grid (ESG) for global climate projection. For more realistic future projection, SimCLIM is supported by different emission scenarios used by the AR5 of IPCC (Amin et al., 2017). Table 4.5 provides a summary of all datasets and their relevant information.

Table 4.4 List of datasets used in this modelling study.

No.	Dataset	Source	Time Series
1	Historical Rainfall	Earth Data	2000–2015
2	Observed Discharge	Kummu et al. (2014)	2000–2012
3	Projected Rainfall	MRC	2030
4	Land Cover	MRC	2010
5	DEM	Earth Data	-

4.5 Methods

This study followed the approach as presented in Figure 4.9 in which three main processes were identified, namely (A) Rainfall-runoff model; (B) Flooded areas mapping; and (C) Flood recession paddy rice areas mapping.

First, observed rainfall and discharge and the DEM were used as inputs for hydrologic software HEC-HMS to calibrate the rainfall-runoff model. Once the model was calibrated and validated, the parameters of the model were used with the projected rainfall for the year 2030 based on three GCMs (GFDL-CM3, GISS-E2-R-CC, and IPSL-CM5A-MR) and two RCPs (RCP4.5 and RCP8.5) to generate projected discharges for the year 2030 of the 11 principal rivers that feed Tonle Sap Lake. This projected discharge is the output for objective 1.

Objective 2 was computed using hydraulic software HEC-RAS. Observed discharge, observed water level and the DEM were used to build a 2D unsteady flow hydraulic model. After calibration and validation, projected discharge from objective 1 was used as input to the model. The result is the projected floodplain for the year 2030.

GIS is the model engine for objective 3. The output from objective 2 along with Land Cover was used in GIS to assess the changes in paddy rice areas by the year 2030.

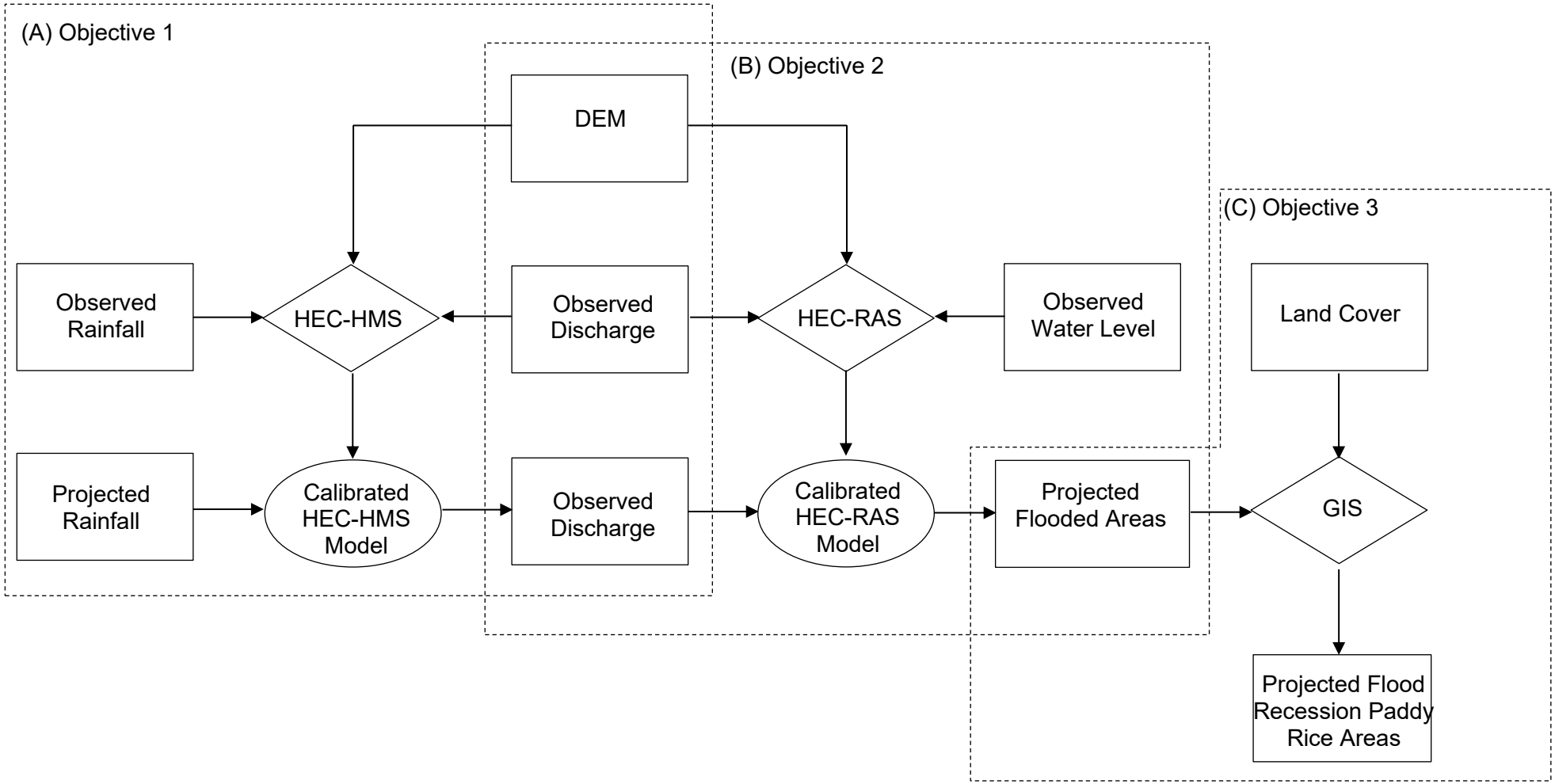

Figure 4.9 General framework used in this study.

4.5.1 Hydrologic Engineering Centre – Hydrologic Modelling System (HEC-HMS)

Runoff in this study was modelled using HEC-HMS, version 4.3. HEC-HMS was developed by the US Army Corps of Engineers (US ACE) in 1998 (Zema et al., 2017). The program has been used and tested worldwide. The model is mainly designed to simulate the rainfall-runoff processes of dendritic basin systems to solve hydrological problems for a wide range of geographic areas ranging from small urban catchments to large river basins (US ACE, 2016a). HEC-HMS, a semi-distributed hydrological model, takes into account all relevant hydrologic processes such as surface runoff, evaporation, infiltration and groundwater recharge (Ali et al., 2011).

The software has an extensive array of capabilities to conduct hydrological simulation, analyse simulations, forecast future flows, analyse water quality and sediment and connect to GIS (US ACE, 2016a). Users are able to prepare spatial data in a GIS platform before directly importing into HEC-HMS (Ali et al., 2011). HEC-HMS can be used to model a single watershed or multiple hydrologically connected watersheds (Abushandi & Merkel, 2013).

The system encompasses losses, runoff transform, analysis of meteorological data, open channel routing, rainfall-runoff simulation, and parameter estimation. Hydrological components are connected in a network to represent a rainfall-runoff process. Available components are sub-basin, source, sink, reach, junction, reservoir and diversion. Computation begins from the upstream elements and proceeds to the downstream ones (Teng et al., 2018). For rainfall-runoff simulation, HEC-HMS uses a number of individual models to represent each component of the runoff process such as models that compute runoff volume, models of baseflow and models of direct runoff. Each model run is a combination of a basin model, meteorological model, and control specifications. Physical datasets describing the watershed properties are stored in the basin model while precipitation, evapotranspiration and snowmelt data necessary for simulating watershed processes are stored in the meteorological model. Six different synthetic and historical precipitation methods, two evapotranspiration methods, and one snowmelt method are included. The control specifications control the time span of simulation including the time step of the simulation run, start date and time, and end date and time (Abushandi & Merkel, 2013; Verma et al., 2010). A detailed description of all the components in HEC-HMS can be found in the HEC-HMS user's manual (US ACE, 2016a).

Basin model

The 90-m resolution DEM obtained from SRTM was projected into the UTM Zone 48 coordinate system. The entire basin was disaggregated into 11 interconnected sub-basins surrounding the Tonle Sap Lake. Geographical features of each sub-basin are summarised in Table 4.5. The shapefile was imported into HEC-HMS and a basin model consisting of one sub-basin and one sink at the outlet was created (Figure 4.10).

Table 4.5 Geographical features of each sub-basin.

No	Sub-basin	Area (km^2)	Mean Elevation (m)
1	Chinit	8,236	60.93
2	Sen	16,344	78.79
3	Staung	4,357	52.58
4	Chikreng	2,713	59.75
5	Siem Reap	3,619	47.26
6	Sreng	9,932	62.67
7	Mongkol Borey	10,858	50.07
8	Sangker	6,052	86.01
9	Dauntri	3,695	63.03
10	Pursat	5,964	155.49
11	Boribor	7,153	69.00

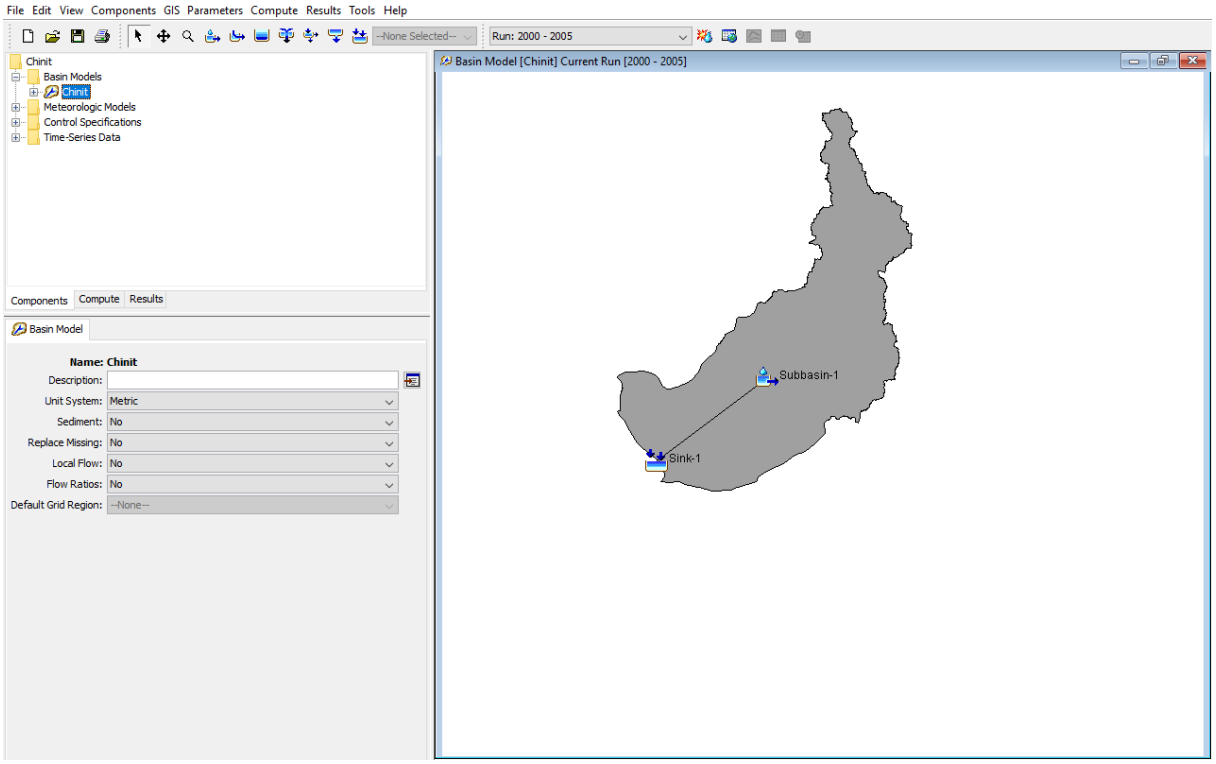

Figure 4.10 Basin Model of one sub-basin in HEC-HMS.

Meteorological model

Precipitation input is computed by the meteorological model. Both gridded and point precipitation data can be used in the meteorological model. Point precipitation data were employed in this particular study. There are 11 rain gauges throughout the study area, one for each sub-basin.

Time series data

Time series data for each rain gauge and discharge gauge were manually entered into the model. Precipitation data from 2000 to 2005 were derived from TRMM while discharge data from 2000 to 2005 were obtained from Kummu et al. (2014), based on rating curves (Table 4.6) developed from observed water levels for each station. Location of each water level measurement used for development of rating curves is shown in Figure 4.11.

Table 4.6 Rating curves for Tonle Sap's tributaries discharges.

No	Sub-basin	Rating curve
1	Chhinit	$Q = 15.49 – 36.8088xH_{KgTmar} + 36.3032xH_{KgTmar}^2 – 8.5957xH_{KgTmar}^3 + 0.7869 \times H_{KgTmar}^4$
2	Sen	$Q = 0.000013 \times (H_{KgThom} – 1.21)^{6.8178} \times F^{0.72}$, where $F = H_{KgThom} – H_{KgLuong}$
3	Staung	$Q = 0.8554 \times H_{KgChen}^{2.7794} \times F^{0.5}$, where $F = H_{KgChen} – H_{KgLuong} + 7.0$
4	Chikreng	$Q = 0.1017 \times H_{KgKdey}^{3.3034} \times F^{0.5}$, where $F = H_{KgKdey} – H_{KgLuong} + 7.0$
5	Siem Reap	$Q = 4.1059 \times (H_{UntacBridge} – 0.0936)^2$
6	Sreng	$Q = 0.01299 \times H_{Kralanh}^{4.3665} \times F^{0.5}$, where $F = H_{Kralanh} – H_{BakPrea} + 4.0$
7	Mongol Borey	$Q = y \times (F + 6.09)^{0.69}$ $y = –0.5665 + 2.212 \times H_{MongolBorey} – 0.8243 \times H_{MongolBorey}^2 – 0.1796 \times H_{MongolBorey}^3$ $F = H_{MongolBorey} – H_{BakPrea} + 6.0$
8	Sangker	$Q = y \times (F + 0.3)^{0.18}$ $y = –28.2541 + 33.8995 \times H_{Battambang} – 9.5551 \times H_{Battambang}^2 – 0.8092 \times H_{Battambang}^3$ $F = H_{MongolBorey} – H_{BakPrea}$
9	Dauntri	$Q = 12.4 \times (H_{MaungRussey} – 1.2439)^2$
10	Pursat	$Q = 25.5 \times (H_{BakTrakuon} – 0.0856)^2$
11	Boribor	$Q = 37.1593 \times H_{Baribor}^{1.6195}$

Source: Kummu et al. (2014)

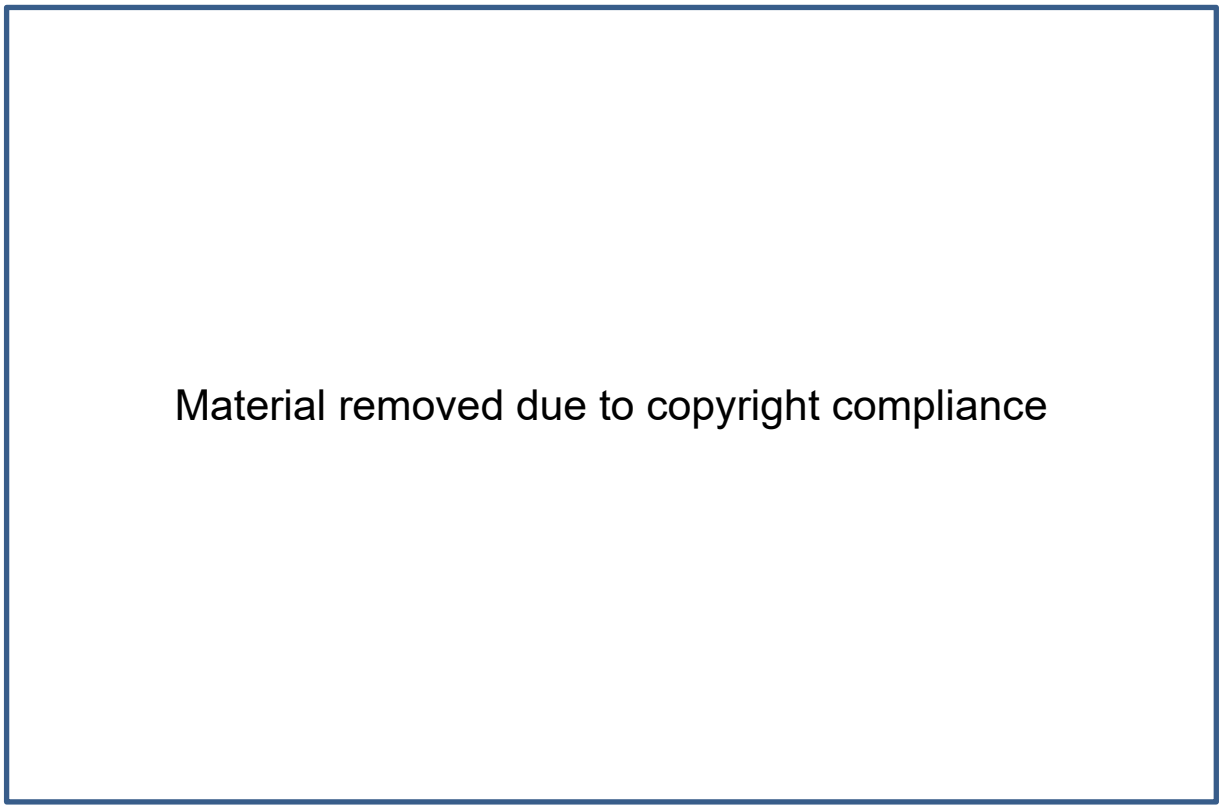

Figure 4.11 Location of each water level measurement (dark triangle) used in rating curve to calculate discharge of each tributary.
Source: Kummu et al. (2014)

Methods

Transform Method

In HEC-HMS, the sub-basin element conceptually represents infiltration, surface runoff, and subsurface processes interacting together. Rainfall excess is calculated into an actual surface runoff by transform method contained within the sub-basin (US ACE, 2016a). HEC-HMS 4.3 offers a total of seven different transform methods including unit hydrograph methods, a linear quasi-distributed method and a kinematic wave implementation. However, some of these methods are not suitable for ungauged basins, as they require more inputs that are not available (Halwatura & Najim, 2013). In this study, the 'Soil Conservation Service – Unit Hydrograph (SCS-UH)' method was selected as it requires only the input of lag time. Also, a previous study by Jin et al. (2015) reported good results from using SCS-UH for direct runoff in basin hydrological modelling.

In SCS-UH, the standard unit hydrograph is defined with 37.5% of unit runoff occurring before the peak flow. This definition agrees with a peak rate factor (PRF) of 484 that incorporates the percentage of unit runoff before the peak, calculated total time base, and unit conversions when applying the equations within the US customary unit system (US ACE, 2016a). Though the percentage of unit runoff occurring before the peak flow may not be uniform across all watersheds due to flow length, ground slope, and other properties of the watershed, HEC-HMS offers the default unit hydrograph with a PRF of 484 (US ACE,

2016a). This study used this default unit hydrograph contained in this transform method to calculate direct surface runoff.

Loss Method

In HEC-HMS, actual infiltration is calculated using a loss method contained within the sub-basin. A total of eleven loss methods are provided in HEC-HMS 4.3. Some of them are designed primarily for continuous simulation, while others are for simulating events (US ACE, 2016a). In this study, the 'Initial and Constant Loss' method was employed. This method is a very simple one and suitable for watersheds that lack detailed soil information (US ACE, 2016a). Only the initial loss, constant rate and percentage of impervious surface for a sub-basin are required. This percentage of impervious surface was calculated for each sub-basin from GIS using MRC Land Cover data.

Baseflow Method

In HEC-HMS, the actual subsurface calculation is computed by baseflow methods contained within the sub-basin. Five different baseflow methods designed for both events and continuous simulation are offered in HEC-HMS 4.3 (US ACE, 2016a). In this study, the 'Recession Baseflow' method was used. Though this method is designed primarily for event simulation, it does have the function to automatically reset after each event, which makes it applicable to also be used for continuous simulation (US ACE, 2016a). Initial discharge and recession constant values are required.

Calibration and validation

Daily discharge output for 2000–2005 from the model was calibrated with observed discharge based on rating curves developed from water levels by Kummu et al. (2014). The option of optimisation in HEC-HMS was used to calibrate the model. To compare a computed hydrograph to an observed hydrograph, HEC-HMS calculates the index of the goodness-of-fit. Algorithms are included in the search method for the model parameters to yield the best value of an index known as objective function (Ali et al., 2011). The objective function measures the goodness-of-fit between the simulated and observed discharge at a selected element (US ACE, 2016a). The daily flows from 2006 to 2007 were used for validation of the model. The performance of the model was assessed graphically and by Nash–Sutcliffe efficiency (NSE) and the coefficient of determination (R^2).

$$NSE = 1 - \frac{\sum_{i=1}^{n}(O_i - S_i)^2}{\sum_{t=1}^{T}(O_i - \bar{O})^2} \quad (1)$$

$$R^2 = \frac{\sum_{i=1}^{n}(O_i - \bar{O})(S_i - \bar{S})}{[\sum_{i=1}^{n}(O_i - \bar{O})^2]^{0.5}[\sum_{i=1}^{n}(S_i - \bar{S})^2]^{0.5}} \quad (2)$$

where *n* is the total number of observations, O_i and S_i are observed and simulated discharge or water level values at a given time step, and $\bar{Q}$ and $\bar{S}$ are the mean observed and simulated values, respectively.

Distribution of projected rainfall

Once the models for all sub-basins had been calibrated and validated, they were used for simulating the runoff for projected rainfall for the year 2030. The datasets for projected precipitation for 2030 were derived from MRC's Climate Change Adaptation. Data were in yearly format. HEC-HMS, on the other hand, requires daily, if not hourly, rainfall data to run the models. The solution was then found by using previous rainfall data for the past 16 years (2000–2015) to infer daily rainfall patterns. The averaging method, nonetheless, does not work because it increases the number of rainy days in a year and decreases the amount of maximum rainfall per day. The best possible alternative option was to distribute the amount of daily rainfall based on the pattern of the year closest to average. First, the number of rainy days within each year (2000–2015) were counted, and the mean of rainy days was calculated. So, the year with the number of rainy days closest to the mean was chosen, and the daily rainfall for 2030 was distributed based on the pattern of that selected year. For example, the average of rainy days for the Pursat rain gauge from 2000 to 2015 is 145 days, and the year 2015 has the closest number of rainy days to this average. So the rainfall pattern for the year 2030 for the Pursat rain gauge was distributed following the pattern of the year 2015. (For the number of rainy days for each rain gauge, see Appendix A.)

4.5.2 Hydrologic Engineering Centre – River Analysis System (HEC-RAS)

HEC-RAS, another piece of hydraulic software developed by the US Army Corps of Engineers, is an integrated system of software, comprising four main modules for river analysis components such as steady flow computation, unsteady flow simulation, sediment transportation computations, and water quality analysis (US ACE, 2016c). The system is designed to make multitasking interaction possible in a multiuser network environment. A graphical user interface (GUI), separate analysis components, data storage and management capabilities, graphics and reporting facilities are all contained in the HEC-RAS system (US ACE, 2016a).

The selected software for the modelling effort is HEC-RAS version 5.0.7. This software was initially developed as a one-dimensional (1D), steady flow hydraulic modelling software package. The later version has the capacity to model unsteady flow, sediment modelling and two-dimensional (2D) flow (US ACE, 2018). The software has been reported to be extensively used due to its compatibility with GIS in creating river geometries, its robust

methods in analysis, and time-saving advantages for simulation (Bhat et al., 2019; Ly et al., 2018; Mohktar et al., 2018).

Method

The hydraulic model in this study is 2D Unsteady Flow. Given the unique seasonal flow reversals of the Mekong River into and out of the flow area, running an unsteady flow model in this situation is more suitable than a steady flow. The geographical features of the study area are wide and flat. Flows enter from multiple directions and go out in multiple flow paths, generating various water surface elevations and velocities in multiple directions. Taking into account all these situations, 2D unsteady flow is highly recommended by the HEC-RAS User's Manual (US ACE, 2016b).

The quality of the hydraulics model can be limited by the quality of terrain data created, making it essential to have a detailed terrain model (US ACE, 2016b). A terrain model can be created in the add-on feature, RAS Mapper. Terrain data such as floating-point grid format (*.flt), ESRI grid files, GeoTIFF (*tif) and other formats like USGS DEM file can be imported to RAS Mapper to create a terrain model (US ACE, 2016b). In this study, a DEM cell size 12.5 m × 12.5 m in GeoTIFF (*.tif) format was loaded into RAS Mapper to create a terrain model as shown in Figure 4.12.

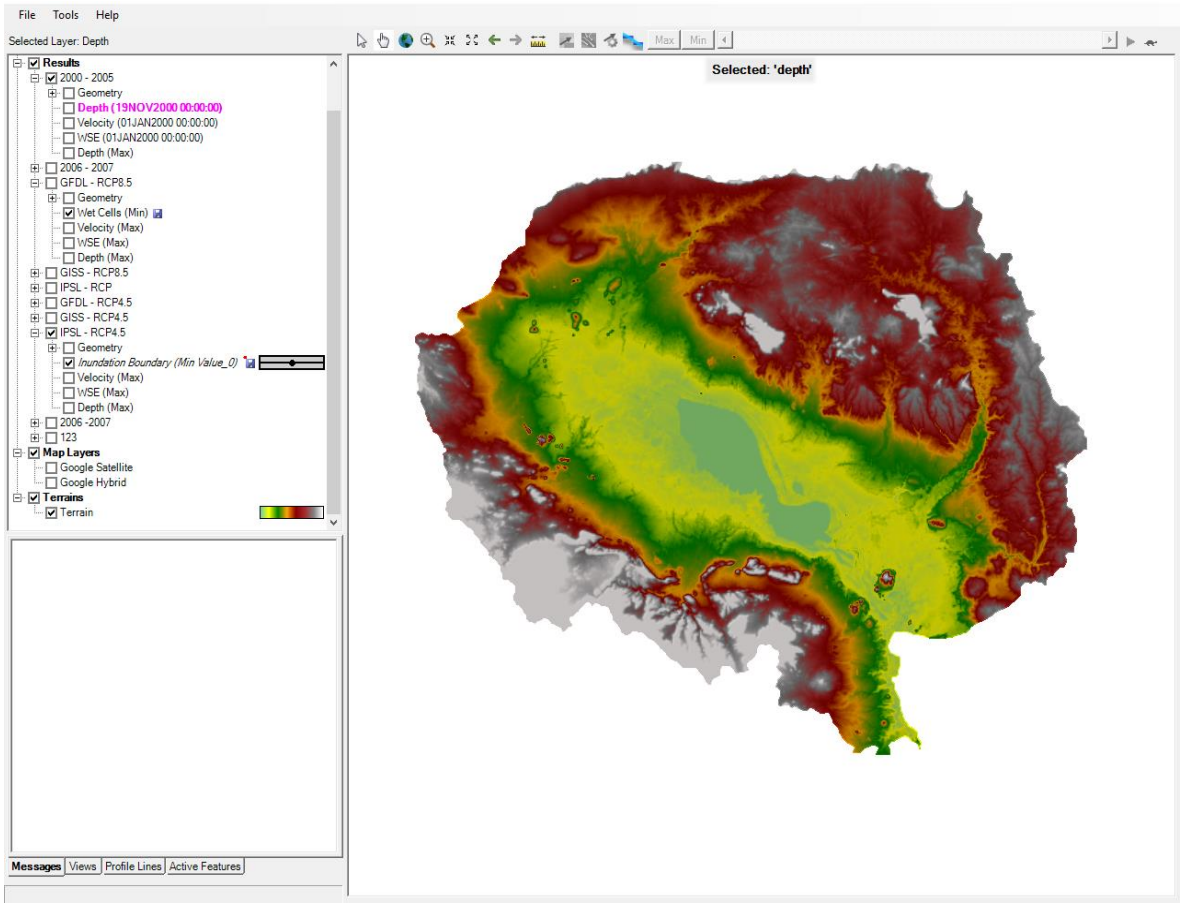

Figure 4.12 2D terrain model in RAS Mapper.

The 2D terrain was then associated with HEC-RAS to generate the geometry of the model. First, a polygon boundary for the 2D flow area was drawn. One of the best ways to do this in HEC-RAS is to bring in aerial imagery in RAS Mapper, in addition to terrain data. Terrain data and various satellite map layers in RAS Mapper can be displayed as background images in the HEC-RAS Geometry editor. The background images help to establish where to draw the 2D flow area boundaries (US ACE, 2016b).

After the boundary for 2D flow area was defined, a computational mesh (or computational grid) was created within the 2D flow area. Each cell of the computational mesh contains three properties: cell centre, cell face and cell point. Spacing between the computational grid-cell centres or cell size (DX and DY) is required to create the computational mesh (US ACE, 2016b). This study used the cell size DX = 500 m, and DY = 500 m. The computational mesh has grids of 500 m × 500 m everywhere within the boundary of the 2D flow area (Figure 4.13). The default Manning's *n* value 0.06 was initially used for the 2D flow area to build the hydraulic model.

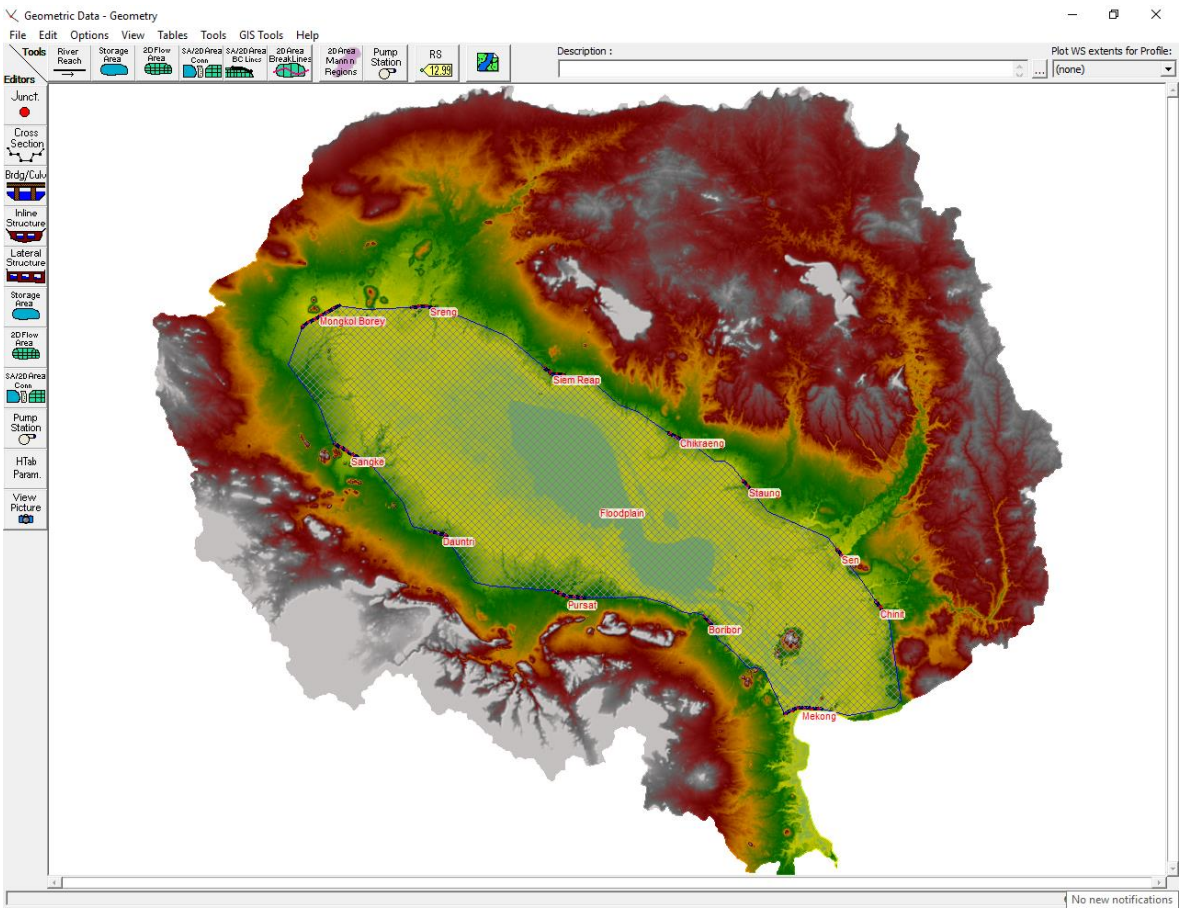

Figure 4.13 Boundary of 2D flow area and external boundary conditions (BC Lines).

External 2D flow area boundary conditions (BC Lines) were set for all 11 tributaries and the Mekong River. Once all the BC Lines were identified, unsteady flow data for each BC was brought in. The type of unsteady flow data used in this study is a flow hydrograph where positive flow values send flow into the 2D flow area, and negative flow values take the flow out of the 2D flow area.

Calibration and validation

In addition to flow records, surface water elevation data are essential pieces of data for both construction and calibration of a hydraulic model in HEC-RAS (US ACE,2016b). The calibration of the model should be the appropriate choice of Manning's *n* value that makes the simulated water level from the HEC-RAS model close to the observed stages along the river (Loliyana & Patel, 2012). The daily water levels from 2006 to 2007 were used for validation of the model. The performance of the model was assessed graphically and by Nash–Sutcliffe efficiency (NSE: Equation 1, page 47).

Tonle Sap River flow

The flow regime of Tonle Sap River into Tonle Sap Lake is mainly driven by the Mekong River. As the longest river in Southeast Asia and flowing across several countries, the Mekong River has a flow regime influenced by many significant determining factors, including natural and anthropogenic factors. The ongoing development of hydropower dams in the basin, the expansion of agricultural areas in the region, and climate change are all concerning factors that modify the natural flow of the Mekong River. Several studies (Arias et al., 2014; Hoang et al., 2019; Yu et al., 2019) have been carried out to comprehensively analyse the changes in the Mekong River flow regime under different drivers with reference to the likely future scenarios and their impacts on the Tonle Sap system.

A recent study by Hoang et al. (2019) was used as the foundation for the best possible scenario of future changes of inflow and outflow of Tonle Sap River driven by hydrological changes of the Mekong River. Hoang et al. (2019) took into account climate change, hydropower developments and irrigation expansions as the drivers of the Mekong's future flow. The time span in the study Hoang et al. (2019) is for the years 2036 to 2065, which is relatively close to this study (i.e., 2030). More importantly, Hoang et al. (2019) used RCP4.5 and RCP8.5 for climate change scenarios, the same as in this study. For the hydropower development scenario, Hoang et al. (2019) used the hydropower dam database of MRC and ADB, which includes 126 dams on both mainstreams and tributaries of the Mekong that are expected to be fully operational by the period 2036–2065. For irrigation, Hoang et al. (2019) developed two basic scenarios (i.e., high and low) using the MIRCA (Global Dataset of Monthly Irrigated and Rain-fed Crop Areas around the Year 2000) and the global projected

irrigation expansion scenarios. The study revealed substantial changes to the Mekong flows. Under the three combined drivers, the dry season flows (March and April) increase remarkably, up to +150% (at Kratie, Cambodia, upper stream of Tonle Sap River). In contrast, the results suggested a decreasing trend for wet season flows starting in June (around −10%) to the lowest reduction of about −25% in July at the same station, Kratie (Figure 4.14).

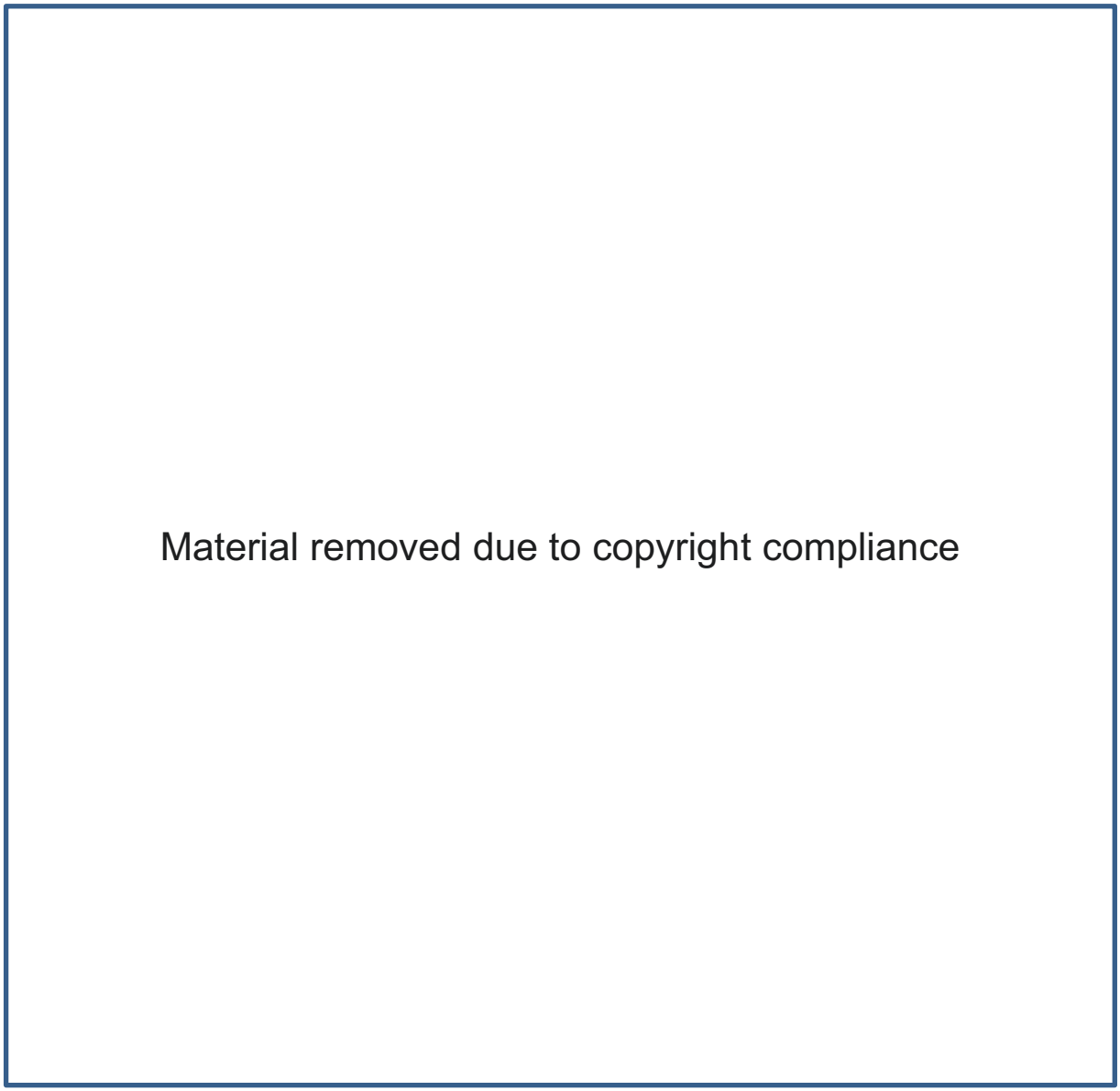

Figure 4.14 Projected changes between 2036 and 2065 to the Mekong River flows under multiple drivers – hydropower dams, agricultural expansion, and climate change.
Source: Hoang et al. (2019)

The magnitude of Tonle Sap River flows for the year 2030 in this study obtained from the average of discharge data (2000–2007) multiplied by the percentage of flow changes for the Mekong River flows at Kratie suggested by Hoang et al. (2019). The percentage of flow changes for combined impacts – Scenario S2 (RCP4.5 + IRR High + Dam) and Scenario S4 (RCP8.5 + IRR High + Dam) were initially targeted. However, the authors further noticed that

flow-change patterns are somewhat similar across all four future scenarios despite relatively negligible differences. So, the percentage of flow changes for each month have been determined as in Table 4.7. These monthly percentage changes were then interpolated into daily changes to align with the simulation time step.

Table 4.7 Estimated changes between 2036 and 2065 in percentage of the monthly flow of the Mekong River at Kratie Station (Cambodia).

No	Month	Flow Changes (%) at Kratie Station
1	January	50
2	February	75
3	March	120
4	April	148
5	May	60
6	June	–10
7	July	–25
8	August	–20
9	September	–5
10	October	0
11	November	24
12	December	25

4.5.3 Geographical Information System (GIS)

In addition to extracting the TRMM and SRTM DEM datasets, this study used GIS to analyse the changes of flood paddy rice areas in the basin.

After the computation, geospatial results from HEC-RAS were managed in RAS Mapper. The simulation results (water depth, velocity, and water surface elevation) were generated in two ways: the dynamic, on-the-fly current view and the stored map data (US ACE, 2016c). In this study, maximum water depth layers as outputs of each scenario were digitised, stored and exported as gridded outputs (raster) and polygon boundaries (shapefile). Each layer demonstrates the maximum inundated areas for each scenario.

The exported files allow further exploitation in ArcGIS. The layers of inundated areas were then overlapped with the land cover layer from MRC. Although there are various types of land cover in the study (see Section 4.4.3), paddy rice area is the only class analysed. Paddy rice areas for the whole basin, as well as each sub-basin, were examined.

4.6 Summary

This chapter began by describing some important characteristics of the study area, the Tonle Sap Basin. It went on to determine the three GCMs (GFDL-CM3, GISS-E2-R-CC and IPSL-CM5A-MR) and two RCPs (RCP4.5 and RCP8.5), the modelling scenarios used in this study.

Due to data limitations, datasets used as inputs for simulating the models were acquired from open sources. Historical rainfall data were extracted from TRMM, whereas DEM was derived from SRTM. Land cover and projected precipitation data were obtained from MRC and observed discharge data were provided by (Kummu et al., 2014), an earlier study that developed discharge rating curves based on observed water levels.

Eleven basin models were built in HEC-HMS to simulate rainfall-runoff for each sub-basin that feeds the Tonle Sap Lake. The models were calibrated and validated using data for the years 2000–2005 and 2006–2007. Projected rainfall data based on climate change scenarios for the year 2030 were input to the calibrated models. A project in HEC-RAS was created to compute inundation areas around the lake. To be consistent with HEC-HMS, the same time steps for calibration, validation and projection were used in the HEC-RAS project. RAS Mapper assisted in exporting geospatial results from HEC-RAS in formats that enabled further analysis in GIS. More than just a tool for extracting raw datasets from STRM DEM and TRMM, GIS was applied to examining changes to paddy rice areas at both basin-scale and sub-basin scales.

Chapter 5
Results

5.1 Introduction

Following the analytical procedures in the previous chapter, this chapter presents results in detail. The chapter is structured into five main sections. The first and second are the evaluation of the performance of HEC-HMS and HEC-RAS, respectively. Section 5.4 moves on to describe the projected changes in flow regimes of the tributary rivers under the climate change impacts. Future changes to Tonle Sap's flood pulse and flood recession paddy rice area are presented in sections 5.5 and 5.6, respectively.

5.2 Performance of HEC-HMS

The hydrologic models were calibrated for the years 2000 to 2005 and validated from 2006 to 2007 for 11 hydrological stations at the outlet of each sub-basin. The statistical indices, NSE and R^2, were used to evaluate the goodness-of-fit for the models. The values of NSE and R^2 for each sub-basin are presented in Table 5.1. During the calibration and validation periods, the values of NSE and R^2 are all above 0.42 and 0.65, respectively. According to the guideline of performance evaluation criteria for models provided by Moriasi et al. (2015), the model precision for daily flow simulation is judged as 'satisfactory' when the values of NSE > 0.40 and $R^2 > 0.60$.

Table 5.1 Nash–Sutcliffe efficiency (NSE) and coefficient of determination (R^2) values for calibration and validation of daily simulation models at 11 sub-basins of Tone Sap Basin.

No.	Sub-basin	Calibration	NSE	R^2	Validation	NSE	R^2
1	Chinit	2000–2005	0.83	0.92	2006–2007	0.91	0.96
2	Sen	2000–2005	0.95	0.98	2006–2007	0.77	0.94
3	Staung	2000–2005	0.72	0.85	2006–2007	0.78	0.88
4	Chikreng	2000–2005	0.71	0.85	2006–2007	0.82	0.91
5	Siem Reap	2000–2005	0.71	0.86	2006–2007	0.45	0.74
6	Sreng	2000–2005	0.81	0.91	2006–2007	0.74	0.90
7	Mongkol Borey	2000–2005	0.68	0.83	2006–2007	0.82	0.92
8	Sangke	2000–2005	0.60	0.78	2006–2007	0.61	0.79
9	Dauntri	2000–2005	0.60	0.78	2006–2007	0.42	0.65
10	Pursat	2000–2005	0.61	0.78	2006–2007	0.60	0.78
11	Boribor	2000–2005	0.64	0.84	2006–2007	0.54	0.82

Visually, the hydrographs show good agreement between the observed and simulated flows, although the simulation models seem to underestimate the discharge for a few sub-basins

(Chikreng, Sangker, and Dauntri) (Figure 5.1) (All hydrographs are shown in Appendix B1). A similar finding of the underperformance of simulated models for the same sub-basin was also reported by Oeurng et al. (2019). In their study, data scarcity and inaccuracy in rainfall and estimated discharge was reported to be the cause of this underestimation. Observed discharge data developed from rating curves used in Oeung et al. were also used in this study to calibrate the models. In general, the flow hydrographs show similar seasonal and inter-annual patterns of both observed and simulated flows for all 11 sub-basins.

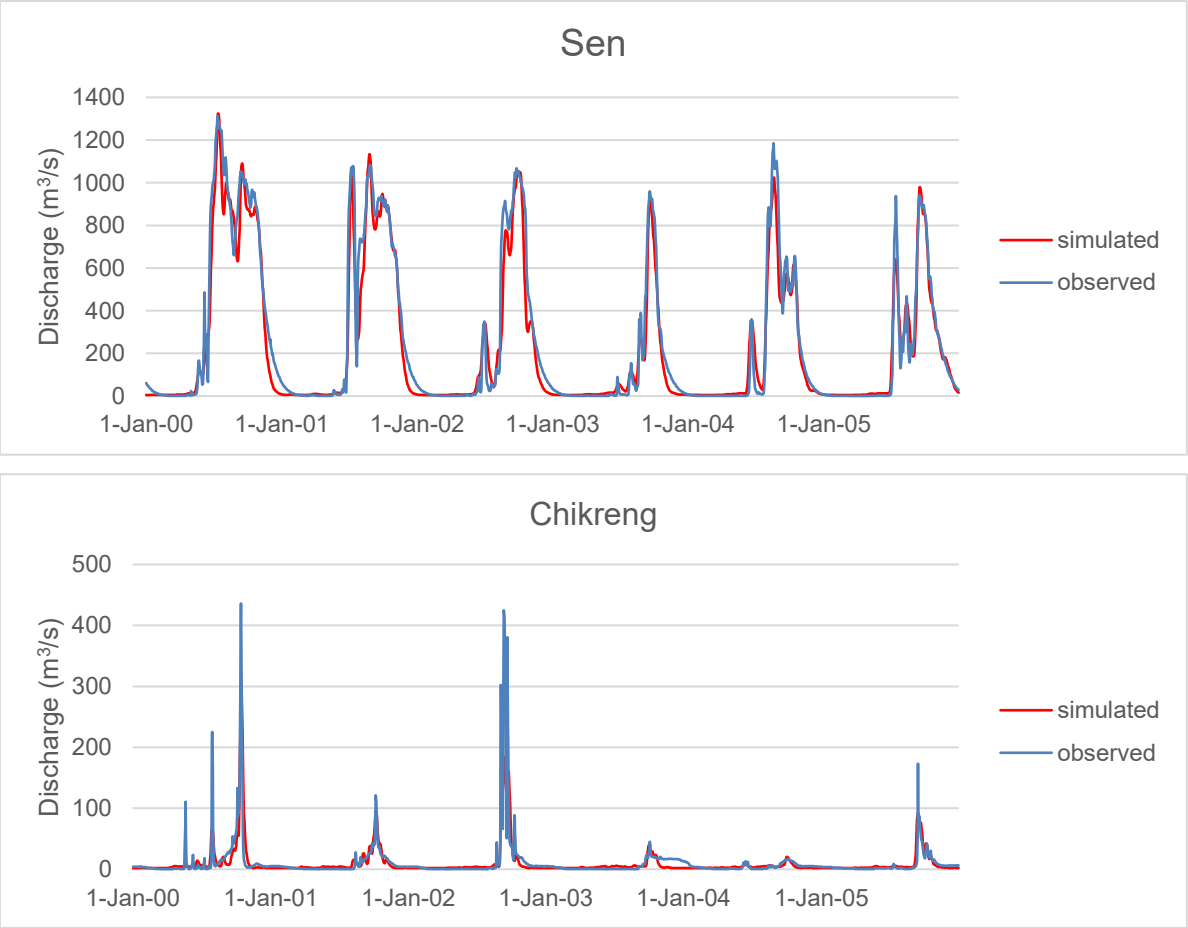

Figure 5.1 Flow hydrographs of Sen and Chikreng sub-basin.

5.3 Performance of HEC-RAS

The hydraulic model was calibrated for the years 2000–2005 and validated from 2006 to 2007. The water level at Kampong Loung station, a hydrological station in Tonle Sap Lake, was used for calibration and validation. According to guidelines offered by Christchurch City Council for hydraulic designs, Manning's roughness coefficient values *n* for floodplains with cultivated areas and scattered shrubbery should be between 0.03 and 0.07 (CCC, 2003). Table 5.2 shows that all values of NSE and R^2 for Manning's *n* values are between 0.03 and 0.07. As a result, a Manning's value for *n* of 0.04 was selected, as it yielded better NSE and R^2 results for both calibration and validation.

Table 5.2 NSE and R^2 values for each Manning's *n* value.

Manning's n value	Calibration (2000–2005)		Validation (2006–2007)	
	NSE	R^2	NSE	R^2
0.03	0.75	0.93	0.67	0.90
0.04	0.75	0.93	0.68	0.90
0.05	0.74	0.92	0.66	0.90
0.06	0.73	0.92	0.67	0.90
0.07	0.71	0.91	0.67	0.90

In a similar manner to the HEC-HMS models, the performance of the HEC-RAS model was also assessed by statistical indices NSE and R^2. The values of NSE are 0.75 and 0.68 for calibration and validation, respectively, where NSE > 0.60 indicates 'good' performance of the hydraulic model, based on the guidelines of performance evaluation criteria for models provided by Moriasi et al. (2015). Figure 5.2 shows the hydrograph of the observed and simulated water level at Kampong Loung station. The graph visually indicates underestimation of high water levels and overestimation of low water levels by the simulated model. This discrepancy may indicate an underestimation of the maximum flooded areas. Seasonal and inter-annual patterns of both simulated and observed water levels, however, show good agreement.

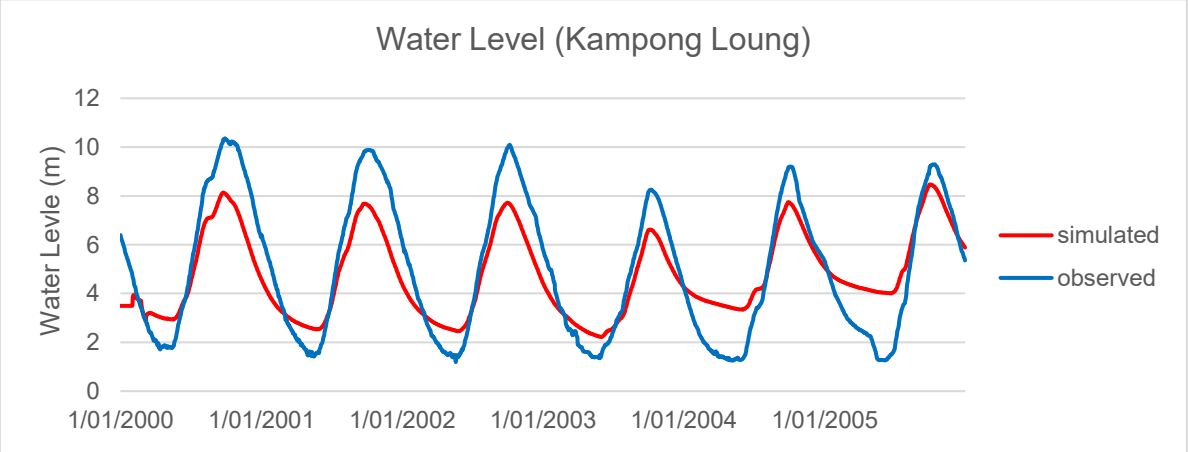

Figure 5.2 Hydrograph of the observed and simulated water level at Kampong Loung station.

5.4 Projected changes in flow regimes of Tonle Sap's tributaries

Future changes in flows of the Tonle Sap's tributaries were analysed by using the rainfalls projected by the three GCMs (GFDL-CM3, GISS-E2-R-CC and IPSL-CM5A-MR) and two RCP (4.5 and 8.5) emission scenarios. The projected streamflow of the year 2030 was compared with the baseline streamflow (2008–2012). Hydrographs of the projected flows are shown in Figure 5.3 (All hydrographs are shown in Appendix B2). The hydrographs suggest a clear trend in changes for most sub-basins, except Sreng and Mongkol Borey, in which flow patterns remain almost unchanged throughout the year, although the volumes of projected flows tend to be slightly lower. Other rivers, except Siem Reap, show flow

reductions in the dry season (November to April) for almost all climate change scenarios. During the wet season (May to October), the hydrographs exhibit stream flow decreases in most rivers with the exceptions being Chinit and Sen and Staung. Although the volumes of high flows remain similar to the baseline for some rivers, the frequency of high flows tends to decrease for rivers such as Chikreng, Siem Reap, Sangker and Dauntri.

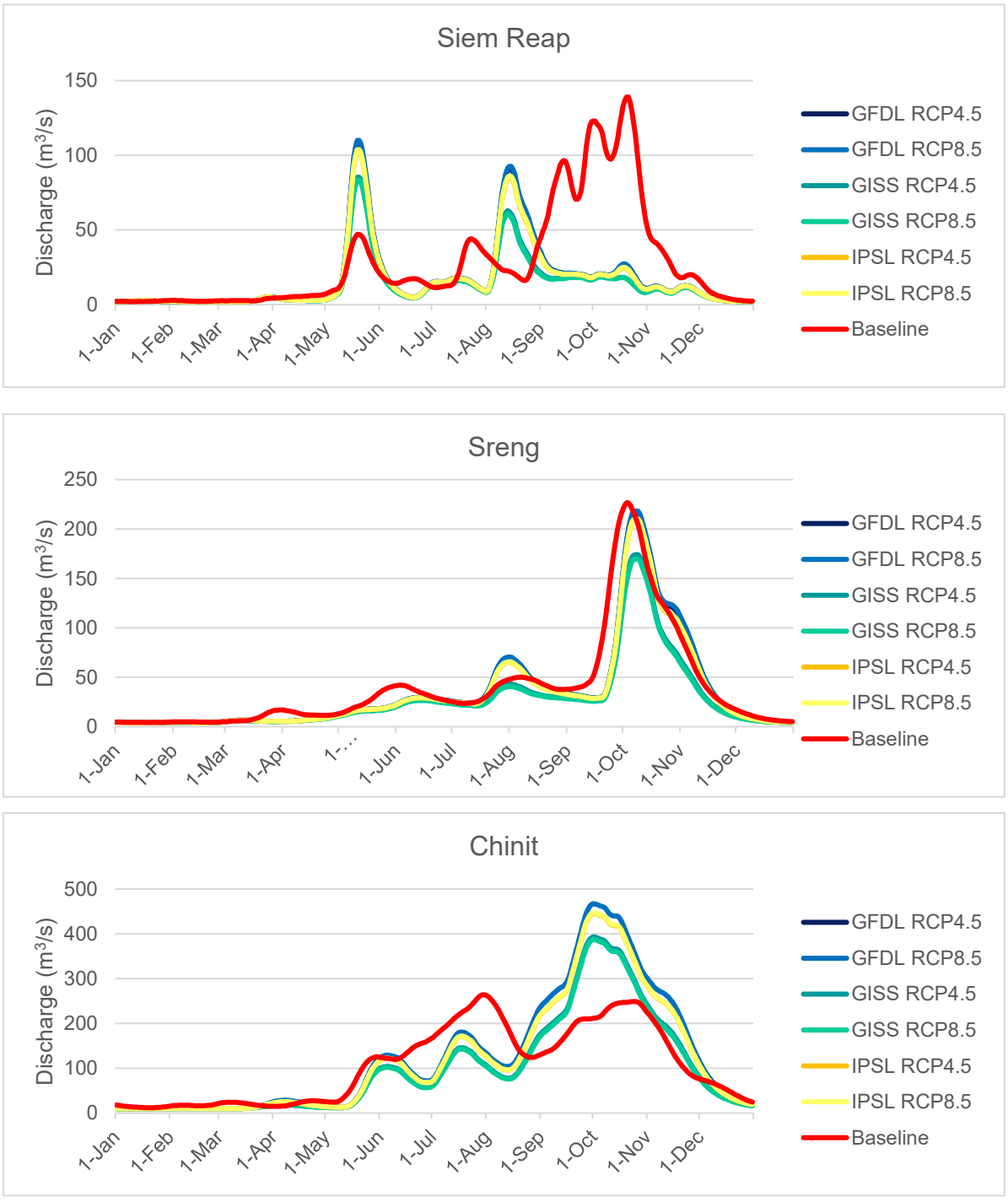

Figure 5.3 Discharge hydrographs of Chinit, Siem Reap and Sreng sub-basin.

The percentage of potential changes for annual stream flow of each sub-basin generated by the outputs of the climate change scenarios is shown in Table 5.3. The comparison of the projected (2030) and the baseline (2008–2012) annual flows shows declines for all sub-

basins under all climate change scenarios. The Dauntri sub-basin shows the highest flow reductions, ranging from 52.23% (GFDL-CM3 RCP8.5) to 62.53% (GISS-E2-R-CC RCP8.5), followed by the two nearby sub-basins, Pursat and Sangker. Annual streamflow decreases in Sangker range from 35.54% (GFDL-CM3 RCP8.5) up to 50.80% (GISS-E2-R-CC RCP8.5), whereas the Pursat River shows a reduction of annual streamflow between 31.43% (GFDL-CM3 RCP8.5) and 45.89% (GISS-CM3 RCP8.5). Sen is the only sub-basin with increasing stream flows under GFDL-CM3 RCP4.5, GFDL-CM3 RCP8.5, IPSL-CM5A-MR RCP4.5 and IPSL-CM5A-MR RCP8.5 scenarios, ranging from 13.21% to 20.24%, while Boribor shows slight increases of 1.95% and 5.34% under the GFDL-CM3 RCP4.5 and GFDL-CM3 RCP8.5 scenarios, respectively. A summary of percentage changes of streamflow for each sub-basin is shown in Table 5.3 and Figure 5.4.

Table 5.3 Percentage changes of stream flow of 11 principal tributaries under different climate change scenarios compared with the baseline stream flow.

Sub-basin	GCMs	RCP 4.5	RCP 8.5
Chinit	GFDL-CM3	−1.73	−0.63
	GISS-E2-R-CC	−20.92	−22.53
	IPSL-CM5A-MR	−6.57	−6.21
Sen	GFDL-CM3	19.09	20.24
	GISS-E2-R-CC	−2.58	−4.67
	IPSL-CM5A-MR	13.21	13.49
Staung	GFDL-CM3	−18.78	−17.82
	GISS-E2-R-CC	−34.91	−36.21
	IPSL-CM5A-MR	−23.23	−22.97
Chikreng	GFDL-CM3	−42.66	−41.68
	GISS-E2-R-CC	−57.36	−58.36
	IPSL-CM5A-MR	−46.85	−46.58
Siem Reap	GFDL-CM3	−39.60	−38.78
	GISS-E2-R-CC	−52.38	−53.35
	IPSL-CM5A-MR	−42.24	−41.82
Sreng	GFDL-CM3	−10.87	−9.97
	GISS-E2-R-CC	−30.37	−32.21
	IPSL-CM5A-MR	−14.35	−13.95
Mongkol Borey	GFDL-CM3	−30.53	−29.85
	GISS-E2-R-CC	−43.57	−44.75
	IPSL-CM5A-MR	−35.82	−35.93
Sangker	GFDL-CM3	−36.31	−35.54
	GISS-E2-R-CC	−49.66	−50.80
	IPSL-CM5A-MR	−41.82	−41.82
Dauntri	GFDL-CM3	−52.89	−52.23
	GISS-E2-R-CC	−61.94	−62.53
	IPSL-CM5A-MR	−56.91	−56.84
Pursat	GFDL-CM3	−32.26	−31.43
	GISS-E2-R-CC	−44.89	−45.89
	IPSL-CM5A-MR	−36.92	−36.83
Boribor	GFDL-CM3	1.95	5.34
	GISS-E2-R-CC	−15.18	−16.64
	IPSL-CM5A-MR	−2.67	−2.44

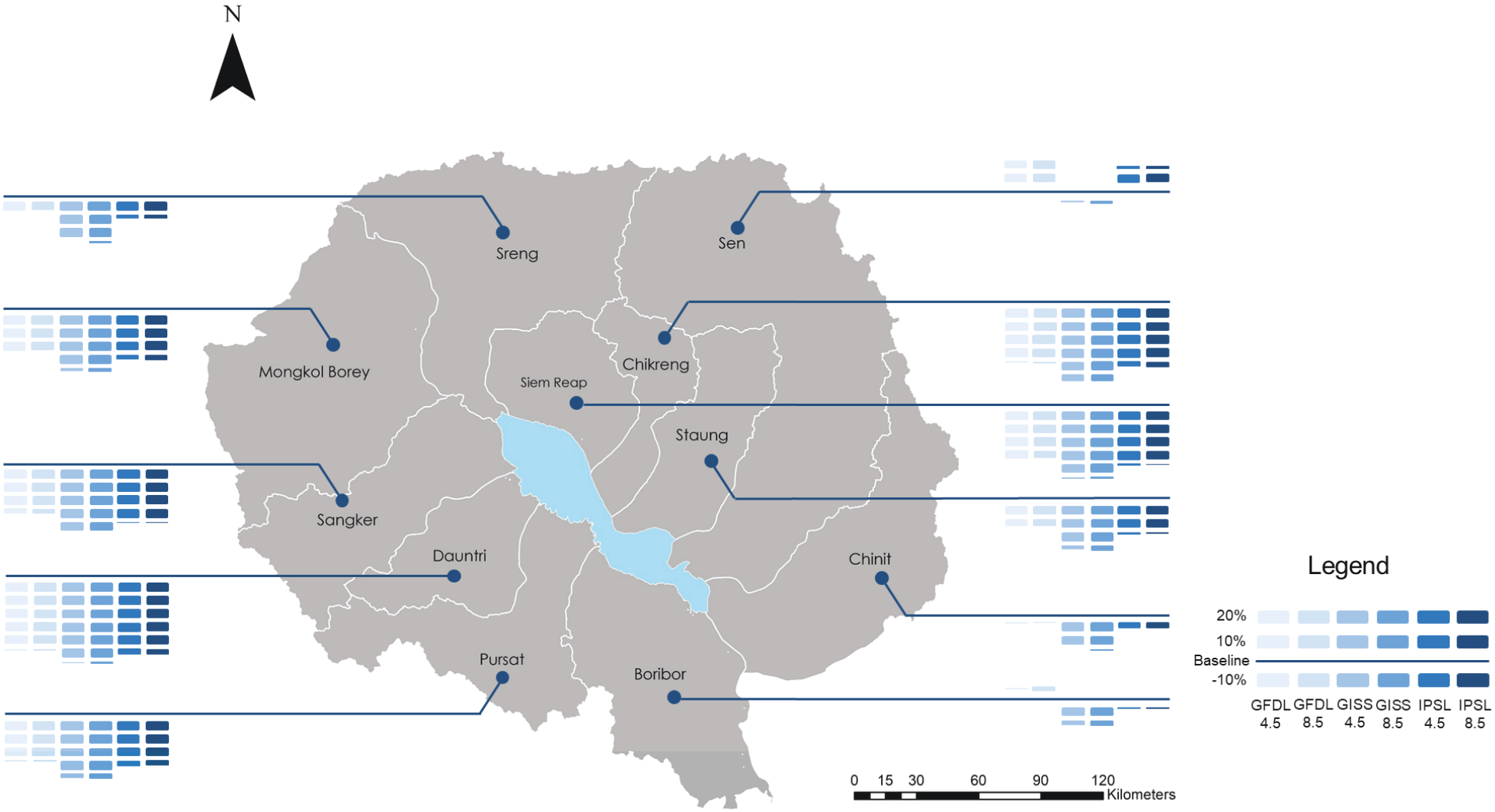

Figure 5.4 Percentage changes of streamflow for each sub-basin.
Note: the blue lines represent the baselines. Each bar above a blue line means projected streamflow increases by 10% and the opposite for bars below

5.5 Projected changes to Tonle Sap's flood pulse contributed by its tributaries

RAS Mapper was used to export the complete geometric datasets of the floodplain from HEC-RAS. Figure 5.5 shows maximum flooded areas of Tonle Sap under different climate change scenarios as the outputs of HEC-RAS computation and RAS Mapper digitalisation. The results identify very similar maximum flooded areas under all climate change scenarios.

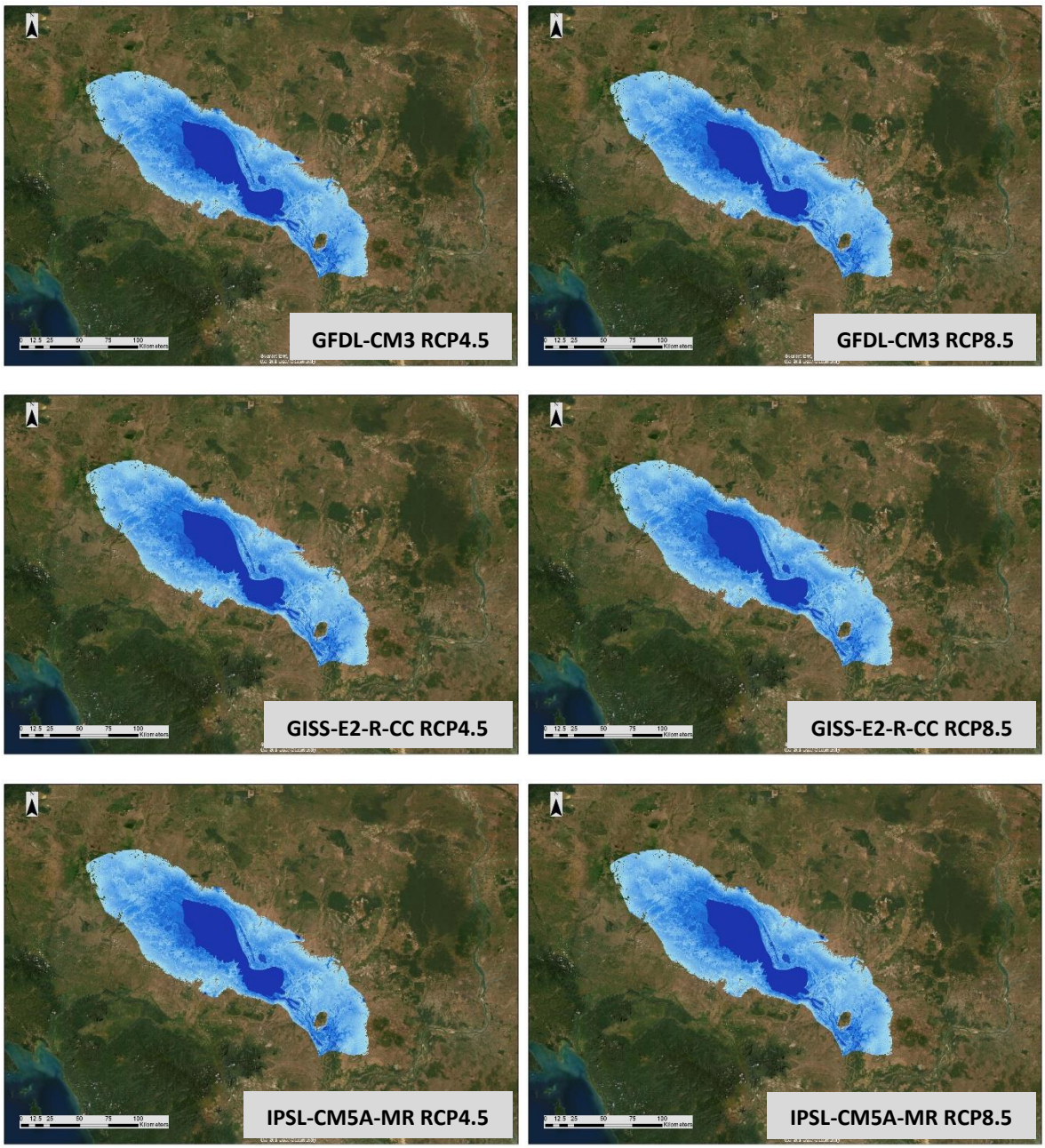

Figure 5.5 Projected flood pulse under different climate change scenarios.

Figure 5.6 shows the overlap of the maximum flooded area under GFDL-CM3 RCP4.5 for the year 2030 (the blue area) over the baseline period of 2008–2012 (the black area), which shows that the areas covered by the flood pulse shrink. Although streamflow decreases are

projected to be higher for sub-basins at the eastern part of the lake (Mongkol Borey, Sangke, Dauntri and Pursat), it does not seem to show correlation with the projected flood pulse.

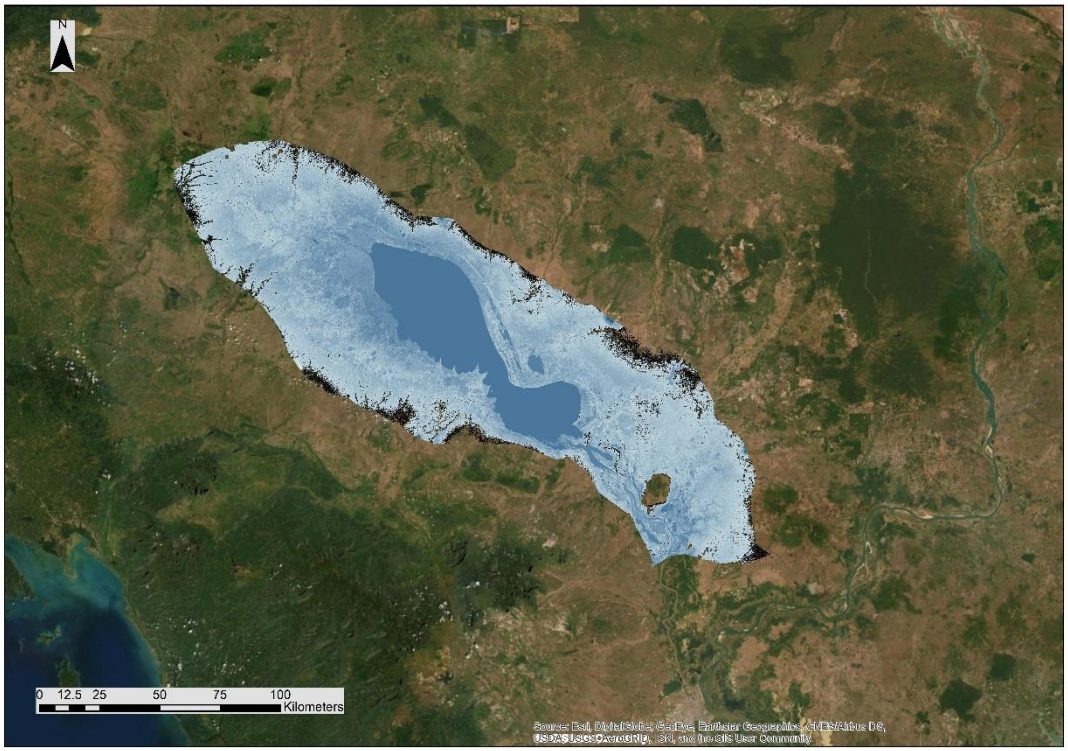

Figure 5.6 Flood pulse of the baseline periods (2008–2012) (the black areas) overlapped by the projected flood pulse of the year 2030 under GFDL-CM3 RCP4.5 climate change scenario (the light blue areas).
Note: The black areas visible on the map are the potential areas of reduced lake extent due to the diminished future flood pulse under the GFDL-CM3 RCP4.5 scenario.

The percentage change in flood pulse area in Table 5.4 is the comparison between the maximum flooded areas for the year 2030 against the maximum flooded areas for the baseline period (2008–2012). At the basin scale, an average across all climate change scenarios shows a reduction in the maximum areas of projected flood pulse of around 10% compared with that of the baseline. The results suggest high similarity between each climate change scenario with deviation of less than 1%.

Table 5.4 Extent of decrease and percentage change of Tonle Sap's flood pulse under different climate change scenarios.

Year	Scenario	Extent (km^2)	Change (km^2)	Change (%)
2008–2012	Baseline	13,893.76	-	-
2030	GFDL-CM3 RCP4.5	12,628.81	−1,264.95	−10.02
	GFDL-CM3 RCP8.5	12,645.34	−1,248.42	−9.87
	GISS-E2-R-CC RCP4.5	12,574.50	−1,319.26	−10.49
	GISS-E2-R-CC RCP8.5	12,580.54	−1,313.22	−10.44
	IPSL-CM5A-MR RCP4.5	12,615.61	−1,278.15	−10.13
	IPSL-CM5A-MR RCP8.5	12,603.81	−1,289.95	−10.23

At the sub-basin scale, Sen is the sub-basin with the highest percentage decrease in flooded area. Areas covered by flood in the Sen sub-basin show an average reduction across all climate change scenarios of 13.82%, followed by Pursat at 12.95%. The Sangker sub-basin shows the least reduction in flooded area, with an average across all climate change scenarios of 2.00%. Chikreng, Staung, Chinit and Boribor also show low reductions, with an average decrease of less than 10%. Summaries of percentage changes of Tonle Sap's flood pulse area by each sub-basin and average percentage change of flooded area for each sub-basin across all climate change scenarios are shown in Table 5.5 and Figure 5.7, respectively.

Table 5.5 Percentage change of Tonle Sap's flood pulse by each sub-basin.

Sub-basin	GCM	RCP 4.5	RCP 8.5
Chinit	GFDL-CM3	−7.59	−7.70
	GISS-E2-R-CC	−7.92	−7.96
	IPSL-CM5A-MR	−7.78	−7.72
Sen	GFDL-CM3	−13.61	−13.65
	GISS-E2-R-CC	−14.05	−14.08
	IPSL-CM5A-MR	−13.78	−13.76
Staung	GFDL-CM3	−9.64	−9.80
	GISS-E2-R-CC	−10.02	−10.10
	IPSL-CM5A-MR	−9.79	−9.79
Chikreng	GFDL-CM3	−8.10	−8.18
	GISS-E2-R-CC	−9.12	−8.71
	IPSL-CM5A-MR	−7.97	−8.23
Siem Reap	GFDL-CM3	−10.99	−11.13
	GISS-E2-R-CC	−11.34	−11.17
	IPSL-CM5A-MR	−11.09	−11.05
Sreng	GFDL-CM3	−10.92	−10.95
	GISS-E2-R-CC	−11.22	−11.24
	IPSL-CM5A-MR	−11.04	−11.03
Mongkol Borey	GFDL-CM3	−10.38	−10.44
	GISS-E2-R-CC	−10.76	−10.78
	IPSL-CM5A-MR	−10.55	−10.52
Sangker	GFDL-CM3	−1.97	−1.97
	GISS-E2-R-CC	−2.03	−2.04
	IPSL-CM5A-MR	−2.00	−1.99
Dauntri	GFDL-CM3	−9.90	−9.92
	GISS-E2-R-CC	−10.14	−10.17
	IPSL-CM5A-MR	−9.99	−9.99
Pursat	GFDL-CM3	−12.94	−10.12
	GISS-E2-R-CC	−14.08	−13.60
	IPSL-CM5A-MR	−12.77	−14.17
Boribor	GFDL-CM3	−9.07	−9.08
	GISS-E2-R-CC	−9.28	−9.30
	IPSL-CM5A-MR	−9.16	−9.15

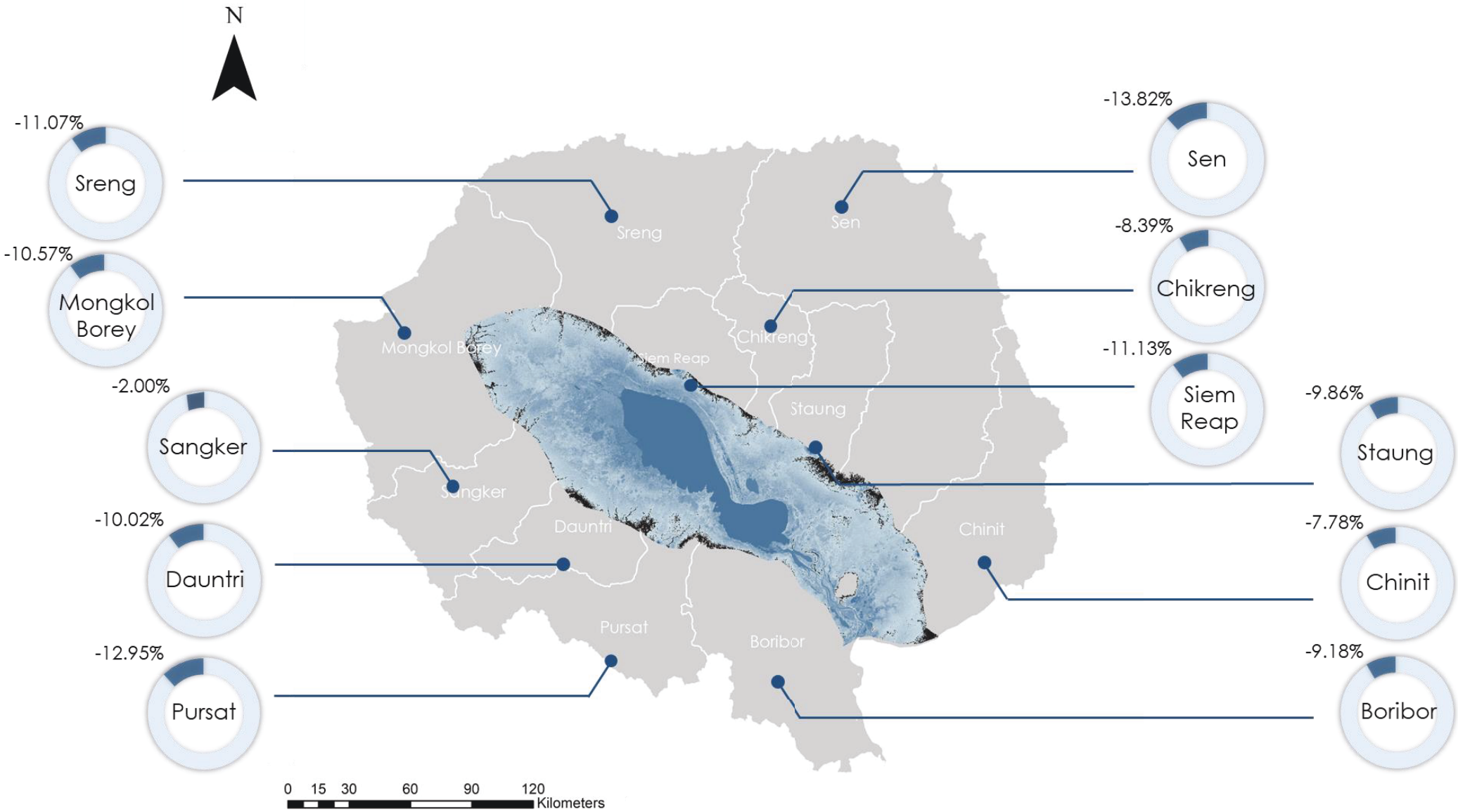

Figure 5.7 **Average percentage change of flooded areas for each sub-basin across all climate change scenarios.**

5.6 Projected changes of flood recession paddy rice area

Flood recession paddy rice areas in this study refer to the paddy rice areas being exposed to the flood pulse. The total area of flood recession rice, thus, decreases accordingly as the projected flood pulse grows smaller. The percentage change of flood recession paddy area between the year 2030 and the baseline period (2008 – 2012) allows a comparison between different climate change scenarios. At the basin scale, an average across all climate change scenarios showed the projected flood recession paddy rice areas decrease by approximately 18%. The deviation between the lowest and highest decrease is around 1%. GFDL-CM3 RCP8.5 shows the lowest percentage change (17.67%) while GISS-E2-R-CC RCP4.5 is the highest (18.96%). A summary of flood recession paddy rice area changes under all climate change scenarios is shown in Table 5.6.

Table 5.6 Areas decrease and percentage change of flood recession paddy rice areas under different climate change scenarios.

Year	Scenario	Area (km^2)	Change (km^2)	Change (%)
2008–2012	Baseline	6,313.53	-	-
2030	GFDL-CM3 RCP4.5	5,352.92	−960.66	−17.95
	GFDL-CM3 RCP8.5	5,365.67	−947.91	−17.67
	GISS-E2-R-CC RCP4.5	5,307.53	−1,006.05	−18.96
	GISS-E2-R-CC RCP8.5	5,313.79	−999.79	−18.82
	IPSL-CM5A-MR RCP4.5	5,341.28	−972.30	−18.20
	IPSL-CM5A-MR RCP8.5	5,332.80	−980.78	−18.39

At the sub-basin level, sub-basins with a lower reduction in flooded areas surprisingly show a higher decrease in flood recession paddy rice areas. Those are Staung, Boribor and Chikreng, with percentage decreases of up to 28.36%, 23.08% and 21.23% respectively. Sen, the sub-basin with the highest flooded area reduction, also shows significant reduction of flood recession paddy rice area with an average decrease across all climate change scenarios of 21.00%. Not surprisingly, as the sub-basin with the lowest reduction of flooded areas, Sangker is also the sub-basin with the lowest reduction of flood recession paddy rice areas with an average reduction across all climate change scenarios of 2.67%. Summaries of percentage change of flood recession paddy rice areas by each sub-basin and average percentage change of flood recession paddy rice areas for each sub-basin across all climate change scenarios are shown in Table 5.7 and Figure 5.8, respectively.

Table 5.7 Percentage change of flood recession paddy rice areas under different climate change scenarios compared with the baseline areas.

Sub-basin	GCMs	RCP 4.5	RCP 8.5
Chinit	GFDL-CM3	−12.93	−13.13
	GISS-E2-R-CC	−13.51	−13.58
	IPSL-CM5A-MR	−13.26	−13.15
Sen	GFDL-CM3	−20.69	−20.75
	GISS-E2-R-CC	−21.33	−21.37
	IPSL-CM5A-MR	−20.94	−20.92
Staung	GFDL-CM3	−27.71	−28.22
	GISS-E2-R-CC	−28.84	−29.09
	IPSL-CM5A-MR	−28.16	−28.16
Chikreng	GFDL-CM3	−20.58	−20.70
	GISS-E2-R-CC	−23.31	−21.97
	IPSL-CM5A-MR	−20.06	−20.80
Siem Reap	GFDL-CM3	−15.02	−15.18
	GISS-E2-R-CC	−15.47	−15.25
	IPSL-CM5A-MR	−15.16	−15.09
Sreng	GFDL-CM3	−18.90	−18.96
	GISS-E2-R-CC	−19.44	−19.48
	IPSL-CM5A-MR	−19.12	−19.09
Mongkol Borey	GFDL-CM3	−10.09	−10.15
	GISS-E2-R-CC	−10.52	−10.56
	IPSL-CM5A-MR	−10.28	−10.26
Sangker	GFDL-CM3	−2.60	−2.61
	GISS-E2-R-CC	−2.74	−2.75
	IPSL-CM5A-MR	−2.66	−2.65
Dauntri	GFDL-CM3	−17.44	−17.49
	GISS-E2-R-CC	−17.89	−17.93
	IPSL-CM5A-MR	−17.62	−17.61
Pursat	GFDL-CM3	−18.14	−14.29
	GISS-E2-R-CC	−20.17	−19.28
	IPSL-CM5A-MR	−18.24	−19.99
Boribor	GFDL-CM3	−22.84	−22.88
	GISS-E2-R-CC	−23.34	−23.38
	IPSL-CM5A-MR	−23.05	−23.02

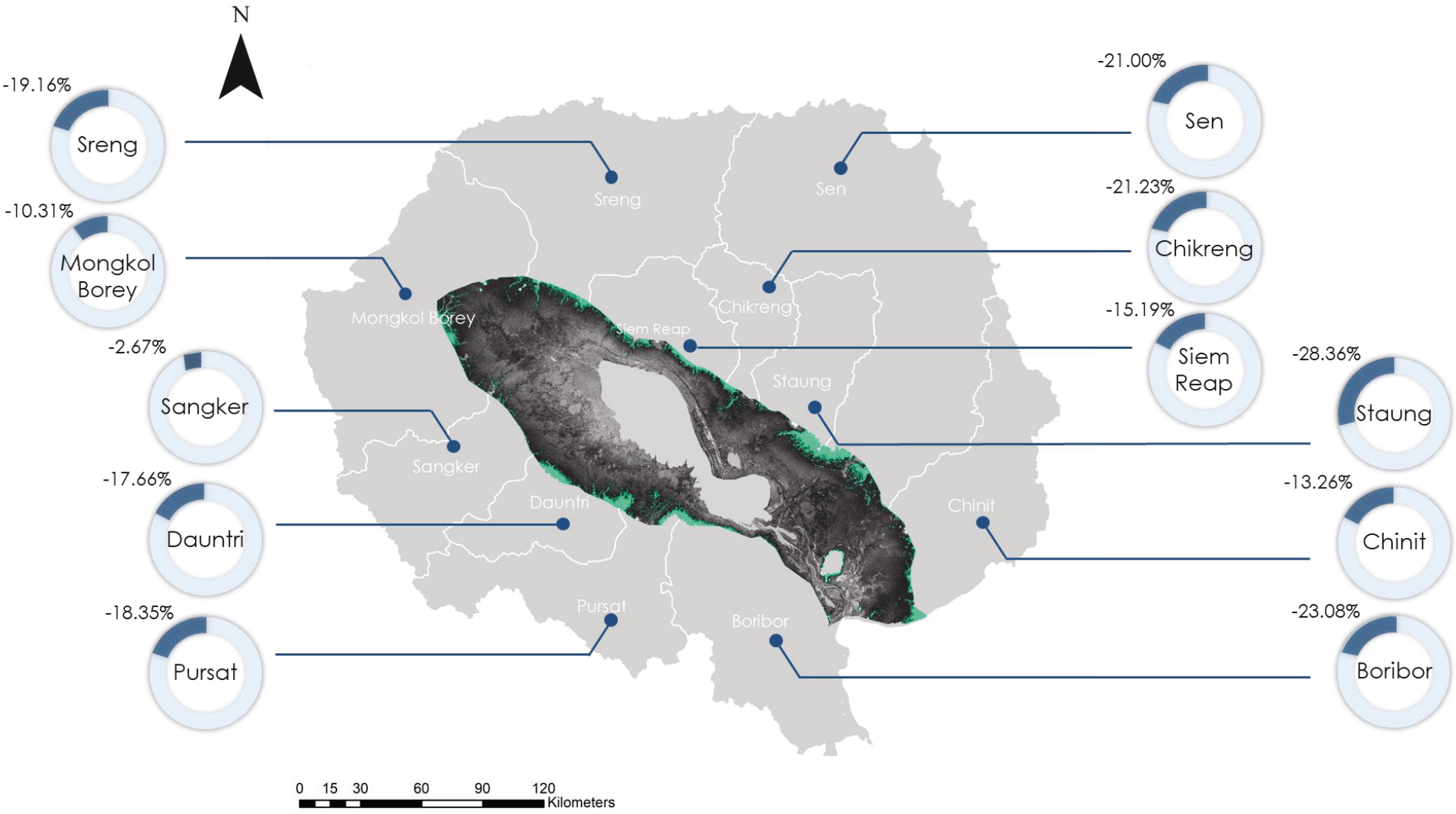

Figure 5.8 Average percentage change of flood recession paddy rice areas for each sub-basin across all climate change scenarios.

5.7 Summary

Evaluation of the goodness-of-fit for HEC-HMS and HEC-RAS models showed satisfactory performance of all simulation models with statistical indices NSE > 0.40 and R^2 > 0.60 for HEC-HMS and NSE > 0.60 and R^2 ≥ 0.90 for HEC-RAS.

Projected discharges as a result of HEC-HMS computation suggest reductions of annual streamflows will occur in all sub-basins under all climate change scenarios for the projected year 2030. The projected decrease could be as high as 62% (Dauntri sub-basin under GISS-E2-R-CC RCP8.5 scenario) compared with the annual streamflow of the baseline periods (2008–2012). Sen and Boribor are the only sub-basins with a slight increase of annual streamflow under both RCPs of GFDL-CM3 and IPSL-CM5A-MR.

Outputs from HEC-RAS show that flood pulse will decrease under all climate change scenarios. The magnitudes of decrease, however, are almost exactly the same between each scenario with an average decrease of around 10% compared with the baseline. On the sub-basin level, Sen shows the greatest reduction of flooded areas, with an average decrease of 13.82% across all climate change scenarios, whereas flooded areas in Sangker are projected to decrease the least (by 2%).

Flood recession paddy rice areas are projected to decrease under all scenarios. The decrease is around 18% for each scenario. Sen, the sub-basin with the highest percentage of flooded area reduction, remains the sub-basin with the highest percentage decreases in paddy rice areas, with an average decrease across all scenarios of 21%. Staung is the sub-basin with the largest percentage reduction in flood recession paddy rice area, 28.36% on average. Sangker also remains as the sub-basin with the least percentage reduction of flood recession paddy rice area, with an average decrease of 2.67% across all climate change scenarios.

Chapter 6
Discussion

6.1 Introduction

The main aim of this thesis was to evaluate the impacts of climate change on major hydrological elements of Tonle Sap Lake, namely the streamflows of the tributary rivers, the extent of the floodplain and the extent of flood recession paddy rice areas supported by the flood pulse. Results from the modelling study set out in Chapter 5 present a wide range of changes that will occur to the lake and surrounding areas. This chapter takes research findings to the next step by comparing the results with previous studies and discussing the likely consequences of the outcomes.

The chapter begins with a general discussion of the results for each objective obtained from the simulations compared with previous studies. It then interprets the implications of the projected changes to tributary streamflow, flood pulse and flood recession paddy rice areas. The chapter concludes by addressing the research limitations in this study.

6.2 General discussion

The first objective of this study was to assess the potential impacts of climate change on streamflow of the 11 principal rivers that flow into Tonle Sap Lake. Results of the hydrologic simulations suggest that most of the sub-basins will likely encounter droughts during both the dry and wet seasons. These reductions are attributed to future precipitation changes in the Lower Mekong Basin, with average annual rainfall predicted to be lower than the historical baseline, as reported in previous studies of the regional climate change (MRC, 2010; Piman et al., 2014).

Flow hydrographs of projected discharges indicate that some sub-basins, including Chikreng, Sangker and Dauntri, will experience a longer dry season and lower annual streamflow. These results are consistent with previous national and regional studies on the effects of climate change (Kirby et al., 2009; MoE & UNDP, 2011; MRC, 2014). Under climate change, longer dry periods and more consecutive drought days are expected in Cambodia and many areas of the Mekong River Basin (Kirby et al., 2009; MoE & UNDP, 2011; MRC, 2014).

Overall, the projected decrease of streamflow in the tributary rivers found in this study is in good agreement with the findings of an earlier study by Oeurng et al. (2019), except for the results for Sen and Boribor sub-basins. This inconsistency could be attributed to the

difference in software used for simulation and the variation in precipitation data used in the calibration processes. However, values of NSE and R^2 for these two sub-basins in this study are higher than those in Oeurng et al., so the simulated models from the current study are likely to be more precise.

The second objective of this study was to evaluate the impact of climate change on the extent of the Tonle Sap's flood pulse. The results of this modelling partly agree with the previous study by Kirby et al. (2009). The simulation in that study projected that the lake would expand more in the wet season and shrink to a smaller extent in the dry season, whereas in this study the lake is projected to grow smaller in both wet and dry seasons. The projection in Kirby et al. was mainly based on the volumes of annual inflows and outflows from the Mekong River (at Phnom Penh) into Tonle Sap Lake, in which the significance of inflows from the tributary rivers was not taken into account. For this reason, results from the current study are likely to be more comprehensive than those in Kirby et al.

The results of this study showed that different climate change scenarios produced similar impacts on Tonle Sap's flood pulse by 2030. This outcome is understandable because the main driver of Tonle Sap's flood pulse, according to an earlier study by Kummu et al. (2014), is the inflow and outflow from the Mekong River, which contributes up to 53.5% of the inflow into Tonle Sap Lake in the wet season and 88.5% of the outflow during the dry season, whereas tributary streamflows account for only 34% of the inflow during the wet season. The tributary rivers have less effect in driving changes to the flood pulse. Though different climate change scenarios resulted in impacts of various sizes on streamflow of the tributary rivers, the magnitudes of impacts on the flood pulse were found to be almost the same under all climate change scenarios because extents are strongly influenced by the flow from the Mekong River.

At the sub-basin scale, the results show that the flooded areas will possibly decrease for all eleven sub-basins under all climate change scenarios. These results are in line with the results of the first objective in which streamflows decrease for all sub-basins, except the Sen and Boribor sub-basins. The results for these two sub-basins appear contradictory, but are explainable. Discharges were the result of rainfall-runoff modelling for individual sub-basins and were computed separately. Unlike streamflow, the flood pulse extent is the balance between inflows and outflows to Tonle Sap Lake. While discharge in the Sen and Boribor catchments increased, the combined decrease in the remaining catchments was greater, leading to lower overall inflows to the lake from the tributaries (Figure 6.1).

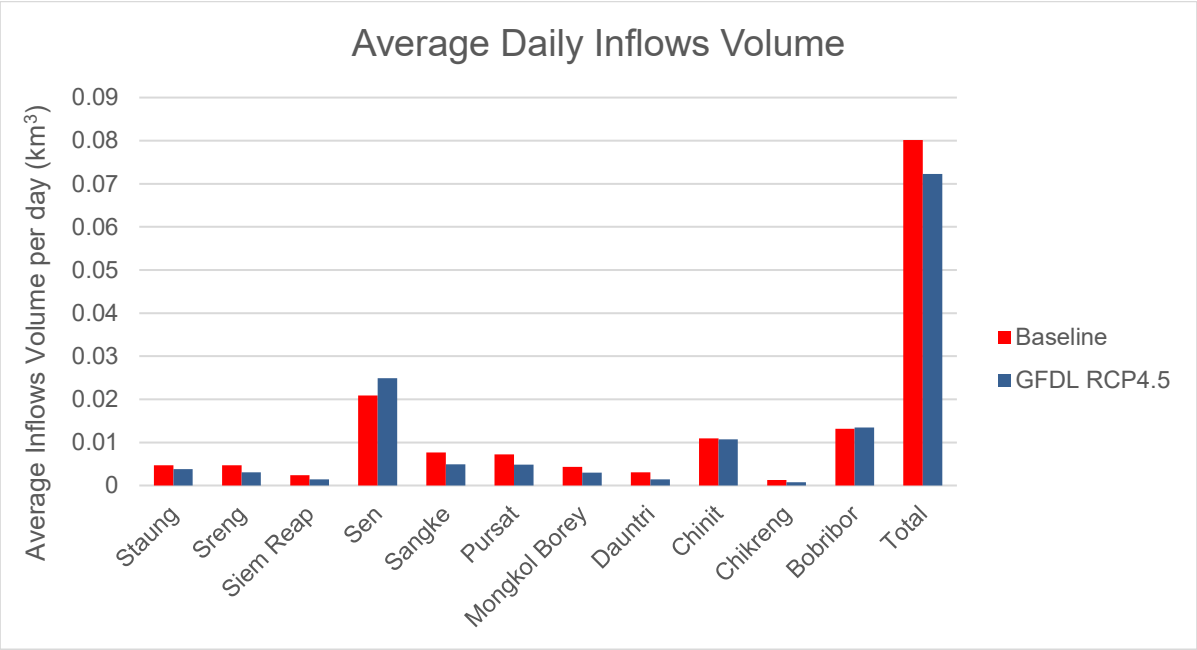

Figure 6.1 Comparison of average daily inflows volume under GFDL RCP4.5 scenario against the baseline.

The third objective of this study was to assess the changes to paddy rice areas under the impact of climate change – research that has not been carried out in the Tonle Sap Basin previously. Therefore, there are no previously published studies to be used as references to support or compare with the results obtained in this study.

6.3 Implications

The results of the simulations indicate that the study area will experience more drought under the impacts of climate change through to 2030. Wihite and Glantz (1985) classified drought-related problems into three kinds of impacts – namely, economic, social and environmental. Discussed below are the primary implications of climate change on the economic, social and environmental aspects of Cambodia through the changes of Tonle Sap Lake.

6.3.1 Changes in streamflow of the tributaries

The results of the climate change simulations on river flows suggest a decrease in future streamflows, and so an increase in drought risk. These seasonal and annual streamflow reductions would consequently affect future freshwater availability in the basin. Domestic water supply and surface irrigation that are highly dependent on water diverted or extracted from those tributary rivers may struggle with higher demands..

Agricultural households that depend on irrigation frequently encounter problems of inadequate supply of water. Lack of water during dry season rice farming is a significant

constraint and occasionally leads to high competition and even severe conflicts among farmers who need water to maintain their paddies in times of drought (CDRI, 2012).

In addition to the scarcity of available drinking water, another common problem during drought is deterioration of water quality in the rivers (Keskinen et al., 2009). The implications for health issues associated with a lack of freshwater availability are beyond the scope of this study, although it is expected that drought risks would increase the risk of water-borne disease and malnutrition.

6.3.2 Changes to the flood pulse

The river flows from all the principal tributaries contribute to maintaining Tonle Sap Lake. The decrease of tributary streamflows leads to a reduction of Tonle Sap's flood pulse. This annual flood pulse supplies nutrients and sediment, making the lake one of the world's most productive ecosystems. Thus, the reduction of flood extent is likely to reduce the productivity of the ecosystem, especially for fisheries that depend on large areas of inundation for food and fish reproduction.

The extent and diversity of habitats of Tonle Sap's floodplain are of regional importance, and the significance of the lake extends far beyond Cambodia's boundary. A strong connection between the floodplain and other ecological systems has been reported in the literature. The flooded areas provide spaces for breeding and nursery grounds for fish that migrate to the Mekong River. It has been reported that fish migration from the Tonle Sap Lake helps to restock fisheries as far upstream as China and in many other tributaries along the way (ADB, 2005). Given this, losses or changes of any parts of the flood pulse system of Tonle Sap Lake could result in disturbance to other wetlands and ecosystems of the Mekong River Basin above the Tonle Sap River. Moreover, the lake also functions as a natural floodwater reservoir that helps reduce the severity of downstream flooding during the wet season and helps control saltwater intrusion and conserve mangrove forests in the Mekong Delta (in Vietnam) during the dry season (ADB, 2005; MRC, 2009). Therefore, the changes to Tonle Sap's flood pulse creates impacts that could spread substantially across the Mekong Basin, from China upstream to the Mekong Delta downstream in Vietnam.

6.3.3 Changes of flood recession paddy areas

The annual flood pulse is essential for replenishing soil fertility lost during drought periods. The flood pulse exerts hydraulic forces that erode sediment and so it carries and deposits organic and inorganic material, restoring fertility to the areas affected (Junk & Wantzen, 2004). Those areas experiencing a reduced flood pulse are likely to be less fertile and less productive for crop cultivation, especially for rice. As highlighted in the literature, rice is the

most crucial food crop in Cambodia and employs a large proportion of the country's population in farming and processing. A reduction of fertile floodplains for farming activities would consequently lead to significant social and economic implications such as food insecurity, unemployment and reduction in economic growth.

Like other countries in the region, at a national level, food insecurity is a thing of the past for Cambodia, as the country is self-sufficient in rice production, and altogether the Lower Mekong Basin is known to be a leading global rice exporter (MRC, 2014). At the local level, however, some districts around Tonle Sap Lake and northern regions of Cambodia are still encountering rice shortages (Cosslett & Cosslett, 2018; MRC, 2014). The result of a simulation study of the impacts of climate change on rice yield in the Lower Mekong Basin suggests rice yields in the Tonle Sap region will decrease from 1% to 5% under all the four RCPs in the 2030s (MRC, 2014). Another simulation study by Kirby et al. (2009) suggested that even wet season rice production in Cambodia will be depressed by climate change. These findings, while preliminary, suggest the possibility of food insufficiency for people who depend solely on farming to sustain their livelihoods, particularly people around Tonle Sap Lake. The decrease of flood recession paddy rice areas found in this study reinforces the findings in previous studies about food insecurity that is likely to happen in the study area due to climate change.

As stated previously, agriculture and fisheries are the only sources of income for people living in the Tonle Sap zone. According to Yu and Fan (2009), 46% of rural Cambodian households are landless or own less than half a hectare per household. With this limited access to land, they can do little when the lands they own become unproductive. Unlike farmers in neighbouring countries, farmers in Cambodia cannot afford to purchase crop insurance or receive any benefits from subsidy implementation programmes: they are left to their own devices. Thus, the shrinkage of fertile ground for agricultural production would substantially affect many households whose sources of income depend solely on farming. The situation will eventually force them to emigrate for other jobs, either in the city or in neighbouring countries.

In the agricultural sector, drought-induced losses have the greatest effect, where crop failure is the primary direct economic impact of drought (Ding et al., 2010). However, thoroughly quantifying the economic impacts of drought-induced losses is challenging and involves many factors. Droughts can cause long-term social and economic impacts which may linger for multiple years. A simplified, worst-case scenario approach to approximate the economic damage that might occur based on the projected results obtained in this study could be carried out using the following equation:

$$ED = (P\ x\ Y\ x\ A)\ x\ \prod \quad (3)$$

where *ED* is the expected annual economic damage (US$), *P* is the price of rice (US$/ton), *Y* is the annual yield of rice per hectare (ton/ha), *A* is the area of paddy rice not being exposed to floods (ha) and ∏ is the annual probability of drought in the study area.

For 2019, the average rice price at the farm gate was 150 US$/ton (CRF, 2019) and the average dry season rice yield per hectare was 3.9 ton/ha (Yu & Fan, 2009) while average projected paddy rice areas not being exposed to floods by 2030 is around 97,700 ha (Table 5.7). The worst-case scenario assumes that those areas are no longer exposed to the flood pulse and have become unproductive for rice cultivation and that farmers have implemented no alternative solutions. Using this basic approach, the economic damage could cost up to US$57.10 million (we also assume the price of rice remains the same in 2030, all crop yield will be lost, and the drought risk probability is one hundred percent). This amount is around 0.21% of the country's GDP in 2019 which was US$26.73 billion (IMF, 2019). At the household level, this outcome could slightly decrease household incomes[2] from US$5880 to US$5867. The average area of household agricultural holdings is 1.6 ha (NIS, 2015), so 61,000 households could be expected to be threatened if the extreme scenario above is applied. This number is equivalent to 1.77% of the total number of households[3] in the country in 2017.

This worst-case scenario is unlikely to happen in the short term because the impact being discussed here is projected to happen gradually and farmers will likely shift to adapt to the change of climate and extreme weather events. One possible option farmers might have is to cultivate other suitable alternative crops such as maize and cassava over the affected areas. The choices for alternative crops could be various depending on the circumstances and individual choices. However, one promising indicator farmers can base decision making on is the gross margin. Gross margin is the outcome of gross revenue less intermediate inputs and hired labour (WB, 2015). A study by the World Bank in 2015 showed that for one hectare under cultivation, Cambodian farmers had a gross margin of US$296 for dry season rice, US$304 for maize, and US$506 for cassava (WB, 2015). Therefore, if the land is suitable and conditions permit, cassava could be set as the prioritised crop in term of profitability.

6.4 Study limitations

The interaction between groundwater and the flood extent was not included in this study. This exclusion stemmed from the previous study of the water balance of Tonle Sap's system by Kummu et al. (2014), which did not include groundwater infiltration processes to the floodplain. As the data for inflow and outflow of the Mekong River to Tonle Sap Lake used in

[2] The latest Cambodia Socio-economic survey in 2017 showed that average household income per month is 1,960,000 Riels (NIS, 2018), which is approximately equal to US$490 (exchange rate 4,000Riels = US$1)
[3] The total number of households in 2017 was 3,438,000 (NIS, 2018)

this study was provided by Kummu et al. (2014), the exclusion of groundwater was predetermined.

Also, both HEC-HMS and HEC-RAS models in this study did not take into account the amount of water withdrawals for surface irrigation and domestic water supply, as these data were unavailable. It is expected that population growth and agricultural expansion will continue to increase for decades to come and are likely to have effects on streamflow of the rivers.

Another assumption in this study is that the land cover is static. The land cover dataset from the year 2010 was used in this study to measure changes in paddy rice areas. As a developing country, Cambodia is expected to change its landscape frequently for years to come with sprawling urbanisation and agricultural expansion. However, those changes were not assumed to occur in the seasonally flooded areas closer to Tonle Sap Lake, as they are unsuitable for urban or agricultural expansion.

Another major assumption of this study is the projected rainfall patterns. Projected rainfall for the year 2030 was based on the daily distribution patterns of observed rainfall from 2000 to 2015. The distribution method employed in this study is thought to be the best possible option when data are insufficient.

6.5 Summary

This chapter discussed the results presented in the previous chapter and compared them with previous literature. Results of the first and second objectives partially agreed with previous studies. It then pointed out several possible explanations that might contribute to the discrepancies. For the third objective, to the best of my knowledge, no similar study has been conducted before, so the discussion was somewhat limited.

The chapter then moved on to interpret some noteworthy implications of the projected changes in terms of social, economic and environmental impacts. The decrease of flows in the tributary rivers suggests an increase in drought risk and consequences for household water supply and surface irrigation that divert or extract water from those rivers. The change of the extent of flood pulse suggested that there will be less nutrients and sediment load, which would substantially affect the ecosystems and other inseparable aspects of the larger Mekong River Basin that interconnects with the lake. The reduction of paddy rice areas found in this study underscores the potential implications for social and economic development such as food insecurity, unemployment and economic impacts.

Lastly, the chapter addressed the limitations in this modelling study. The study did not include groundwater and water withdrawals for surface irrigation and household water supply

in the simulations. Also, the study assumed no change to land cover in or outside the study area. Lastly, projected rainfall patterns were daily distributed based on the patterns of the observed rainfall, which might leave some biases. The following chapter summarises the results and conclusions by revisiting the objectives and making recommendations for future studies.

Chapter 7
Conclusions

7.1 Introduction

The objective of this final chapter is to look back at the study's findings and reflect on the research objectives. In addition, it provides some suggestions for future research, based on the gaps found when pursuing this study. Finally, the chapter ends with an overall conclusion of the researcher's thoughts about the processes and the findings in this study.

7.2 Revisiting the research objectives

(1) Determining the impacts of climate change on streamflow of Tonle Sap's tributaries

The first objective of this study was to examine climate change impacts on streamflow of Tonle Sap's tributaries. The results of this objective indicated that streamflow will likely decrease in almost every tributary river, except Boribor and Sen, in which slight increases were projected. The implication is the possibility that there will be more drought risks than floods under the effects of future change of climate. This can be attributed to the decrease of projected rainfall in the basin.

This finding has significant implications for domestic water supply and household agricultural irrigation that are dependent on water withdrawals from those rivers. The insights gained from this objective may be of assistance to relevant authorities at local levels who oversee water use. Regardless of the effects of climate change and frequent drought conditions, water should be used efficiently and be equitably allocated to ensure adequate water for household use and agricultural production, while at the same time maintaining sufficient flows to sustain ecosystems in the rivers. The impacts will be exacerbated due to climate change.

(2) Assessing the impacts of climate change on Tonle Sap's flood pulse contributed by its tributaries

The second significant finding in this study was the decrease in the extent of Tonle Sap's flood pulse. HEC-RAS model analysis revealed that the extent of flood pulse under the effects of climate change would decrease by about 10%. Although the current study is limited because it did not analyse sediment transport in and out of the lake, sediment loads are expected to decrease as the flood pulse decreases. A reduction in area of approximately 10% of floodplain exposed to the pulse highlights a concern for ecosystems, especially fish,

which depend on the nutrients and sediment loads brought by the flood pulse. The disturbance to Tonle Sap's floodplain and its system could lead to various issues in other areas far beyond the lake itself, as discussed in Chapter 6.

Previous literature mainly focused on the impacts of upstream developments on Tonle Sap's flood pulse through the changes in the Mekong's streamflow. However, few studies have investigated the effects of climate change. This study added to knowledge about the impacts of climate change on Tonle Sap Lake by modelling the effects on tributary streamflow and the resulting flood pulse reduction. In addition, the findings of this objective have gone some way towards establishing the basis for national and regional authorities in preparation for future changes that will likely take place in Tonle Sap Lake. Policies, regulations and a mitigation framework can be designed to deal with these upcoming changes.

(3) Evaluating the impacts of climate change on flood recession paddy rice areas in Tonle Sap Basin

This thesis has provided more thorough insights into the potential impact of climate change, not only to the hydrology of Tonle Sap Lake but also to the agricultural production that depends on Tonle Sap's system. The study has identified a possible decrease in area of up to 1,000 km^2 for paddy rice cultivation that is typically supported by the rich nutrients of Tonle Sap's flood pulse. This decrease is in line with the shrinkage of the flood pulse extent. The reduction, however, does not necessarily mean the areas will be wasted or unproductive. The findings in this objective identified the areas that are susceptible to loss of rice paddy production because the areas will no longer be or will be less exposed to floods.

Despite its exploratory nature, this analysis should help to improve predictions of the change of climate on flood recession paddy rice areas. Also, the findings lay the groundwork for future research into an economic impact assessment of climate change on rice cultivation and the study of crop alternatives (such as maize or cassava) to minimise the economic loss in the areas not being exposed to floods.

7.3 Recommendations for future research

While working on this thesis, several emerging topics arose that would be interesting and useful to explore further.

1. Streamflows are driven by runoff from the basin. Although rainfall is the primary driver, there are other factors that contribute to varying runoff, such as changes to land cover. Therefore, more work should be carried out to determine the change in runoff under the combined effects of land-use change and climate change.

2. The connection between surface water and groundwater is significant. However, groundwater was not included in this modelling study due to data limitation. Thus, future study should expand the scope of modelling to cover both surface water and groundwater.
3. Sediment is transported in and out of the lake through the flow of the Tonle Sap River, which is, in turn, driven by the flow of the Mekong River. Alteration in the flow of the Mekong River also contributes to the changes in Tonle Sap's flood pulse. The findings of this study suggest that the flood pulse will grow smaller. However, sediment transport was out of the scope of this study, and therefore, further research could be usefully conducted to determine the changes in sediment loads, and their effects as the flood pulse changes.
4. The damage to rice areas and rice production due to shrinkage of flood pulse in this study was not thoroughly examined. Further work is needed to fully understand these potential economic losses. Future research should be undertaken to investigate how replacing rice with alternative crops such as maize or cassava over the affected areas might reduce the extent of economic impacts, while taking into account the environmental consequences of planting these crops and the changes that might have to the hydrological regime of the basin.

7.4 Final conclusions

Overall, this study aimed to evaluate the impacts of climate change on major hydrological elements of Tonle Sap Lake. The focus of this study was the impacts of climate change by the year 2030 on Tonle Sap's tributary rivers, flood pulse and floodplain paddy rice areas. Data availability constraints were the most significant limitation for this modelling study. The modelling software HEC-HMS, HEC-RAS and GIS were practically useful and complemented each other well.

The findings from this study make several contributions to the current body of literature. First, the study helped to address the uncertainties of climate change impacts on future water availability at the basin scale. Second, the findings enhance understanding of potential changes to Tonle Sap's flood pulse by considering the changes to tributaries' inflows and the changes to Mekong River inflow and outflow. The results, therefore, fill a gap in current knowledge. Lastly, this study is the first of its kind to attempt to draw attention to the flood recession paddy rice areas that are prone to be adversely affected by climate change, though further work is needed to fully assess the magnitude of damage and its cost. At least in this area of Cambodia, climate change has been confirmed as posing various negative impacts, which threaten the livelihoods and well-being of humans and animals that are dependent on the resources provided by the lake.

Again, the findings from this study remind us that climate change affects not only the environment but also the economy and society as a whole. Thus, it should not be overlooked, and should always be taken into account in each step of any decisions to be made.

References

Abushandi, E., & Merkel, B. (2013). Modelling rainfall runoff relations using HEC-HMS and IHACRES for a single rain event in an arid region of Jordan. *An International Journal - Published for the European Water Resources Association (EWRA), 27*(7), 2391-2409. doi:10.1007/s11269-013-0293-4

ADB (Asian Development Bank). (2005). *The Tonle Sap Basin strategy*.

ADB (Asian Development Bank). (2009). *The economics of climate change in Southeast Asia: A regional review*. Manila: ADB.

ADB (Asian Development Bank). (2012). *Cambodia: Water supply and sanitation sector assessment, strategy and roadmap*. Mandaluyong City, Philippines: ADB.

ADB (Asian Development Bank). (2013). *Asia-Pacific aspirations: Perspectives for a post 2015 development agenda*. Bangkok: ESCAP, ADB, UNDP.

Akhtar, R. (2016). Climate change and geoecology of South and Southeast Asia: An introduction. In R. Akhtar (Ed.), *Climate Change and Human Health Scenario in South and Southeast Asia* (pp. 1-10). Cham, Heidelberg, New York, Dordrecht, London: Springer.

Ali, M., Khan, S. J., Aslam, I., & Khan, Z. (2011). Simulation of the Impacts of land-use change on surface runoff of Lai Nullah Basin in Islamabad, Pakistan. *Landscape and Urban Planning, 102*, 271-279. doi:10.1016/j.landurbplan.2011.05.006

Amin, A., Nasim, W., Mubeen, M., Kazmi, D. H., Lin, Z., Wahid, A., Sultana, S. R., Gibbs, J., & Fahad, S. (2017). Comparison of future and base precipitation anomalies by SimCLIM statistical projection through ensemble approach in Pakistan. *Atmospheric Research, 194*(C), 214-225. doi:10.1016/j.atmosres.2017.05.002

Anirudh, R., & Giridhar, M. V. S. S. (2015). *Digital elevation model generation using SRTM*. Paper presented at the 2nd National Conference on Water, Environment and Society, Hyderabad, India.

AQUASTAT. (2011). *Irrigation areas factsheets: Cambodia*. Retrieved from: http://www.fao.org/aquastat/en/countries-and-basins/country-profiles/country/KHM

Arias, M. E., Piman, T., Lauri, H., Cochrane, T. A., & Kummu, M. (2014). Dams on Mekong tributaries as significant contributors of hydrological alterations to the Tonle Sap floodplain in Cambodia. *Hydrology and Earth System Sciences, 18*, 5303-5315. doi:10.5194/hess-18-5303-2014

Aydinalp, C., & Cresser, M. S. (2008). The effects of global climate change on agriculture. *American-Eurasian Journal of Agriculture and Environmental Sciences, 3*(5), 672-676.

Bhat, M. S., Ahmad, B., Alam, A., Farooq, H., & Ahmad, S. (2019). Flood hazard assessment of the Kashmir Valley using historical hydrology. *Journal of Flood Risk Management, 12*(1), 1-13. doi:10.1111/jfr3.12521

Boncori, J. P. M. (2016). Caveats concerning the use of SRTM DEM version 4.1 (CGIAR-CSI). *Remote Sensing, 8*(10), 793. doi:10.3390/rs8100793

Bündnis Entwicklung Hilft and Ruhr University Bochum. (2018). *World risk report 2018*. Retrieved from https://reliefweb.int/sites/reliefweb.int/files/resources/WorldRiskReport-2018.pdf

Campbell, I. C., Say, S., & Beardall, J. (2009). Tonle Sap Lake, the heart of the Lower Mekong. In I. C. Campbell (Ed.), *The Mekong: Biophysical Environment of an International River Basin* (pp. 251-270). New York: Academic Press, Elsevier.

CCC (Christchurch City Council). (2003). *Waterways, wetlands and drainage guide*.

CDRI (Cambodia Development Resource Institute). (2012). *Annual development review 2011-12*. Phnom Penh, Cambodia: CDRI.

CIFOR (Center for International Forestry Research). (2012). *Forests and water: What policymakers should know*. Retrieved from https://www.cifor.org/publications/pdf_files/factsheet/4061-factsheet.pdf

Cosslett, T. L., & Cosslett, P. D. (2018). *Sustainable development of rice and water resources in Mainland Southeast Asia and Mekong River Basin*. Singapore: Singapore: Springer Singapore.

CRF (Cambodia Rice Federation). (2019). Paddy price. Retrieved from http://www.crf.org.kh/

Dhar, S., & Mazumdar, A. (2009). Impacts of climate change under the threat of global warming for an agricultural watershed of the Kangsabati River. *International Journal of Agricultural and Biosystems Engineering, 3*(3), 136-145.

Ding, Y., Hayes, M. J., & Widhalm, M. (2010). Measuring economic impacts of drought: A review and discussion. *Papers in Natural Resources, 196*.

Doyle, S. (2012). *City of water: Architecture, infrastructure and the floods of Phnom Penh*. Retrieved from https://www.acsa-arch.org/proceedings/Fall%20Conference%20Proceedings/ACSA.FALL.13/ACSA.FALL.13.3.pdf

FA (Forest Administration of Cambodia). (2010). *National forest programme 2010 - 2029*. Retrieved from http://www.cdc-crdb.gov.kh/cdc/documents/Sector_Strategy/6_Forestry_Reform/National_Forest_Programme_2010_2029_Eng.pdf.

FAO (Food and Agriculture Organisation). (2009). *How to feed the world in 2050*. Retrieved from http://www.fao.org/fileadmin/templates/wsfs/docs/expert_paper/How_to_Feed_the_World_in_2050.pdf

FAO (Food and Agriculture Organisation). (2016). *AQUASTAT database glossary*. Retrieved from: http://www.fao.org/nr/water/aquastat/data/glossary/search.html

FAO (Food and Agriculture Organisation). (2017). *Drought characteristics and management in Central Asia and Turkey*. Retrieved from http://www.fao.org/3/a-i6738e.pdf

FAO (Food and Agriculture Organisation), IFAD (International Fund for Agricultural Development), UNICEF (United Nations Children's Fund), WFP (World Food Programme), & WHO (World Health Organisation). (2019). *The state of food security and nutrition in the world 2019. Safeguarding against economic slowdowns and downturns.* Rome: FAO.

Fox, J. M., & Ledgerwood, J. (1999). Dry-season flood-recession rice in the Mekong Delta: Two thousand years of sustainable agriculture? *Asian Perspective, 38*(1), 37-50.

Germanwatch. (2019). *Global climate risk index 2019*. Germany: Germanwatch.

Global Carbon Atlas. (2018). Carbon dioxide emissions: 2016. Retrieved from http://emission2015.globalcarbonatlas.org/en/CO2-emissions

Halwatura, D., & Najim, M. M. M. (2013). Application of the HEC-HMS model for runoff simulation in a tropical catchment. *Environmental Modelling and Software, 46*(C), 155-162. doi:10.1016/j.envsoft.2013.03.006

Hoang, L. P., van Vliet, M. H., Kummu, M., Lauri, H., Koponen, J., Supit, I., Leemans, R., Kabat, P., & Ludwig, F. (2019). The Mekong's future flows under multiple drivers: How climate change, hydropower developments and irrigation expansion drive hydrological changes. *Science of the Total Environment, 649*, 601-609. doi:10.1016/j.scitotenv.2018.08.160

Huang, Y., Chen, S., Cao, Q., Hong, Y., Wu, B., Huang, M., Qiao, L., Zhang, Z., Li, Z., Li, W., & Yang, X. (2014). Evaluation of version-7 TRMM multi-satellite precipitation analysis product during the Beijing extreme heavy rainfall event of 21 July 2012. *Water, 6*(1), 32-44. doi:10.3390/w6010032

Huntington, T. G. (2006). Evidence for intensification of the global water cycle: Review and synthesis. *Journal of Hydrology, 319*, 83-95. doi:10.1016/j.jhydrol.2005.07.003

IMF (International Monetary Fund). (2019). GDP, current prices. Retrieved from https://www.imf.org/external/datamapper/NGDPD@WEO/OEMDC/ADVEC/WEOWORLD/KHM

IPCC (Intergovernmental Panel on Climate Change). (2014). *Climate change 2014: Synthesis report. Contribution of working groups I, II and III to the Fifth Assessment Report of the Intergovernmental Panel on Climate Change.* Geneva, Switzerland: IPCC.

Jha, A. K., Bloch, R., & Lamond, J. (2012). *Cities and flooding: A guide to integrated urban flood risk management for the 21st century* (T. W. Bank Ed.). Washing, D.C.: The World Bank.

Jin, H., Liang, R., Wang, Y., & Tumula, P. (2015). Flood-runoff in semi-arid and sub-humid regions, a case study: A simulation of Jianghe watershed in northern China. *Water (Switzerland), 7*(9), 5155-5172. doi:10.3390/w7095155

Johnston, R., Try, T., & Silva, S. (2013). *Agricultural water management planning in Cambodia*.

Junk, W. J. (1989). Flood tolerance and tree distribution in central Amazonian floodplains. In L. B. Holm-Nielsen, I. C. Nielsen, & H. Balslev (Eds.), *Tropical forests: Botanical dynamics, speciation and diversity* (pp. 47-64). London: Academic Press.

Junk, W. J., & Wantzen, K. M. (2004). The flood pulse concept: New aspects, approaches and application - an update. In R. L. Welcomme & T. Petr (Eds.), *Proceedings of the second international symposium on the management of large rivers for fisheries* (pp. 117-149). Bangkok, Thailand: Food and Agriculture Organisation (FAO) and Mekong River Commission (MRC).

Karl, T. R., Meehl, G. A., Peterson, T. C., Kunkel, K. E., Gutowski, W. J., & Easterling, D. R. (2008). Executive Summary. In T. R. Karl, G. A. Meehl, C. D. Miller, S. J. Hassol, A. M. Waple, & W. L. Murray (Eds.), *Weather and climate extremes in a changing climate. Regions of focus: North America, Hawaii, Caribbean, and U.S. Pacific Islands* (pp. 1-10). Washington, DC: Department of Commerce, NOAA's National Climatic Data Center.

Keane, J., Page, S., Kergna, A., & Kennan, J. (2009). *Climate change and developing country agriculture: An overview of expected impacts, adaptation and mitigation challenges, and funding requirements*. International Centre for Trade and Sustainable Development, Geneva, Switzerland and International Food & Agricultural Trade Policy Council, Washington DC, USA: ICTSD-IPC Platform on Climate Change, Agriculture and Trade.

Keskinen, M., Chinvanno, S., Kummu, M., Nuorteva, P., Snidvongs, A., Varis, O., & Västilä, K. (2009). *Water and climate change in the Lower Mekong Basin: Diagnosis & recommendations for adaptation.* Helsinki University of Technology, Espoo, Finland: Water & Development Publications.

Keskinen, M., Käkönen, M., Tola, P., & Varis, O. (2007). The Tonle Sap Lake, Cambodia: water-related conflicts with abundance of water. *2007, 2*(2), 49-59.

Kim, S., & Chem, P. (2014). *Climate change vulnerability and adaptation assessment methods and tools applied in Cambodia*. Phnom Penh: CDRI.

Kim, S., Sohn, H., Kim, M., & Lee, H. (2019). Analysis of the relationship among flood severity, precipitation, and deforestation in the Tonle Sap Lake Area, Cambodia using multi-sensor approach. *KSCE Journal of Civil Engineering, 23*(3), 1330-1340. doi:10.1007/s12205-019-1061-7

Kimsun, T., & Bopharath, S. (2013). Poverty and the environment in rural Cambodia. In A. Ananta, A. Bauer, & M. Thant (Eds.), *Environments of the Poor in Southeast Asia, East Asia and the Pacific*. Singapore: Institute of Southeast Asian Studies.

Kirby, M., Krittasudthacheewa, C., Mainuddin, M., Kemp-Benedict, E., Swartz, C., & de la Rosa, E. (2009). *Mekong Basin focal project: Final report*. Colombo, Sri Lanka: Challenge Program on Water and Food.

Kumar, N., Tischbein, B., Kusche, J., Laux, P., Beg, M. K., & Bogardi, J. J. (2017). Impact of climate change on water resources of upper Kharun catchment in Chhattisgarh, India. *Journal of Hydrology: Regional Studies, 13*(C), 189-207. doi:10.1016/j.ejrh.2017.07.008

Kummu, M., Koponen, J., & Sarkkula, J. (2004). *Upstream impacts on Lower Mekong floodplains: Tonle Sap case study*. Paper presented at the International Conference on Advances in Integrated Mekong River Management, Vientiane.

Kummu, M., Penny, D., Sarkkula, J., & Koponen, J. (2008). Sediment: curse or blessing for Tonle Sap Lake? *Ambio, 37*(3), 158-163. doi:10.1579/0044-7447(2008)37[158:SCOBFT]2.0.CO;2

Kummu, M., & Sarkkula, J. (2008). Impact of the Mekong River flow alteration on the Tonle Sap flood pulse. *Ambio, 37*(3), 185-192.

Kummu, M., Tes, S., Yin, S., Adamson, P., Jozsa, J., Koponen, J., Richey, J., & Sarkkula, J. (2014). Water balance analysis for the Tonle Sap Lake-floodplain system. *Hydrological Processes, 28*, 1722-1733. doi:10.1002/hyp.9718

Lauri, H., Räsänen, T. A., & Kummu, M. (2014). Using reanalysis and remotely sensed temperature and precipitation data for hydrological modeling in monsoon climate: Mekong River case study. *Journal of Hydrometeorology, 15*(4), 1532-1545. doi:10.1175/JHM-D-13-084.1

Liu, Z., Ostrenga, D., Teng, W., & Kempler, S. (2012). Tropical Rainfall Measuring Mission (TRMM) precipitation data and services for research and applications. *Bulletin of the American Meteorological Society, 93*(9), 1317-1325. doi:10.1175/BAMS-D-11-00152.1

Loliyana, V. D., & Patel, P. L. (2012). *Calibration and performance of HEC-RAS hydrodynamic model for stage prediction in Lower Tapi River*. Paper presented at the Hydraulic and Water Resources (HYDRO 2012), Bombay, India.

Ly, S., Kim, L., Demerre, S., & Heng, S. (2018). Flood mapping along the Lower Mekong River in Cambodia. *Engineering Journal, 22*(1). doi:10.4186/ej.2018.22.1.269

McCracken, K., & Phillips, D. R. (2016). Climate change and the health of older people in Southeast Asia. In R. Akhtar (Ed.), *Climate Change and Human Health Scenario in South and Southeast Asia* (pp. 29-54). Cham, Heidelberg, New York, Dordrecht, London: Springer.

Men, B., Liu, H., Tian, W., Wu, Z., & Hui, J. (2019). The impact of reservoirs on runoff under climate change: A case of Nierji Reservoir in China. *Water, 11*(5). doi:10.3390/w11051005

Misra, A. K. (2014). Climate change and challenges of water and food security. *International Journal of Sustainable Built Environment, 3*(1), 153-165. doi:10.1016/j.ijsbe.2014.04.006

MoE (Ministry of Environment). (2009). *Cambodia environment outlook*. Retrieved from https://wedocs.unep.org/bitstream/handle/20.500.11822/8689/Cambodia_environment_outlook.pdf?sequence=3&isAllowed=y

MoE (Ministry of Environment). (2015). *Cambodia's second national communication (SNC)*. Cambodia: MoE.

MoE (Ministry of Environment). (2016a). *Climate change action plan 2016-2018*. Phnom Penh: MoE.

MoE (Ministry of Environment). (2016b). *A second study on understanding of public perception of climate change in Cambodia: Knowledge, attitudes and practices.* Phnom Penh: MoE.

MoE (Ministry of Environment), & UNDP (United Nations Development Programme). (2011). *Building resilience: The future of rural livelihoods in the face of climate change. Cambodia human development report 2011*.

Mohktar, E. S., Pradhan, B., Ghazali, A. H., & Shafri, H. Z. M. (2018). Assessing flood inundation mapping through estimated discharge using GIS and HEC-RAS model. *Arabian Journal of Geosciences, 11*, 1-20. doi:10.1007/s12517-018-4040-2

MoP (Ministry of Planning). (2009). *General population census of Cambodia 2008 (National report on final census result)*. Phnom Penh: National Institute of Statistics.

Moriasi, D. N., Gitau, M. W., Pai, N., & Daggupati, P. (2015). Hydrologic and water quality models: Performance measures and evaluation criteria. *Hydrologic and Water Quality Models: Performance Measures and Evaluation Criteria, 58*(6), 1763-1785. doi:10.13031/trans.58.10715

Moss, R. H., Edmonds, J. A., Hibbard, K. A., Manning, M. R., Rose, S. K., van Vuuren, D. P., Carter, T. R., Emori, S., Kainuma, M., Kram, T., Meehl, G. A., Mitchell, J. F. B., Nakicenovic, N., Riahi, K., Smith, S. J., Stouffer, R. J., Thomson, A. M., Weyant, J. P., & Wilbanks, T. J. (2010). The next generation of scenarios for climate change research and assessment. *Nature, 463*, 747-756. doi:10.1038/nature08823

MoWRAM (Ministry of Water Resources and Meteorology). (2013). *Climate change strategic plan for water resources and meteorology*. Phnom Penh.

MRC (Mekong River Commission). (2009). *The flow of the Mekong*. Retrieved from http://www.mrcmekong.org/assets/Publications/report-management-develop/MRC-IM-No2-the-flow-of-the-mekong.pdf

MRC (Mekong River Commission). (2010). *State of the Basin Report 2010*. Retrieved from http://www.mrcmekong.org/AF69E849-8579-4E69-9CC2-42B23FDD84A4/FinalDownload/DownloadId-7BF012216959827E427CF16B2D9A072D/AF69E849-8579-4E69-9CC2-42B23FDD84A4/assets/Publications/basin-reports/MRC-SOB-Summary-reportEnglish.pdf

MRC (Mekong River Commission). (2011). *Flood situation report 2011*. Retrieved from http://www.mrcmekong.org/assets/Publications/technical/Tech-No36-Flood-Situation-Report2011.pdf

MRC (Mekong River Commission). (2012). *The impact & management of floods & droughts in the Lower Mekong Basin & the implications of possible climate change*. Retrieved from http://www.mrcmekong.org/assets/Publications/basin-reports/FMMP-working-paper-110820.pdf

MRC (Mekong River Commission). (2014). *Irrigation for food security, poverty alleviation and rural development in the LMB*. Retrieved from http://www.mrcmekong.org/assets/Publications/basin-reports/AIP211-DFV1907CEdNSTLpj260914.pdf

MRC (Mekong River Commission). (2016). *Land cover map of the Lower Mekong Basin*.

Muis, S., Güneralp, B., Jongman, B., Aerts, J. C. J. H., & Ward, P. J. (2015). Flood risk and adaptation strategies under climate change and urban expansion: A probabilistic analysis using global data. *Science of the Total Environment, 538*, 445-457. doi:10.1016/j.scitotenv.2015.08.068

NIS (National Institute of Statistics). (2015). *Census of Agriculture of the Kingdom of Cambodia 2013*. Retrieved from https://www.nis.gov.kh/nis/CAC2013/Final_Report_En.pdf

NIS (National Institute of Statistics). (2018). *Cambodia socio-economic survey 2017*. Retrieved from https://www.nis.gov.kh/nis/CSES/Final%20Report%20CSES%202017.pdf

OECD (Organisation for Economic Cooperation and Development). (2013). *Water and climate change adaptation: Policies to navigate uncharted waters*. Retrieved from https://www.oecd.org/env/water-and-climate-change-adaptation-9789264200449-en.htm

OECD (Organisation for Economic Cooperation and Development). (2015). *The economic consequences of climate change*. Paris: OECD.

Oeurng, C., Cochrane, T. A., Chung, S., Kondolf, M. G., Piman, T., & Arias, M. E. (2019). Assessing climate change impacts on river flows in the Tonle Sap Lake Basin, Cambodia. *Water, 11*(3), 1-27. doi:10.3390/w11030618

Perera, E. D. P., Sayama, T., Magome, J., & Hasegawa, A. (2017). RCP8.5-based future flood hazard analysis for the Lower Mekong River Basin. *Hydrology, 55*(4). doi:10.3390/hydrology4040055

Piman, T., Cochrane, T. A., Arias, M. E., Dat, N. D., & Vonnarart, O. (2014). Managing hydropower under climate change in the Mekong tributaries. In S. Shrestha, A. K. Anal, P. A. Salam, & M. van der Valk (Eds.), *Managing Water Resources under Climate Uncertainty: Examples from Asia, Europe, Latin America, and Australia* (pp. 223-248). Cham, Switzerland: Springer International Publishing.

Quirino, D. T., Casaroli, D., Jucá, R. A., Mesquita, M., Pego, A. W., & Alves, J. (2017). Evaluation of TRMM satellite rainfall estimates (algorithms 3B42 V7 & RT) over the Santo Antônio county (Goiás, Brazil). *Revista Facultad Nacional de Agronomía Medellín, 70*(3), 8251-8261. doi:10.15446/rfna.v70n3.61805

RGC (Royal Government of Cambodia). (2014). *Post-flood early recovery need assessment report*. Retrieved from http://www.kh.undp.org/content/dam/cambodia/docs/PovRed/Cambodia%20post-flood%20recovery%20need%20assessment%20report.pdf

RGC (Royal Government of Cambodia). (2018). *Rectangular strategy phase IV for growth, employment, equity and efficiency: Building the foundation toward realizing the Cambodia Vision 2050*. Cambodia: Royal Government of Cambodia.

Rodríguez, E., Morris, C. S., & Eric Belz, J. (2006). A global assessment of the SRTM performance. *Photogrammetric Engineering & Remote Sensing, 72*(3), 249-260.

Sahoo, A. K., Sheffield, J., Pan, M., & Wood, E. F. (2015). Evaluation of the tropical rainfall measuring mission multi-satellite precipitation analysis (TMPA) for assessment of large-scale meteorological drought. *Remote Sensing of Environment, 159*, 181-193. doi:10.1016/j.rse.2014.11.032

Schmeling, M. (2019). Cambodia, shaded relief map. Retrieved from https://www.123rf.com/photo_10768866_cambodia-shaded-relief-map-colored-according-to-elevation-with-major-urban-areas-includes-clip-path-.html

Sharma, A., & Tiwari, K. N. (2014). A comparative appraisal of hydrological behavior of SRTM DEM at catchment level. *Journal of Hydrology, 519*(PB), 1394-1404. doi:10.1016/j.jhydrol.2014.08.062

Shrestha, S. (2014). *Climate change impacts and adaptation in water resources and water use sectors: Case studies from Southeast Asia*. Cham, Heidelberg, New York, Dordrecht, London: Springer.

Smith, D., & Hornbuckle, J. (2013). A review on rice productivity in Cambodia and water use measurement using direct and indirect methods on a dry season rice crop.

Tan, M. L., & Duan, Z. (2017). Assessment of GPM and TRMM precipitation products over Singapore. *Remote Sensing, 9*(7), 720. doi:10.3390/rs9070720

Teng, F., Huang, W., & Ginis, I. (2018). Hydrological modeling of storm runoff and snowmelt in Taunton River Basin by applications of HEC-HMS and PRMS models. *Journal of the International Society for the Prevention and Mitigation of Natural Hazards, 91*(1), 179-199. doi:10.1007/s11069-017-3121-y

Tol, R. S. J. (2018). The economic impacts of climate change. *Review of Environmental Economics and Policy, 12*(1), 4-25. doi:10.1093/reep/rex027

Turunen, J., Snäkin, J.-P., Panula-Ontto, J., Lindfors, H., Kaisti, H., Luukkanen, J., Magistretti, S., & Mang, C. (2011). *Livelihood resilience and food security in Cambodia: Results of a household survey, knowledge for development project: Creating rural resources database for sustainable livelihoods in Cambodia*. Retrieved from Helsinki, Finland: https://www.utu.fi/fi/yksikot/ffrc/julkaisut/e-tutu/Documents/eTutu_2011-1.pdf

UN-Water (United Nations Water). (2010). *Climate change adaptation: The pivotal role of water*.

UN (United Nations). (2018). *Sustainable development goal 6: Synthesis report on water and sanitation*. New York: UN.

UN (United Nations). (2019). World population prospects 2019. Retrieved from https://population.un.org/wpp/

UN OCHA (United Nations Office for the Coordination of Humanitarian Affairs). (2017). *Cambodia: Country profile*. Retrieved from https://www.unocha.org/asia-and-pacific-roap/cambodia

UNESCAP (United Nations Economic and Social Commission for Asia and the Pacific). (2010). *Protecting development gains: Reducing disaster vulnerability and building resilience in Asia and the Pacific*. Bangkok: UNESCAP.

UNFPA (United Nations Population Fund). (2019). *State of world population 2019*.

UNISDR (United Nations International Strategy for Disaster Reduction). (2010). *ASEAN disaster risk management initiative: Synthesis report on ten ASEAN countries disaster risks assessment*. Retrieved from https://www.unisdr.org/files/18872_asean.pdf

US ACE (US Army Corps of Engineers). (2016a). *Hydrologic modeling system (HEC-HMS): User's manual (version 4.2)*.

US ACE (US Army Corps of Engineers). (2016b). *River analysis system (HEC-RAS): 2D modeling user's manual (version 5.0)*.

US ACE (US Army Corps of Engineers). (2016c). *River analysis system (HEC-RAS): Hydraulic reference manual (version 5.0)*.

US ACE (US Army Corps of Engineers). (2018). *HEC-RAS two-dimensional modeling: Lake Wausau, Wisconsin River and tributaries Big Rib River and Eau Claire River*.

van Vuuren, D. P., Edmonds, J., Kainuma, M., Riahi, K., Thomson, A., Hibbard, K., Hurtt, G. C., Kram, T., Krey, V., Lamarque, J., Masui, T., Meinshausen, M., Nakicenovic, N., Smith, S. J., & Rose, S. K. (2011). The representative concentration pathways: An overview. *Climate Change, 109*, 5-31. doi:10.1007/s10584-011-0148-z

Varis, O., & Keskinen, M. (2003). Socio-economic analysis of the Tonle Sap Region, Cambodia: Building links and capacity of targeted poverty alleviation. *Water Resources Development, 19*(2), 295-310. doi:10.1080/0790062032000089374

Varis, O., Kummu, M., Keskinen, M., Sarkkula, J., Koponen, J., & Heinonen, U. (2006). Integrated water resources management on the Tonle Sap Lake, Cambodia. *Water Science & Technology: Water Supply, 6*(5), 51-58. doi:10.2166/ws.2006.843

Verma, A., Jha, M., & Mahana, R. (2010). Evaluation of HEC-HMS and WEPP for simulating watershed runoff using remote sensing and geographical information system. *Paddy and Water Environment, 8*(2), 131-144. doi:10.1007/s10333-009-0192-8

Warrick, R. A., Ye, W., Kouwenhoven, P., Hay, J. E., & Cheatham, C. (2005). *New developments of the SimCLIM model for simulating adaptation to risks arising from climate variability and change*. Conference held at Melbourne, Australia. Conference Contribution retrieved from https://hdl.handle.net/10289/5486

WB (World Bank). (2013). *Turn down the heat: climate extremes, regional impacts, and the case for resilience.* Washington DC: World Bank.

WB (World Bank). (2015). *Cambodian agriculture in transition: Opportunities and risks*. Retrieved from http://documents.worldbank.org/curated/en/805091467993504209/pdf/96308-ESW-KH-White-cover-P145838-PUBLIC-Cambodian-Agriculture-in-Transition.pdf

WB (World Bank). (2017). *Cambodia - Sustaining strong growth for the benefit of all. Overview.* Washington, D.C: World Bank Group.

Wihite, D. A., & Glantz, M. H. (1985). Understanding the drought phenomenon: The role of definitions. *Drought Mitigation Center Faculty Publications, 20*.

Yu, B., & Fan, S. (2009). *Rice production response in Cambodia*. Paper presented at the International Association of Agricultural Economists Conference, Beijing, China.

Yu, W., Kim, Y., Lee, D., & Lee, G. (2019). Hydrological assessment of basin development scenarios: Impacts on the Tonle Sap Lake in Cambodia. *Quaternary International, 503*, 115-127. doi:10.1016/j.quaint.2018.09.023

Yusuf, A. A., & Francisco, H. (2009). *Climate change vulnerability mapping for Southeast Asia*. St. Louis: Federal Reserve Bank of St Louis.

Zema, D. A., Labate, A., Martino, D., & Zimbone, S. M. (2017). Comparing different infiltration methods of the HEC-HMS model: The case study of the Mésima Torrent (Southern Italy). *Land Degradation & Development, 28*, 294-308. doi:10.1002/ldr.2591

Appendix A

Number of Rainy Days

	Santuk	Kampong Thom	Staung	Chikreng	Siem Reap	Oddar Meanchey	Banteay Meanchey	Battambong	Maung Russey	Pursat	Rolea B'ier
2000	161	153	141	149	146	148	115	141	140	169	172
2001	146	135	138	149	126	161	142	143	142	144	149
2002	141	140	136	140	141	149	143	149	159	147	138
2003	144	119	123	139	120	130	123	146	132	124	138
2004	160	133	118	136	120	120	128	161	133	126	128
2005	140	126	125	133	142	154	153	133	154	140	182
2006	142	130	132	132	127	149	189	173	165	149	159
2007	157	135	130	151	135	138	145	154	154	155	150
2008	162	136	146	140	141	154	146	152	153	152	144
2009	147	146	138	144	139	163	147	157	139	151	149
2010	131	122	126	131	127	132	138	152	151	149	133
2011	141	135	132	142	148	140	141	144	140	150	137
2012	141	137	127	141	145	155	157	146	154	141	160
2013	142	130	131	137	146	136	145	151	154	146	131
2014	155	135	128	135	127	138	131	130	134	138	134
2015	126	119	118	113	121	124	117	145	125	145	122

Appendix B

Hydrographs

B.1 Hydrographs of the Observed and Simulated Discharge

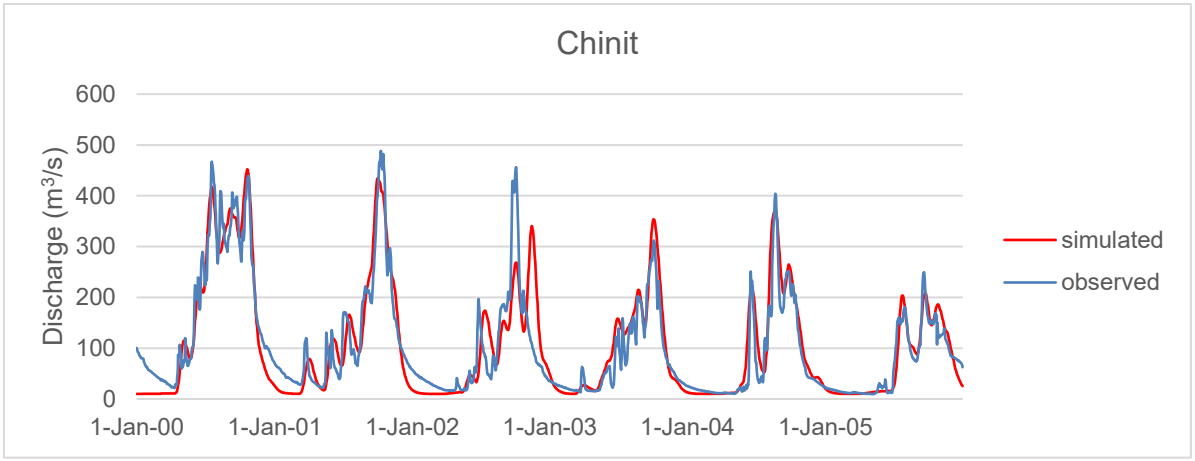

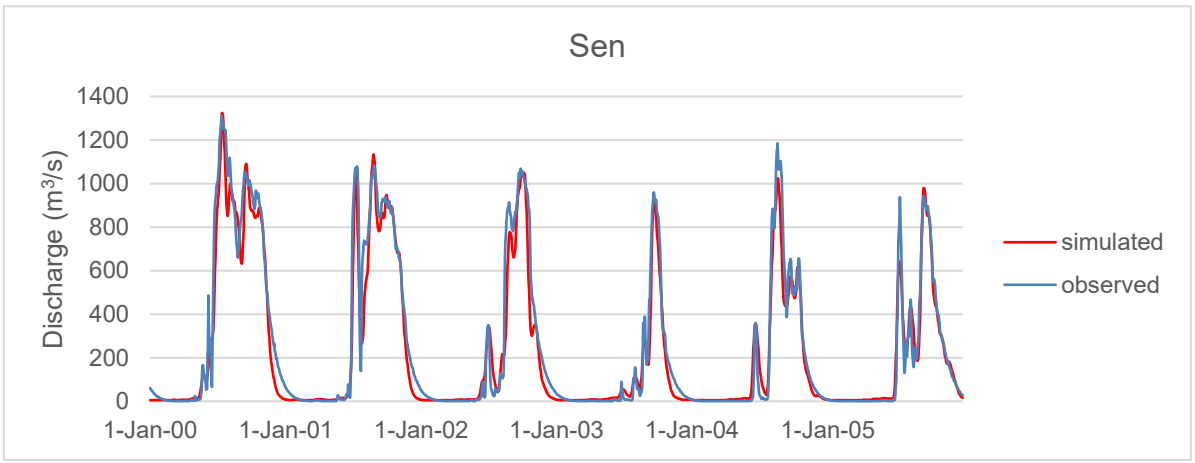

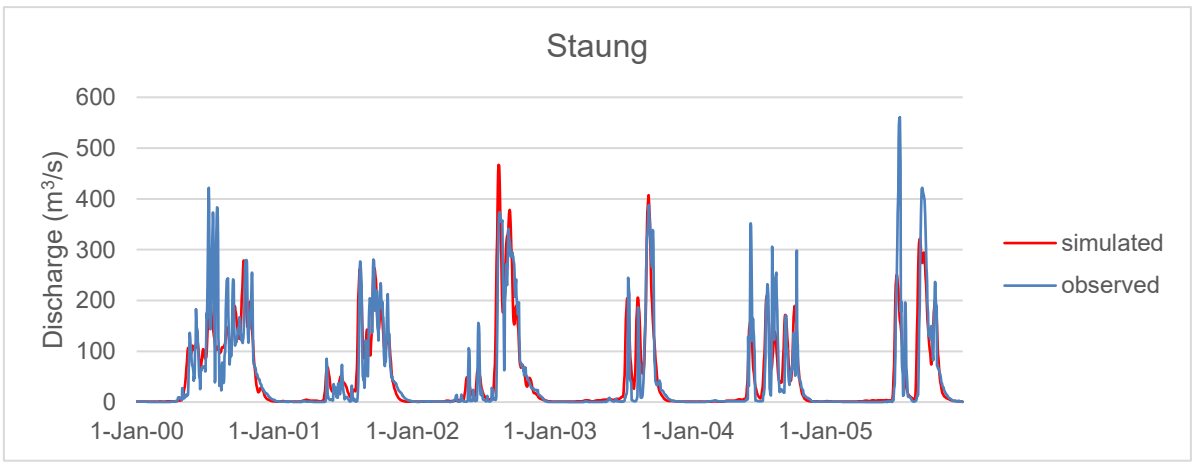

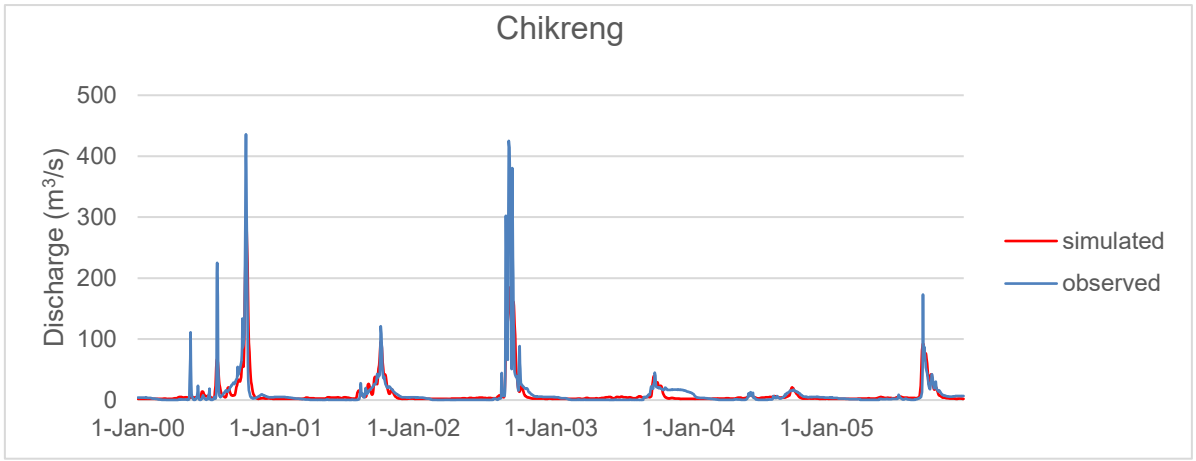
Chikreng
Discharge (m3/s)
500
400
300
200
100
0
1-Jan-00
1-Jan-01
1-Jan-02
1-Jan-03
1-Jan-04
1-Jan-05
simulated
observed

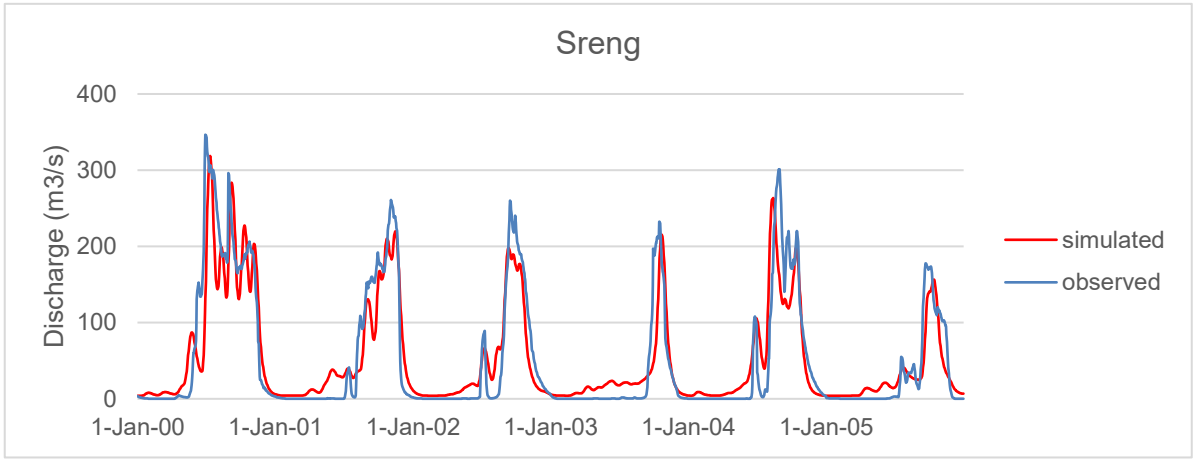
Sreng
Discharge (m3/s)
400
300
200
100
0
1-Jan-00
1-Jan-01
1-Jan-02
1-Jan-03
1-Jan-04
1-Jan-05
simulated
observed

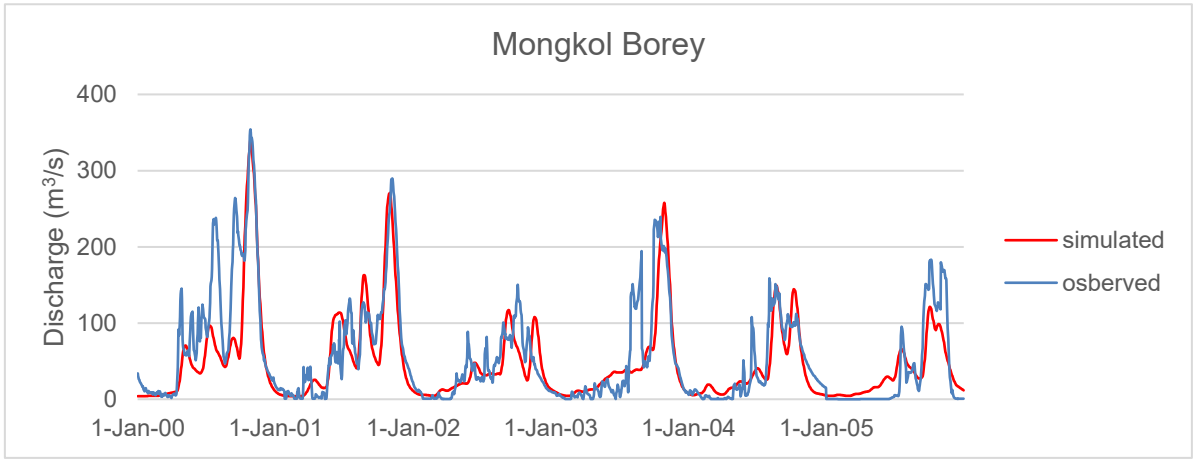
Mongkol Borey
Discharge (m3/s)
400
300
200
100
0
1-Jan-00
1-Jan-01
1-Jan-02
1-Jan-03
1-Jan-04
1-Jan-05
simulated
osberved

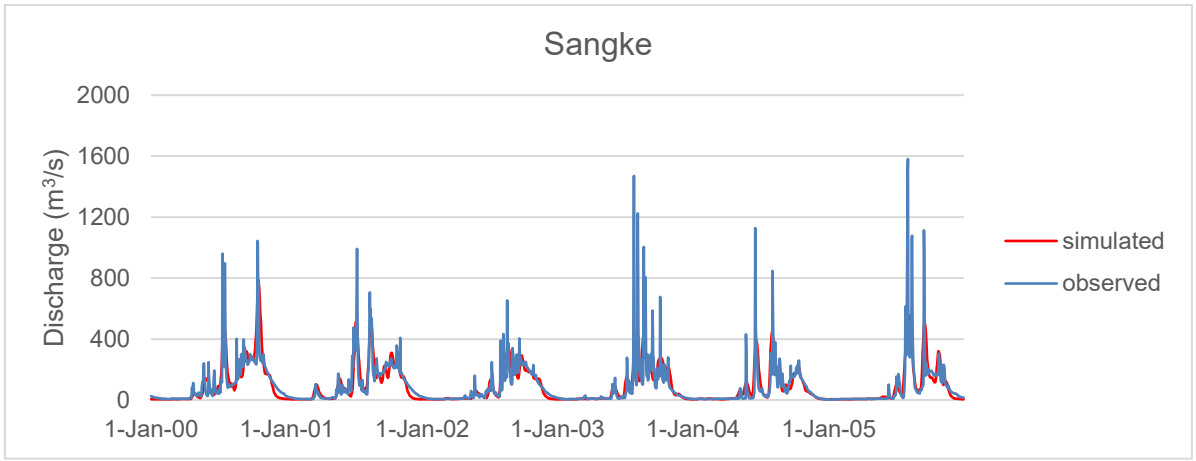
Sangke
Discharge (m3/s)
2000
1600
1200
800
400
0
1-Jan-00
1-Jan-01
1-Jan-02
1-Jan-03
1-Jan-04
1-Jan-05
simulated
observed

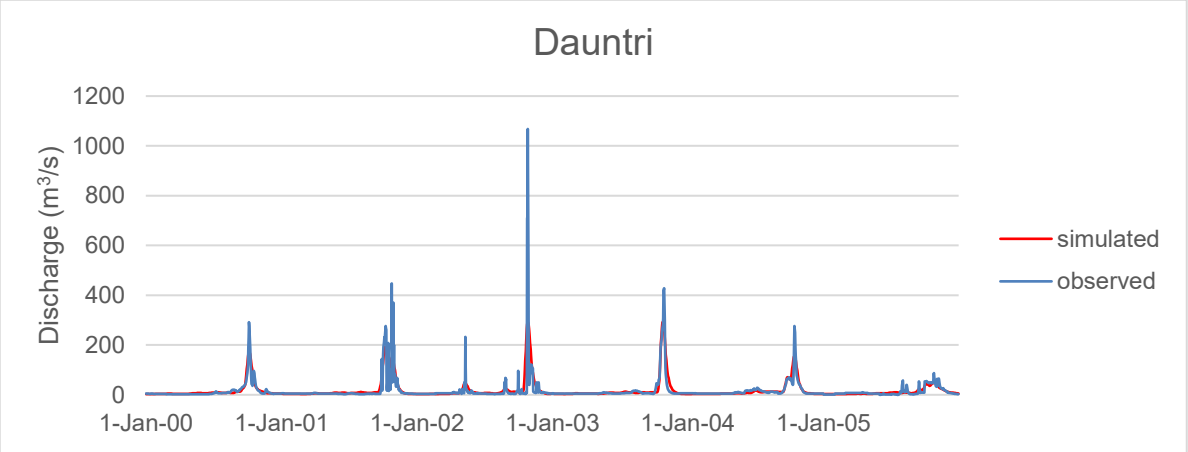
Dauntri
Discharge (m³/s)
1200
1000
800
600
400
200
0
1-Jan-00
1-Jan-01
1-Jan-02
1-Jan-03
1-Jan-04
1-Jan-05
simulated
observed

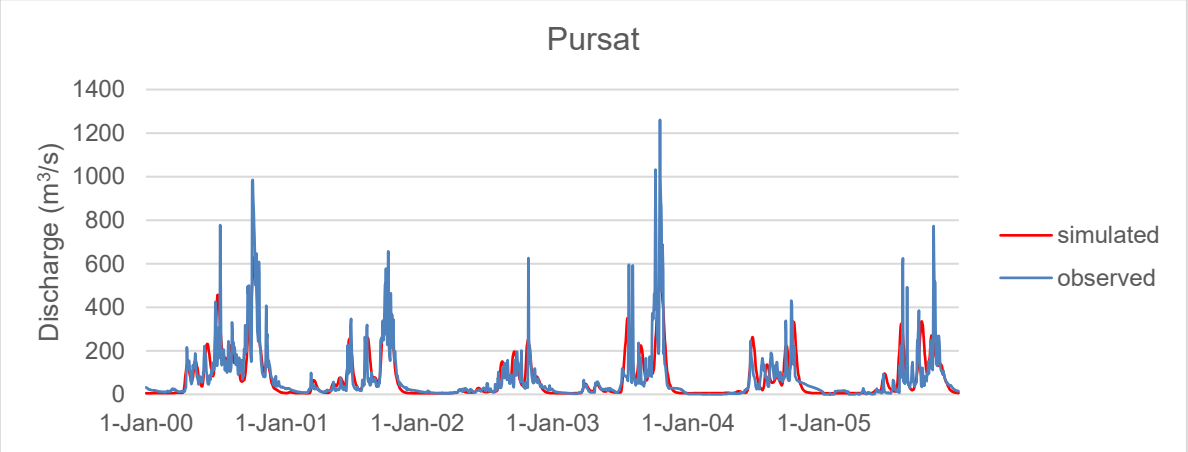
Pursat
Discharge (m³/s)
1400
1200
1000
800
600
400
200
0
1-Jan-00
1-Jan-01
1-Jan-02
1-Jan-03
1-Jan-04
1-Jan-05
simulated
observed

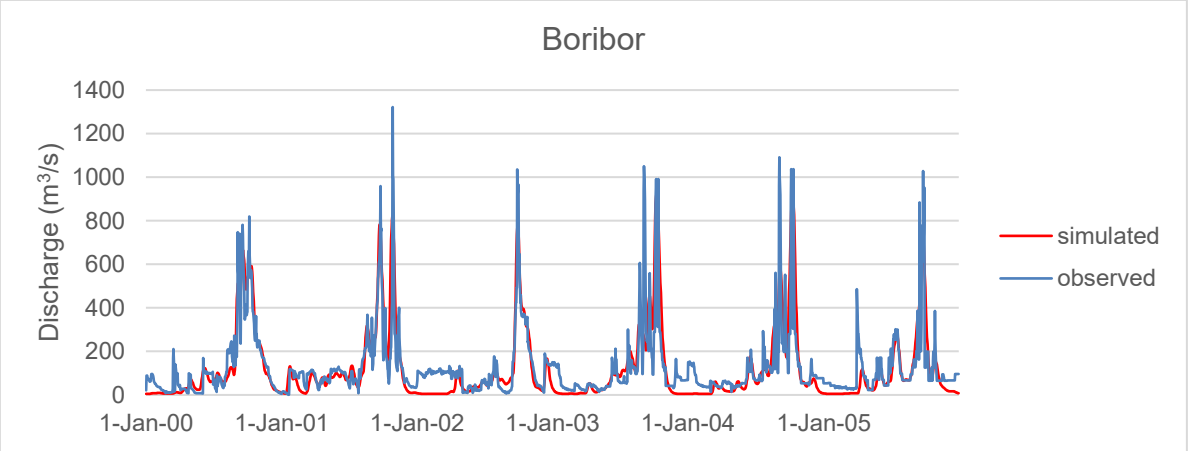
Boribor
Discharge (m³/s)
1400
1200
1000
800
600
400
200
0
1-Jan-00
1-Jan-01
1-Jan-02
1-Jan-03
1-Jan-04
1-Jan-05
simulated
observed

B.2 Hydrographs of the Baseline and Projected Discharge

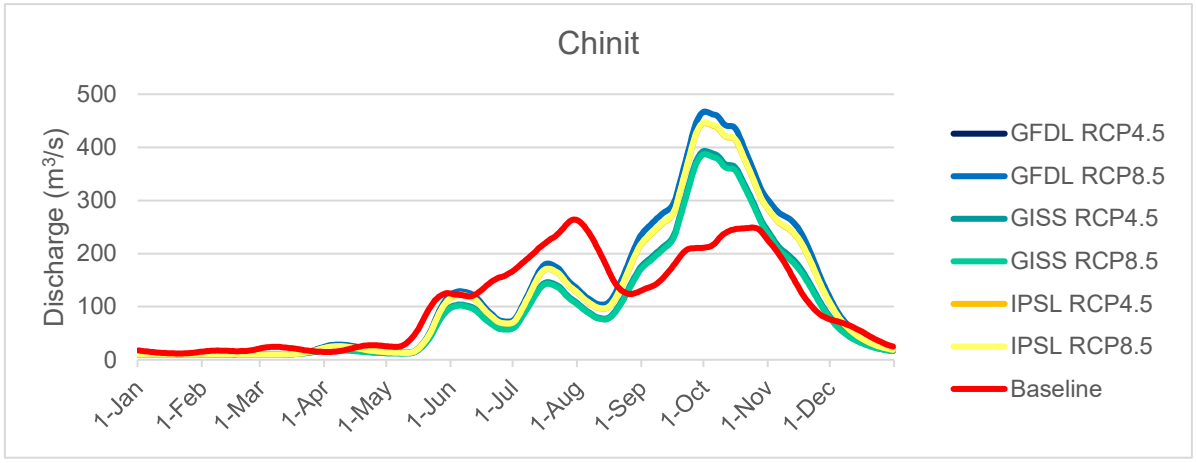

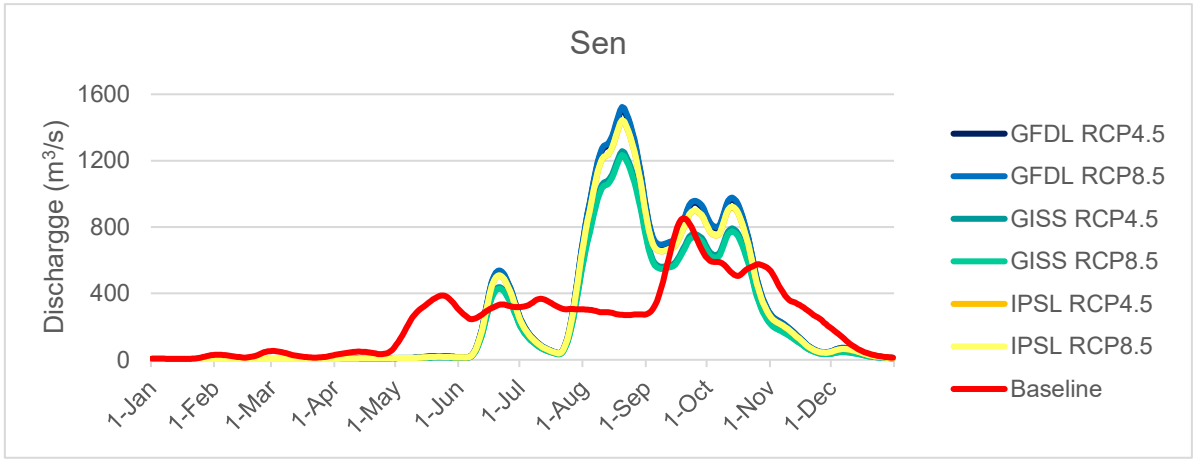

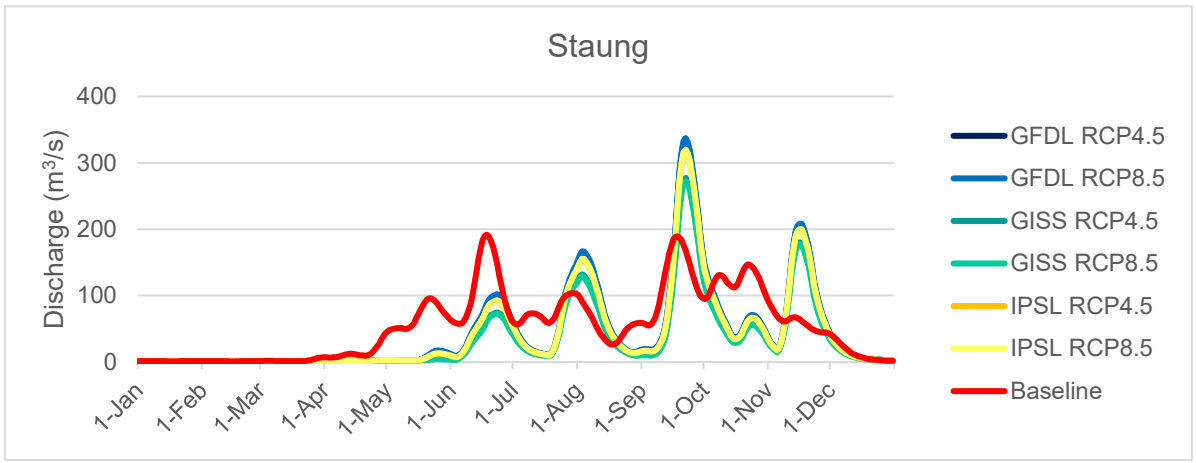

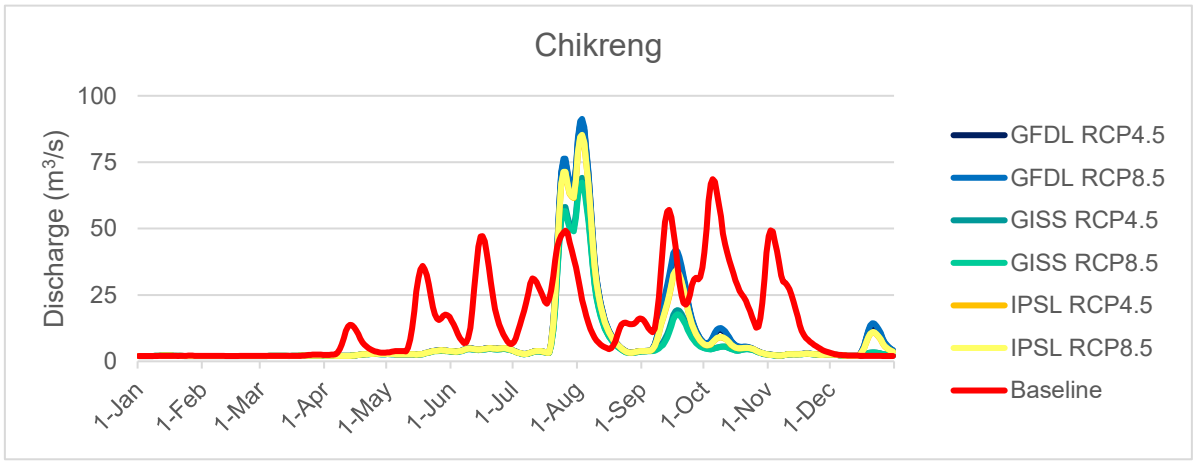

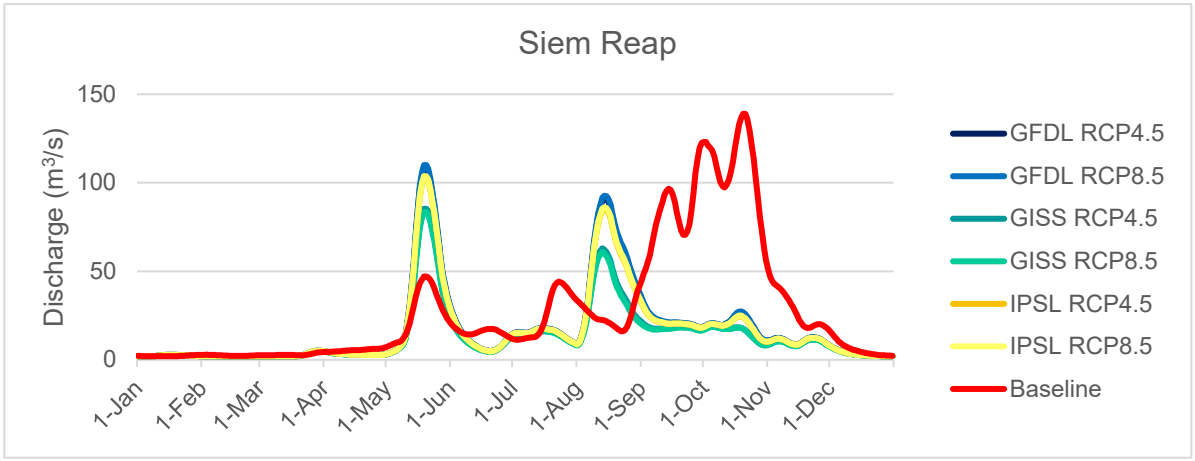
Siem Reap
Discharge (m³/s)
150
100
50
0
1-Jan
1-Feb
1-Mar
1-Apr
1-May
1-Jun
1-Jul
1-Aug
1-Sep
1-Oct
1-Nov
1-Dec
GFDL RCP4.5
GFDL RCP8.5
GISS RCP4.5
GISS RCP8.5
IPSL RCP4.5
IPSL RCP8.5
Baseline

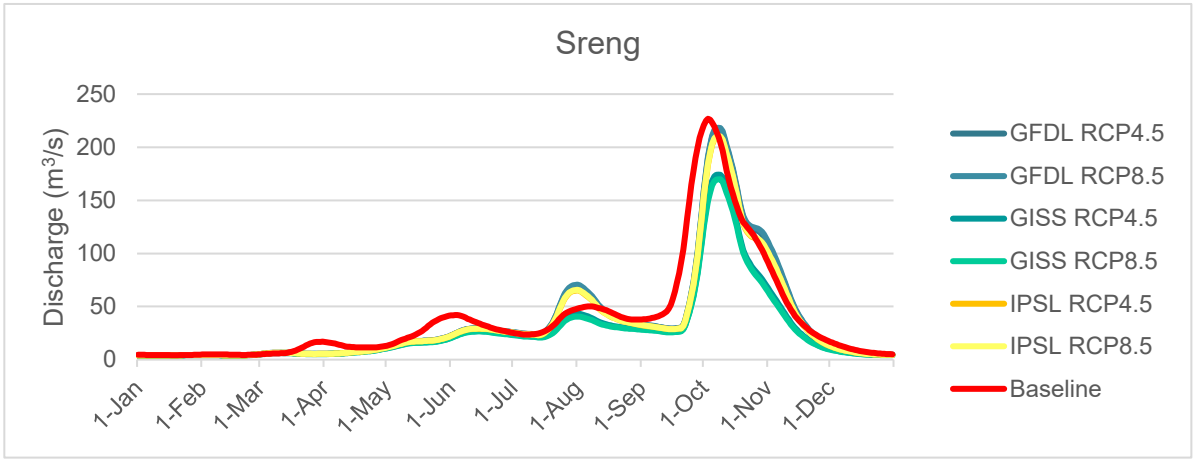
Sreng
Discharge (m³/s)
250
200
150
100
50
0
1-Jan
1-Feb
1-Mar
1-Apr
1-May
1-Jun
1-Jul
1-Aug
1-Sep
1-Oct
1-Nov
1-Dec
GFDL RCP4.5
GFDL RCP8.5
GISS RCP4.5
GISS RCP8.5
IPSL RCP4.5
IPSL RCP8.5
Baseline

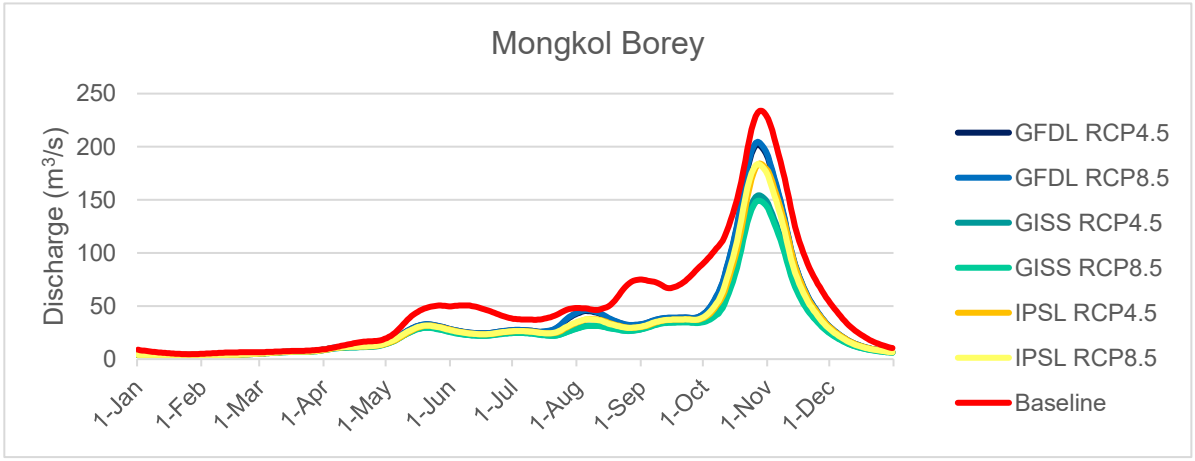
Mongkol Borey
Discharge (m³/s)
250
200
150
100
50
0
1-Jan
1-Feb
1-Mar
1-Apr
1-May
1-Jun
1-Jul
1-Aug
1-Sep
1-Oct
1-Nov
1-Dec
GFDL RCP4.5
GFDL RCP8.5
GISS RCP4.5
GISS RCP8.5
IPSL RCP4.5
IPSL RCP8.5
Baseline

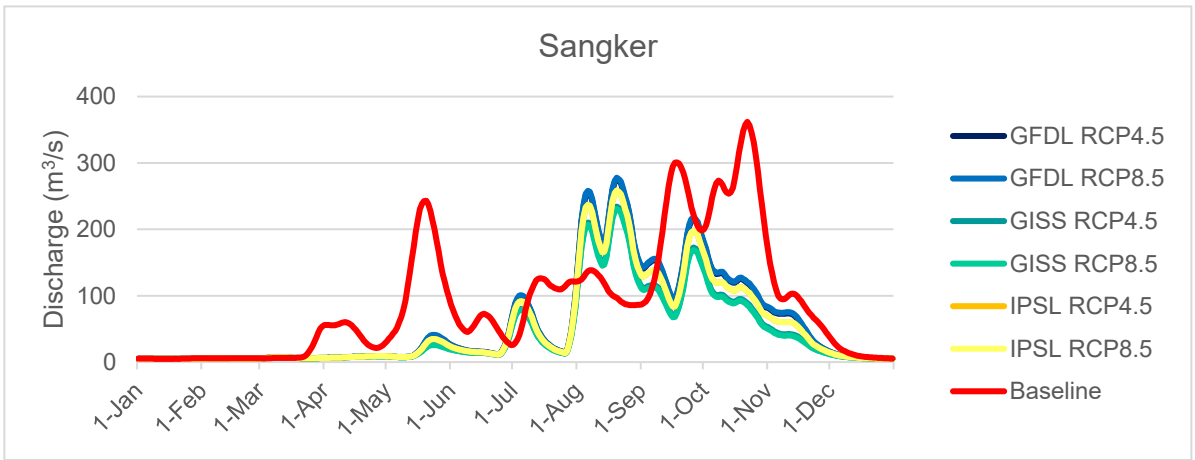
Sangker
Discharge (m³/s)
400
300
200
100
0
1-Jan
1-Feb
1-Mar
1-Apr
1-May
1-Jun
1-Jul
1-Aug
1-Sep
1-Oct
1-Nov
1-Dec
GFDL RCP4.5
GFDL RCP8.5
GISS RCP4.5
GISS RCP8.5
IPSL RCP4.5
IPSL RCP8.5
Baseline

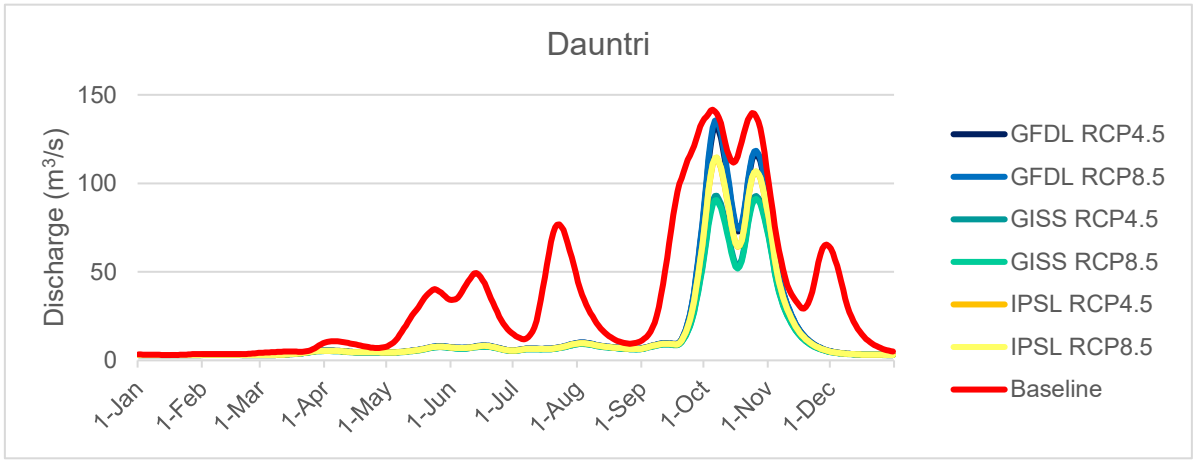
Dauntri
Discharge (m3/s)
150
100
50
0
1-Jan
1-Feb
1-Mar
1-Apr
1-May
1-Jun
1-Jul
1-Aug
1-Sep
1-Oct
1-Nov
1-Dec
GFDL RCP4.5
GFDL RCP8.5
GISS RCP4.5
GISS RCP8.5
IPSL RCP4.5
IPSL RCP8.5
Baseline

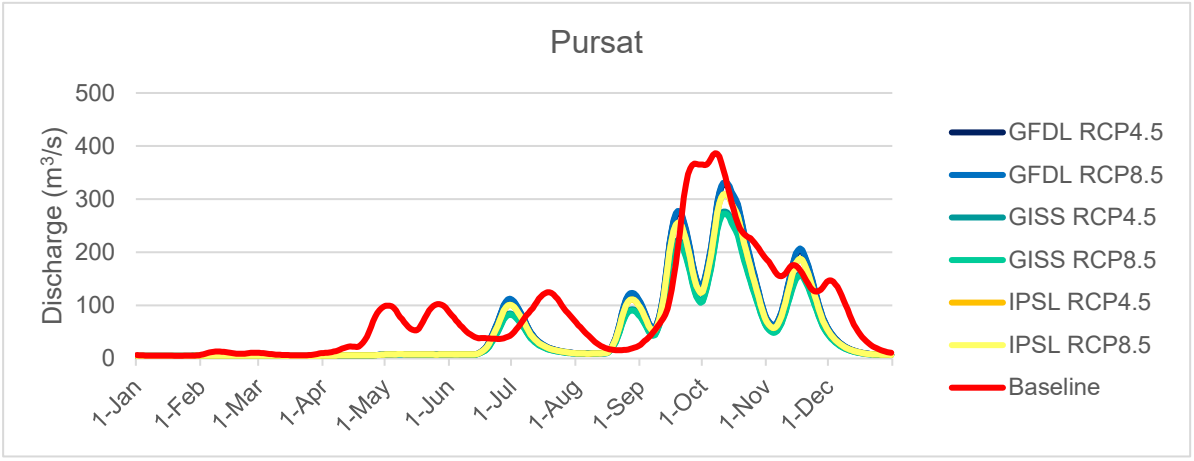
Pursat
Discharge (m3/s)
500
400
300
200
100
0
1-Jan
1-Feb
1-Mar
1-Apr
1-May
1-Jun
1-Jul
1-Aug
1-Sep
1-Oct
1-Nov
1-Dec
GFDL RCP4.5
GFDL RCP8.5
GISS RCP4.5
GISS RCP8.5
IPSL RCP4.5
IPSL RCP8.5
Baseline

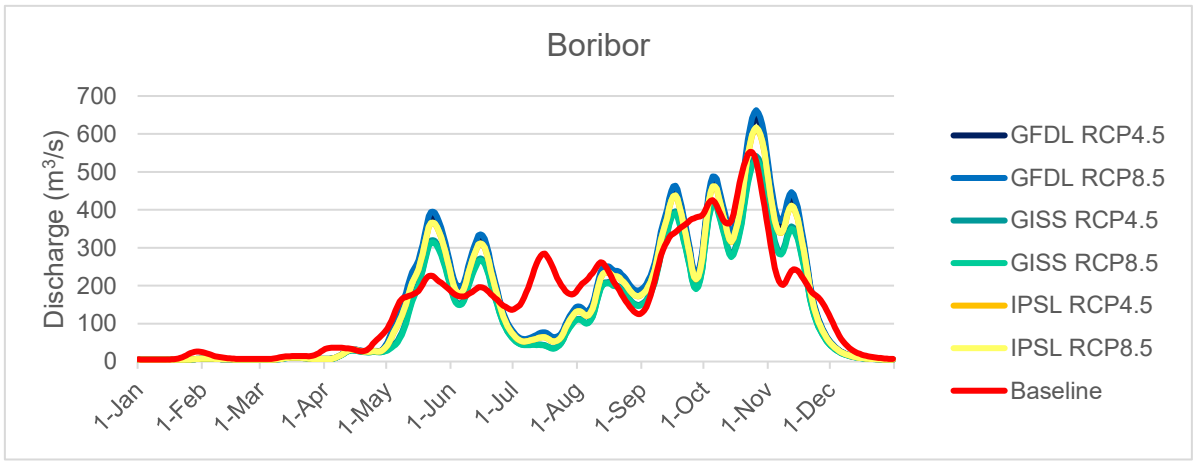
Boribor
Discharge (m3/s)
700
600
500
400
300
200
100
0
1-Jan
1-Feb
1-Mar
1-Apr
1-May
1-Jun
1-Jul
1-Aug
1-Sep
1-Oct
1-Nov
1-Dec
GFDL RCP4.5
GFDL RCP8.5
GISS RCP4.5
GISS RCP8.5
IPSL RCP4.5
IPSL RCP8.5
Baseline